

**UNIVERSIDADE ESTADUAL DE CAMPINAS  
FACULDADE DE ENGENHARIA ELÉTRICA E DE COMPUTAÇÃO  
DEPARTAMENTO DE SISTEMAS E ENERGIA**



**PEDRO PABLO VERGARA BARRIOS**

**CONTROL AND ENERGY MANAGEMENT SYSTEM OF A MICROGRID USING  
A GENETIC ALGORITHM**

***SISTEMA DE CONTROLE E GESTÃO DE ENERGIA DE UMA MICRORREDE  
UTILIZANDO ALGORITMOS GENÉTICOS***

**CAMPINAS  
2015**

**UNIVERSIDADE ESTADUAL DE CAMPINAS  
FACULDADE DE ENGENHARIA ELÉTRICA E DE COMPUTAÇÃO  
DEPARTAMENTO DE SISTEMAS E ENERGIA**



**PEDRO PABLO VERGARA BARRIOS**

***CONTROL AND ENERGY MANAGEMENT SYSTEM OF A MICROGRID USING  
A GENETIC ALGORITHM***

**SISTEMA DE CONTROLE E GESTÃO DE ENERGIA DE UMA MICRORREDE  
UTILIZANDO ALGORITMOS GENÉTICOS**

**Orientador: Prof. Dr. Luiz Carlos Pereira da Silva**

Dissertação de Mestrado apresentada ao Programa de Pós-Graduação em Engenharia Elétrica da Faculdade de Engenharia Elétrica e de Computação da Universidade Estadual de Campinas para obtenção do título de Mestre em Engenharia Elétrica, área de concentração em Energia Elétrica (AF).

Este exemplar corresponde à versão final da dissertação de mestrado defendida pelo aluno Pedro Pablo Vergara Barrios, e orientada pelo Prof. Dr. Luiz Carlos Pereira da Silva.

---

Prof. Dr. Luiz Carlos Pereira da Silva

**CAMPINAS  
2015**

**Agência(s) de fomento e nº(s) de processo(s):** FAPESP, 2013/22451-4

Ficha catalográfica  
Universidade Estadual de Campinas  
Biblioteca da Área de Engenharia e Arquitetura  
Luciana Pietrosanto Milla - CRB 8/8129

V586c Vergara Barrios, Pedro Pablo, 1990-  
Control and energy management system of a microgrid using a genetic algorithm / Pedro Pablo Vergara Barrios. – Campinas, SP : [s.n.], 2015.

Orientador: Luiz Carlos Pereira da Silva.  
Dissertação (mestrado) – Universidade Estadual de Campinas, Faculdade de Engenharia Elétrica e de Computação.

1. Sistemas de gestão de energia. 2. Algoritmos genéticos. 3. Fontes renováveis. I. Silva, Luiz Carlos Pereira da, 1972-. II. Universidade Estadual de Campinas. Faculdade de Engenharia Elétrica e de Computação. III. Título.

Informações para Biblioteca Digital

**Título em outro idioma:** Sistema de controle e gestão de energia de uma microrrede utilizando algoritmos genéticos

**Palavras-chave em inglês:**

Energy management systems

Genetic algorithm

Renewable sources

**Área de concentração:** Energia Elétrica

**Titulação:** Mestre em Engenharia Elétrica

**Banca examinadora:**

Luiz Carlos Pereira da Silva [Orientador]

Márcio Venício Pilar Alcântara

Marcos Julio Rider Flores

**Data de defesa:** 04-11-2015

**Programa de Pós-Graduação:** Engenharia Elétrica

## COMISSÃO JULGADORA – DISSERTAÇÃO DE MESTRADO

**Candidato:** Pedro Pablo Vergara Barrios RA: 153774

**Data da Defesa:** 4 de novembro de 2015

**Título da Tese:** “ Control and energy management system of a microgrid using a genetic algorithm / Sistema de controle e gestão de energia de uma microrrede utilizando algoritmos genéticos”.

Prof. Dr. Luiz Carlos Pereira da Silva (Presidente, FEEC/UNICAMP)

Dr. Márcio Venício Pilar Alcântara (ANEEL)

Prof. Dr. Marcos Julio Rider Flores (FEEC/UNICAMP)

A ata de defesa, com as respectivas assinaturas dos membros da Comissão Julgadora, encontra-se no processo de vida acadêmica do aluno.

## **DEDICATORY**

A mi familia, por su paciencia al estar tan lejos de ellos, a mi madre, padre, hermanos y abuela. Lo son todo para mí.

A mis amigos, David, Nelly, Silvia, Marcos. Los llevo siempre conmigo.

A Ruan, porque al final la espera ha valido la pena.

Y finalmente, a cada una de las personas que siempre han contribuido, de alguna u otra forma, para llegar a donde estoy.

## **ACKNOWLEDGMENTS**

This master dissertation was supported by the São Paulo Research Foundation (FAPESP) under the research grant 13/22451-4.

To my advisor, Prof. Dr. Luiz Carlos Pereira da Silva and all the professors at the DSE/FEEC.

To my colleagues and friends at DSE/FEEC/UNICAMP at the LE19 and LE23.

## ABSTRACT

A microgrid, as a controllable intelligent electric network, composed of distributed energy systems (DERs), energy storage systems (ESS) and controllable loads, require an Energy Management System (EMS) as a central entity responsible for coordinate control of DERs, for the dispatch of units under supply and demand uncertainty, for managing instantaneous active power balance, power flows and network voltage profiles, among others. Considering this central control structure, in this master dissertation it is proposed an Energy Management System composed of two optimization stages: a long-term and a short-term stage.

The main function of the long-term stage is to solve the energy management problem considering an operational horizon of 24-hours to minimize simultaneously the operational cost and the power losses. To do this, it is used the Non-dominated Sorting Genetic Algorithm II (NSGA-II) complemented with a Quadratic Programming (QP) algorithm, to reduce the final complexity of the energy management problem. For the short-term stage, it is used a QP algorithm. The main function of the short-term stage is to guarantee power balance and reduce the impact of the forecast error in the operation of the distribution system.

To develop the optimization algorithm MATLAB and GridLab-D are used to implement and simulate the EMS in a microgrid composed of a residential distribution network including batteries, renewable and fuel-based generation systems. To evaluate the developed EMS two main cases are studied, a perfect forecast case and real operational case. Finally, dynamic simulations are carried on in GridLabD to technically assess the impact of the optimal solution in the distribution system.

**Keywords:** Energy management systems, genetic algorithms, microgrid, renewable energy systems.

## RESUMO

As microrredes, como redes elétricas controláveis e inteligentes, compostas por sistemas distribuídos de energias (DES), sistemas de armazenamento e cargas controláveis, exigem o uso de um Sistema de Gestão de Energia (EMS) como entidade central encarregada de coordenar e controlar os SDE, despachar as unidades de geração sob incerteza da demanda e da geração, controlar o balanço instantâneo de potência ativa, fluxo de carga e perfis de tensão, entre outras. Considerando as funções desta entidade central, nesta dissertação propõe-se um Sistema de Gestão de Energia composto por duas etapas de otimização: uma etapa a longo-prazo e outra a curto-prazo.

A principal função da etapa de longo-prazo é resolver o problema de gestão de energia considerando um horizonte de planejamento de 24 horas, visando minimizar simultaneamente os custos operacionais e as perdas de potência. Para isto, é utilizado o algoritmo *Non-dominated Sorting Genetic Algorithm II* (NSGA-II), complementado com uma técnica de Programação Quadrática, visando reduzir a complexidade do problema de gestão de energia. A principal função da etapa de curto-prazo é garantir o balanço de potência e reduzir o impacto do erro de previsão na operação do sistema de distribuição.

Para desenvolver o algoritmo de otimização proposto são utilizados os pacotes MATLAB e GridLabD para implementar e simular o SGE em uma microrrede composta por uma rede de distribuição residencial, incluindo baterias, sistemas de geração convencionais e baseados em energias renováveis. Para avaliar o SGE desenvolvido dois casos de estudos são propostos, denominados como um caso com perfeita previsão e um caso de operação real. Finalmente, simulações dinâmicas são desenvolvidas no GridLabD para avaliar o impacto técnico das soluções ótimas no sistema de distribuição.

**Palavras-chave:** Sistema de gestão de energia, algoritmos genéticos, microrrede, sistemas de energias renováveis.

## LIST OF FIGURES

Figure 1. Basic structure of a Low Voltage Microgrid .....	24
Figure 2. Information exchange between the primary, secondary and tertiary control level. ....	28
Figure 3. PQ inverter controller structure. ....	29
Figure 4. Frequency/active power and voltage/reactive power droop characteristics [28]. ....	30
Figure 5. Information flow (inputs/outputs) of a general EMS. ....	33
Figure 6. MPC/RH Strategy in an EMS. ....	35
Figure 7. Proposed Hierarchical Control Structure of a LV Microgrid. ....	39
Figure 8. Structure of a house in GridLabD, composed of four Triplex Meter (TM), a solar system, a battery bank, an EV and a thermodynamic and electric model. ....	44
Figure 9. Residential LV microgrid developed in GridLabD. ....	42
Figure 10. Charging profile of the Nissan Altra battery (lithium-ion) [71]. ....	54
Figure 11. Power losses characterization of a distribution transformer (DT) in GridLabD. ....	56
Figure 12. Triplex line power losses estimated by GridLabD, the linear model and the quadratic model as a function of the input power for a DT. ....	56
Figure 13. Schedule of the EV. ....	62
Figure 14. Schematic example of mutation. ....	70
Figure 15. Schematic example of crossover. ....	71
Figure 16. Computational flow of the proposed NSGA-II+QP algorithm. ....	73
Figure 17. Computational flow of the short-term stage algorithm. ....	77
Figure 18. Solar and Wind System models compared to the GridLabD models. ....	79
Figure 19. Load consumption used for the cases of study in Scenario I and II. ....	80
Figure 20. Scenario I: Pareto Front results obtained for the Perfect Forecast case. ....	81
Figure 21. Scenario I: Output power for the battery system, PV and wind system, diesel generator and main grid for the Perfect Forecast case given by the long-term stage. ....	83
Figure 22. Scenario I: State-of-Charge (SOC) for the Perfect Forecast case. ....	84
Figure 23. Scenario I: Pareto Front results obtained for the Real Operational case. ....	86
Figure 24. Scenario I: Output power for the battery system, PV and wind system, diesel generator and main grid for the Real Operational case given by the long-term stage. ....	89
Figure 25. Scenario I: State-of-Charge (SOC) for the Real Operational case. ....	90
Figure 26. Scenario I: Relative Error (RE) for the SOC for both operational cases considered. ....	91
Figure 27. Output power for the battery system, PV and wind system, diesel generator and main grid for the Perfect Forecast case, limiting the power supplied by the MV grid. ....	94
Figure 28. Scenario I: Output power for the battery system, PV and wind system, diesel generator and main grid for the Perfect Forecast case, considering the LLC of the battery system given by the long-term stage. ....	94
Figure 29. Scenario I: Output power for the battery system, PV and wind system, diesel generator and main grid for the Perfect Forecast case given by the short-term stage. ....	98
Figure 30. Scenario I: Output power for the battery system, PV and wind system, diesel generator and main grid for the Real Operational case given by the short-term stage. ....	101

Figure 31. Scenario II: Pareto Front results obtained for the Perfect Forecast case.....	104
Figure 32. Scenario II: Output power for the battery and EV system, PV and wind system, diesel generator and main grid for the Perfect Forecast case given by the long-term stage.....	106
Figure 33. Scenario II: State-of-Charge (SOC) for the Perfect Forecast case.....	107
Figure 34. Scenario II: Pareto Front results obtained for the Real Operational case. ....	110
Figure 35. Scenario II: Output power for the battery and EV system, PV and wind system, diesel generator and main grid for the Real Operational case given by the long-term stage. ....	114
Figure 36. Scenario II: State-of-Charge (SOC) for the Real Operational case. ....	114
Figure 37. Scenario II: Relative Error (RE) for the SOC of the ESS for both operational case considered. ....	115
Figure 38. Scenario II: Relative Error (RE) for the SOC of the EV for both operational case considered. ....	115
Figure 39. Scenario II: Output power for the battery and EV system, PV and wind system, diesel generator and main grid for the Perfect Forecast case, limiting the maximum MV power given by the long-term stage.....	119
Figure 40. Scenario II: Output power for the battery and EV system, PV and wind system, diesel generator and main grid for the Perfect Forecast case, if the LLC is considered.....	120
Figure 41. Scenario II: State-of-Charge (SOC) for the Real Operational case, if the LLC is considered..	121
Figure 42. Scenario II: Output power for the battery system, PV and wind system, diesel generator and main grid for the Perfect Forecast case given by the short-term stage.....	124
Figure 43. Scenario II: Output power for the battery system, PV and wind system, diesel generator and main grid for the Real Operational case given by the short-term stage. ....	127
Figure 44. Scenario I: Triplex line voltage variations: Line 1 (red) and Line 2(blue). ....	131
Figure 45. Scenario I: Voltage Unbalance (VU) at the PCC, node N4. Scenario I.....	133
Figure 46. Scenario I: Triplex line voltage variations: Line 1 (red) and Line 2(blue) for the cases where the diesel generator is dispatched.....	135
Figure 47. Scenario II: Triplex line voltage variations: Line 1 (red) and Line 2(blue).....	137
Figure 48. Scenario II: Voltage Unbalance (VU) at the PCC, node N4.....	138

## LIST OF TABLES

Table 1. Characteristics of the five type of residential consumers implemented in GLD.....	43
Table 2. Parameters of the PV and Wind system model.....	45
Table 3. Parameters of the battery model.....	48
Table 4. Fuel consumption of a 60 kW diesel generator unit.....	49
Table 5. Parameters of the diesel generator model. ....	50
Table 6. Parameters of the EV Nissan Altra. ....	54
Table 7. Parameters of the two line power loss models. ....	57
Table 8. Time-of-use pricing scheme used by the Sao Paulo's utility (CPFL-Paulista).....	59
Table 9. States of the EV during one day of schedule. ....	62
Table 10. Scenario I: OC, PL and Energy provided by the MV grid for different operational scenarios....	85
Table 11. Scenario I: Comparative results for the Min OC, the Min PL and the BCS Sol for the both operational cases considered. ....	92
Table 12. Scenario I: OC, FC, PL and Energy provided by the MV grid for the cases where the diesel generator is more attractive. ....	95
Table 13. Scenario I: Comparative results for the solution obtained using the EMS and the simulated solution in GridLab-D for the Perfect Forecast case.....	97
Table 14. Scenario I: Comparative results for the solution obtained using the EMS and the simulated solution in GridLab-D for the Real Operational case.....	99
Table 15. Scenario I: Comparative results for the Min OC, the Min PL and the BCS Sol for both operational cases considered. ....	101
Table 16. Scenario II: OC, PL and Energy provided by the MV grid for different operational scenarios.	110
Table 17. Scenario II: Comparative results for the Min OC, the Min PL and the BCS Sol for both operational cases considered in the scenario II. ....	117
Table 18. Scenario II: OC, FC, PL and Energy provided by the MV grid for the cases where the diesel generator is more attractive. ....	121
Table 19. Scenario II: Comparative results for the solution obtained using the EMS and the simulated solution in GridLab-D for the Perfect Forecast case.....	125
Table 20. Scenario II: Comparative results for the Min OC, the Min PL and the BCS Sol for both operational cases considered. ....	128

## ABBREVIATIONS

BCS	Best Compromise Solution
ANEEL	Brazilian Electricity Regulatory Agency
CD	Crowding Distance
DM	Decision Maker
DSM	Demand Side Management
DER	Distributed Energy Resources
DGS	Distributed Generation Systems
DG	Distributed Generators
DMS	Distribution Management System
DNO	Distribution Network Operator
DT	Distribution Transformer
ELD	Economic Load Dispatch
EV	Electric Vehicle
EMS	Energy Management System
ESS	Energy Storage System
FPF	Final Pareto front
GLD-FPF	Final Pareto front after simulating the solution in GRIDLABD
FC	Fuel Consumption
GA	Genetic Algorithm
LLC	Life Loss Cost
LC	Load Controller
LPSP	Loss of Power Supply Probability
LV	Low Voltage
MPPT	Maximum Power Point Tracking
MV	Median Voltage
MG	Microgrid
MGCC	Microgrid Central Controller
MS	Micro-Source Controller
MINLP	Mixed-Integer Non-Linear problem
MPC	Model Predictive Control
MMO	Multi-Master Operation
MOGA	Multi-Objective Genetic Algorithm
MGSA	Multi-period Gravitational Search Algorithm
NSGA-II	Non-dominated Sorting Genetic Algorithm II
OC	Operational Cost
PNNL	Pacific Northwest National Laboratory
PSO	Particle Swarm Optimization
PF	Perfect Forecast
PV	Photovoltaic
PCC	Point of Common Coupling
PL	Power Losses
PMS	Power Management System
PRODIST	Procedures for Electricity Distribution in the National Electric System
QP	Quadratic Programming
RO	Real Operational
RE	Relative Error
RES	Renewable Energy System
RH	Rolling Horizon
SMO	Single Master Operation

SG	Smart Grid
Min OC Sol	Solution with the minimum OC
Min PL Sol	Solution with the minimum PL
STC	Standard Test Conditions
SOC	State of Charge
TM	Triplex Meters
TMY	Typical Meteorological Year
UC	Unit Commitment
V2G	Vehicle-to-grid
VPP	Virtual Power Plant
VSI	Voltage Source Inverter
VU	Voltage Unbalance

## NOMENCLATURE

$P_{GD}^t$	Active power output of the diesel generator at time $t$ (kW)	$P_{BAT,min}^t$	Minimum charging/discharging battery power (kW)
$SR$	Active power reserve (%)	$P_{GD,min}$	Minimum output power of the diesel generator (kW)
$R_{BAT}^t$	Active power reserve of the battery system at time $t$ (kW)	$MUT_{GD}$	Minimum running time for the diesel generator (min)
$R_{GD}^t$	Active power reserve of the diesel generator at time $t$ (kW)	$S_{min}$	Minimum shifting coefficient
$R_G^t$	Active power reserve of the main grid at time $t$ (kW)	$SOC_{min}$	Minimum SOC
$T_A^t$	Ambient temperature at time $t$ (K)	$MDT_{GD}$	Minimum stopping time for the diesel generator (min)
$\gamma(v, C_i^s)$	Amount of energy used by the EV (kWh)	$F_{min}$	Minimum value of the objective $i$
$A_s$	Area of the PV system (m <sup>2</sup> )	$v_N$	Nominal velocity (m/s)
$\eta_{BAT}$	Battery efficiency (%)	$V_{BAT}$	Nominal voltage of the battery (V)
$C_{BAT}$	Capacity of the battery bank (Ah)	$N_{BAT}$	Number of batteries in the distribution system
$C_{EV}$	Capacity of the EV (kWh)	$N_{EV}$	Number of EV
$tl_0, tl_1$	Coefficient of the linear model for the triplex line losses model	$N_{pop}$	Number of individuals in the population
$tlq_0, tlq_1, tlq_2$	Coefficient of the quadratic model for the triplex line losses model	$N_{obj}$	Number of optimization objectives
$g_0, g_1, g_2$	Coefficients of the fuel consumption model for the diesel generator.	$T$	Number of time-step considered
$p_1, p_2, p_3, p_4$	Coefficients of the power curve model for the wind turbine	$OC$	Operational cost objective (USD\$)
$C_G^t$	Cost of the energy supply by the MV grid (USD\$/kWh)	$B_{BAT}^t$	Operational state of the battery system (charging/discharging)
$v_{CO}$	Cutoff velocity (m/s)	$U_{GD}^t$	Operational state of the diesel generator
$DOD_{EV}$	Deep of Discharge of an EV	$P_{DT,out}$	Output power of the distribution transformer (kW)
$DOD$	Depth-of-Discharge of the ESS (%)	$P_G^t$	Power from the MV grid at time $t$ (kW)
$C_{GD}$	Diesel cost (USD\$/l)	$P_{CH}^t$	Power input of the battery system in charging mode at time $t$ (kW)
$RD_{BAT}$	Down-rate for the battery (kWh)	$PL^t$	Power losses at time $t$ (kW)

$RU_{GD}$	Down-rate for the diesel generator (kW)	$P_{TL, Loss}$	Power losses in the triplex line (kW)
$\eta_{DT}$	Efficiency of the distribution transformer (%)	$PL$	Power Losses objective (kW)
$\eta_{STC}$	Efficiency of the PV panel at the Standard Test Conditions (STC) (%)	$P_{U, WT}^t$	Power output of one wind turbine at time $t$ (kW)
$P_{L, PP}^t$	Expected load consumption for the PF case at time $t$ (kW)	$P_{BAT}^t$	Power output of the battery system at time $t$ (kW)
$P_{L, RO}^t$	Expected load consumption for the RO case at time $t$ (kW)	$P_{DCH}^t$	Power output of the battery system in discharging mode at time $t$ (kW)
$k, d$	Experimental parameters for the Life Loss Cost model of the battery system	$P_{GD}^t$	Power output of the diesel generator at time $t$ (kW)
$FC(\cdot)$	Fuel consumption (l/h)	$P_{EV}^t$	Power output of the EV at time $t$ (kW)
$FC_{GD}^t$	Fuel consumption at time $t$ (l/h)	$P_{PV}^t$	Power output of the PV system (kW)
$C_{ini}$	Initial investment of one battery (USD\$)	$P_{WT}^t$	Power output of the wind system at time $t$ (kW)
$P_{DT, in}$	Input power of the distribution transformer (kW)	$\Delta$	Random value used for the mutation genetic operator
$\eta_{INV}$	Inverter's efficiency (%).	$\gamma$	Random value used to create the RO case from the PF case.
$G_A^t$	Irradiance (W/m <sup>2</sup> )	$C_i^s$	Seasonal coefficient of the EV model
$C_{Life}$	Life Loss Cost of the battery system (USD\$)	$S^t$	Shifting coefficients of the DSM at time $t$
$\tilde{P}_L^t$	Load consumption after applying the DSM strategy in kW	$SOC_{EV, max}$	SOC maximum of the EV
$P_L^t$	Load consumption at time $t$ (kW)	$SOC_{EV, min}$	SOC minimum of the EV
$P_{DT, Loss}$	Losses due to the efficiency of the distribution transformer (kW)	$SOC_{EV}^t$	SOC of the EV system
$P_{BAT, max}^t$	Maximum charging/discharging battery power (kW)	$SOC^t$	State of Charge of the battery system at time $t$
$g_{max}$	Maximum number of generations	$T_{STC}$	STC temperature (K)
$P_{BAT, Total}$	Maximum output power of the aggregated battery system model (kW)	$K_p$	Temperature coefficient for the active power (1/K)
$P_{EV, Total}^t$	Maximum output power of the aggregated EV model (kW)	$\Delta t$	Time-step (1/4-hour) for the long-term stage/ (1/12-hour) for the short-term stage
$P_{PV, Total}$	Maximum output power of the aggregated PV system model (kW)	$E_{CH}$	Total amount of energy purchased by ESS in charging mode (kWh)
$P_{WT, max}$	Maximum output power of the aggregated wind system model (kW)	$E_{DCH}$	Total amount of energy supplied by ESS in discharging mode (kWh)

$P_{GD,max}$	Maximum output power of the diesel generator (kW)	$E_G$	Total amount of energy supplied by the MV grid (kWh)
$P_{EV,max}$	Maximum output power of the EV (kW)	$T_{GD,OFF}^t$	Total off-line of the diesel generator (min)
$P_{G,max}$	Maximum power of the main grid (kW)	$T_{GD,ON}^t$	Total on-line of the diesel generator (min)
$S_{max}$	Maximum shifting coefficient	$\eta$	Uniform random value used by the NSGA-II+QP algorithm
$SOC_{max}$	Maximum SOC	$RU_{BAT}$	Up-rate for the battery (kWh)
$F_{max}$	Maximum value of the objective $i$	$RD_{GD}$	Up-rate for the diesel generator (kW)
$v$	Mean velocity of an EV (m/s)	$VU$	Voltage unbalance factor (%)
$\mu^k$	Membership function		

## SUMMARY

DEDICATORY	
ACKNOWLEDGMENTS	
ABSTRACT	
RESUMO	
ABBREVIATIONS	
NOMENCLATURE	
INTRODUCTION	19
1.1 OBJECTIVES	20
1.2 STRUCTURE OF THE DISSERTATION	21
2 CONTROL AND ENERGY MANAGEMENT OF MICROGRIDS	23
2.1 HIERARCHICAL CONTROL	25
2.1.1 PRIMARY CONTROL	28
2.1.2 SECONDARY CONTROL	31
2.1.3 TERTIARY CONTROL	31
2.2 ENERGY MANAGEMENT SYSTEMS	32
2.3 STRUCTURE OF THE PROPOSED ENERGY MANAGEMENT SYSTEM	38
3 SYSTEM MODELING AND STATEMENT OF THE PROBLEM	41
3.1 RESIDENTIAL FEEDER	41
3.2 PV AND WIND SYSTEM	44
3.3 ENERGY STORAGE SYSTEM	46
3.4 DIESEL GENERATOR	49
3.5 DEMAND-SIDE MANAGEMENT	50
3.6 ELECTRIC VEHICLE	52
3.7 LINES AND TRANSFORMERS POWER LOSS MODELS	55
3.8 STATEMENT OF THE ENERGY MANAGEMENT PROBLEM	57
3.8.1 TECHNICAL CONSTRAINS	59
4 THE OPTIMIZATION STRATEGY	63
4.1 LONG-TERM OPTIMIZATION STAGE: NSGA-II+QP ALGORITHM	65
4.2 SHORT-TERM OPTIMIZATION STAGE	74
5 CASE STUDY I: BASIC MICROGRID	78
5.1 WEATHER DATA AND RES SYSTEM MODEL VALIDATION	78
5.2 CASES OF STUDY	79
5.3 LONG-TERM STAGE	80
5.4 SHORT-TERM STAGE	95
6 CASE STUDY II: A MORE INTELLIGENT MICROGRID	103
6.1 LONG-TERM STAGE	103
6.2 SHORT-TERM STAGE	122
7 TECHNICAL ASSESSMENT OF THE EMS IN THE DISTRIBUTION SYSTEM	129
7.1 SCENARIO I: BASIC MICROGRID	129

7.2 SCENARIO II: A MORE INTELLIGENT MICROGRID .....	135
8 CONCLUSIONS.....	139
8.1 FUTURE WORKS.....	142
8.2 PUBLICATIONS .....	143
9 REFERENCES.....	144
10 APPENDIX.....	150
10.1 APPENDIX A .....	150
10.2 APPENDIX B.....	152

---

## 1 INTRODUCTION

---

MICROGRIDS, composed of Distributed Energy Resources (DERs) such as Distributed Generation Systems (DGS), Energy Storage Systems (ESS) and intelligent loads, requires a central control system capable of controlling and managing its operation, aiming to guarantee an efficient and reliable operation [1]. This central entity is a system that forecast microgrid's (MG) operation and provides operational set-points to the DGS in agreement with load energy demand, defining electrical parameters such as currents and voltages, ensuring stability, frequency regulation and others important characteristic of MG's operation [2].

These management functions are the main concern of the Energy Management System (EMS), designed to manage the multi-constraint and multi-decision environment in which these electric systems are operated [3]. Due to the inherent operating characteristics of MGs, the EMS requires fast response, compared to a traditional EMS for large power systems [4].

The main motivations for the study of these systems relies on the development of microgrids, which can be considered as emerging technologies that can ensure energy supply in the future and reduce the environmental impact of generation on the planet, especially in systems with high renewable energy penetration [5], [6]. Moreover, as this EMS aims to reduce consumption of the main grid, this system will allow the development of new strategies to reduce peak demand, reduce grid congestion, improve power quality and develop new demand side frameworks. In a future scenario, these systems will fulfill the function of optimizing the operation of the electricity demand, heating and water supply, among other

resources, accomplishing with the minimization of objectives and increasing efficiency and reliability [7] [8].

It is possible to consider the MG's operation as an optimization problem with multiple objectives, where the EMS must supply local demand, minimize economic operation and minimize environmental impact (emissions, noise, residues); while limiting the maximum energy that is extracted from the main grid [5]. The development of EMS for microgrids composed with different DGS and ESS is a first step towards the integration of microgrids in the current electrical system, without affecting its operation or requiring major updates in its architecture or operation.

## **1.1 OBJECTIVES**

Considering all the discussion presented above, the main objective of this master dissertation is to develop an Energy Management System (EMS) for a Low Voltage (LV) MG composed of ESSs, renewable energy and fuel-based generation systems for a residential microgrid in grid-connected mode. To do this, it will be used a Multi-Objective Genetic Algorithm (MOGA) as the optimization strategy, considering two operation objectives: operational cost and power losses, both in conflict. Also, the next objectives can be considered:

- Characterize the operation of an Energy Management System (EMS) in a hierarchical control structure.
- Develop a multi-objective EMS using a genetic algorithm for a LV residential microgrid composed of a long- and a short-term optimization stage.

- Model and simulate the EMS using GridLabD Software, including micro-source systems (such as photovoltaic and wind system), energy storage (such batteries and electric vehicles) and not-shedding loads.
- Study technical aspects related to the energy management and control in LV microgrids, such as decreasing energy losses, load management, voltage profile improvement, increasing the reliability and efficiency of the system, among others.

## 1.2 STRUCTURE OF THE DISSERTATION

This master dissertation is organized as follows:

- ✓ Chapter 2 presents the concept of microgrids, special attention is given to the energy management system framed in a hierarchical control structure. Also, it is presented a short review of trends related to the Energy Management System (EMS) structure and optimization algorithms. Finally, it is presented the structure of the proposed EMS.
- ✓ Chapter 3 presents the LV microgrid that will be used to asses and evaluate the performance of the proposed EMS. This LV microgrid is developed and modeled in GridLabD software. Additionally, all the models used for the generations and storage systems are presented. Finally, it is presented a statement of the energy management problem and the operational constraints that the EMS has to guarantee to operate according to the power quality requirements of the Procedures for Electricity Distribution in the National Electric System, PRODIST by its Portuguese acronym.
- ✓ Chapter 4 presents the optimization algorithm developed for the long-term and short-term stage of the EMS. For the long-term stage, the Non-dominated Sorting Genetic Algorithm II (NSGA-II) is used. This MOGA is complemented with a QP technique. Also, the mutation and crossover genetic operator are presented. Finally, for the short-term stage a QP algorithm is used and presented.

- ✓ Chapter 5 presents the first scenario of study. In this scenario it is not considered the Demand Side Management (DSM) system and the Electric Vehicle (EV) technology. This first scenario tends to model a basic microgrid. To do this, a performance assessment of the final solutions provided by the long-term and short-term stage is presented. Also, a validation of the Renewable Energy Systems (RES) models proposed and the weather data used to solve the energy management problem is presented.
- ✓ Chapter 6 presents the second scenario of study, in which the DSM system and the Electric Vehicles (EV) are considered in the energy management problem. This second scenario tends to model a more intelligent and futuristic operational case, in which residential users participates actively in a demand-side management program and all the users have an electric vehicle available for the management of the LV Microgrid. To do this, a performance assessment of the final solutions provided by the long-term and short-term stage is presented.
- ✓ Chapter 7 presents some dynamic simulation carried on in GridLabD to assess technically the impact of the optimal solutions in the distribution system. This technical assessment includes an analysis of the voltage variation at the most remote nodes of the distribution system and an analysis of the voltage unbalance (VU) factor.
- ✓ Chapter 8 presents the main findings and conclusions of this thesis. Also, some topics for future works are summarized.

---

## 2 CONTROL AND ENERGY MANAGEMENT OF MICROGRIDS

---

The concept of microgrid was first introduced in the technical literature in [9], as a solution to implement many Smart Grid (SG) functions without requiring redesign or reengineering of all the distribution system [10], especially for the reliable integration of DERs, including Energy Storage Systems and controllable loads. This electric system can be defined as a cluster of micro-sources, ESSs and controllable loads, which presents itself to the grid as a single entity, that can operate in grid-connected mode or isolated from the main grid [11]. The MGs can provide multiple benefits to the actual electric power systems, such as reducing carbon emissions, increasing power quality and reliability, reducing line losses, increasing efficiency, allowing a high penetration of renewable energy systems (RES) and electric vehicle (EV) technologies, and postponing investments in new transmission and large-scale generation systems [11]–[13].

Based on this, important efforts have been undertaken by the energy sector, in order to develop appropriate technologies and techniques for the reliable and economic exploitation of renewable energy sources, and their integration into the power system. In Brazil, for instance, the Brazilian Electricity Regulatory Agency (ANEEL) has published recently the 482/2012 resolution, which establishes the technical and commercial regulations for small distributed generation units connected to the low voltage network, including residential PV arrays [14]. This resolution aims to reduce the barriers to the interconnection of small-scale distributed generation in low voltage networks, and increase the installed capacity of renewable generation systems, such as solar and wind systems [15].

A typical LV microgrid is shown in Figure 1. In general, a low voltage (LV) MG comprises small distributed generators (DG) with power electronic interfaces, ESSs, critical and non-critical loads and a control infrastructure composed of micro-source controllers (MSs), load controllers (LC) and a Microgrid Central Controller (MGCC), coupled to the medium voltage (MV) grid through the Point of Common Coupling (PCC). The MGCC is commanded by the Energy Management System (EMS), responsible for long-term economic operation, short-term dispatch, control of dispatchable units and security operation, among others [16]. Meanwhile, the MSs are responsible for stability operation of all generation's units and must autonomously respond to system changes without requiring information or controls signals from the MGCC, the static-switch or loads [9]. This is mainly because in a MG with many micro-sources, fast communication between sources is impractical and reduce peer-to-peer operation concept. The MSs are usually implemented into the inverters control logic. The main function of the LC is to disconnect non-critical loads in case of low generation aiming to maintain power balance and voltage and frequency stability.

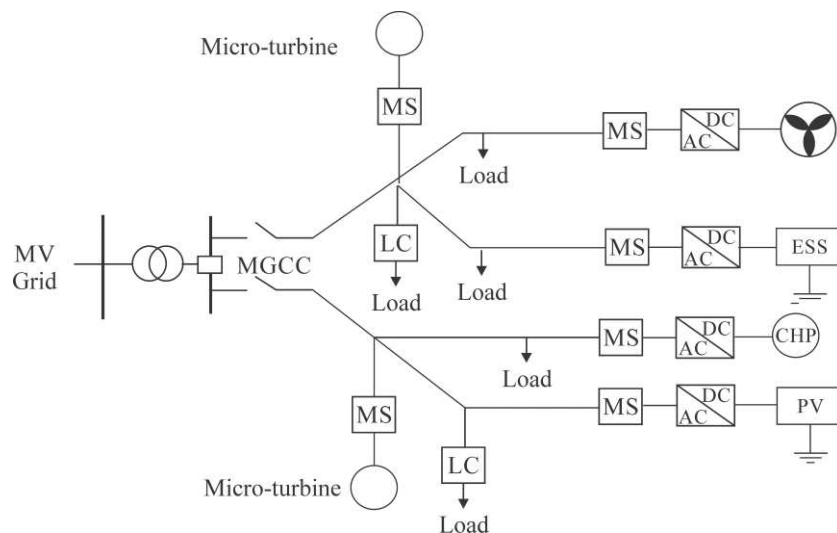


Figure 1. Basic structure of a Low Voltage Microgrid

One of the most important issues in the process of integration of MG is the control and management of dispatchable units in conjunction with non-dispatchable RES, like wind and solar systems, which are characterized by an unpredictable behavior. Considering this, it is clear that this complex electric system requires an entity capable of controlling DG units, ESSs and loads, aiming to optimally operate under some electric, environmental and economic objectives.

In this master dissertation it is proposed a hierarchical control structure composed of three control levels. The most important level correspond to the second one, denominated Energy Management System (EMS) which function is based on the solution of two optimization problems, known as Unit Commitment (UC) and Economic Load Dispatch (ELD) problems. In this chapter it is presented a general hierarchical control structure to operate a LV MG. Also, the main characteristics of an EMS are presented. Finally, a short State-of-the-Art is included.

## **2.1 HIERARCHICAL CONTROL**

The microgrid's control system is responsible for voltage and frequency regulation, proper load sharing, DER coordination, re-synchronization with the main grid, power control and optimization of operational cost [17]. Since MGs can operate connected to the main grid and in stand-alone mode, it requires a different control approach compared to those actually applied to conventional power systems [18], [19], mainly because [4]:

- The steady-state and dynamic characteristic of DER units, especially electronically coupled units, are different from conventional turbine-generator units.

- The degree of unbalance could be significant due to the presence a non-balanced loads.
- Most of the generators units, especially in MGs with high penetration of renewable generation systems, can be non-controllable sources, e.g. wind and photovoltaic systems.
- Short- and long-term ESSs can play a major role in control and operation, especially in the transition between the connected and stand-alone mode of operation.
- A MG is designed to provide a high and pre-specified power quality level.

In grid connected mode, the frequency and voltage at the PCC are defined by the MV grid. On the other hand, in the standalone mode, the MG operates as an independent and isolate entity, thus voltage and frequency must be fully controlled by DERs units, meanwhile a central control strategy determine the operation set points of all DER units to control power balance and guarantee power quality constrains.

Based on their interface with the electric grid, DERs units can be classified as conventional (or rotatory units) and electronically coupled units, which utilize power electronic converters to coupling with the AC electric system [4]. One of the most important features of the electronically interface source is their capability for fast dynamic response, but low tendency to maintain frequency. In a scenario with high penetration of electronically coupled units, it may occur excessive voltage rise, faults level, may increase harmonic distortion and stability problems may arise if it is not applied an adequate control strategy [20]. Thereby, to successfully integrate DERs units in the power system, many technical challenges must be overcome to ensure that high levels of efficiency and reliability will be fully harnessed. In this sense, some of the main challenges are related to [21], [22]:

- Coordinated control of a large number of DERs with probably conflicting requirements.
- Schedule and dispatch of units under supply and demand uncertainty, and determination of appropriate levels of reserves.
- Reliable and economical operation of MG with high penetration levels of intermittent generation, especially in the stand-alone mode of operation.
- Design of appropriate Demand Side Management (DSM) schemes to allow customer to react to the grid needs.
- Reengineering of the protection schemes at the distribution level to account for bidirectional power flows.
- Develop new voltage and frequency control techniques to account for the increase in power electronically interface units.
- Management of instantaneous and real-time active and reactive power balances, power flows and network voltage profiles.

Different approaches have been proposed for microgrid's control, including Decentralized control [23]–[25], Hierarchical and Centralized control [3], [26] and Expert Systems or Fuzzy Systems controls [7], [27]. In the Hierarchical and Centralized control structure, three levels of control has been already proposed [17], [18], [28], [29], each one with its own functionalities and objectives. The adoption of a hierarchical and centralized control structure become more interesting when it is analyzed the different processing time required to execute two of the main process to control a MG: (1) a fast dynamic control of voltage and frequency in the DER units aiming to maintenance of system's stability, and (2) a slower dynamics in the long-term economic dispatch. However, some of its characteristics make it difficult to

support plug-and-play characteristics, increasing the difficulty to introduce new DER units once the system is in operation. In addition, this central controller does not allow to develop the peer-to-peer concept, mainly because the control and management functions will depend of one central control entity [3], [28].

In Figure 2 it is shown the hierarchical control structure proposed. The main advantage of this hierarchical structure is the cooperation between the EMS and others levels of control aiming to achieve all controls and operations objectives. This centralized control structure is composed of three different levels: (i) the primary, (ii) the secondary and (iii) the tertiary control level. The idea behind using three different control levels is that each of them operates with its own speed of response (processing time) and infrastructure requirements. All the three control levels are briefly discussed as follows.

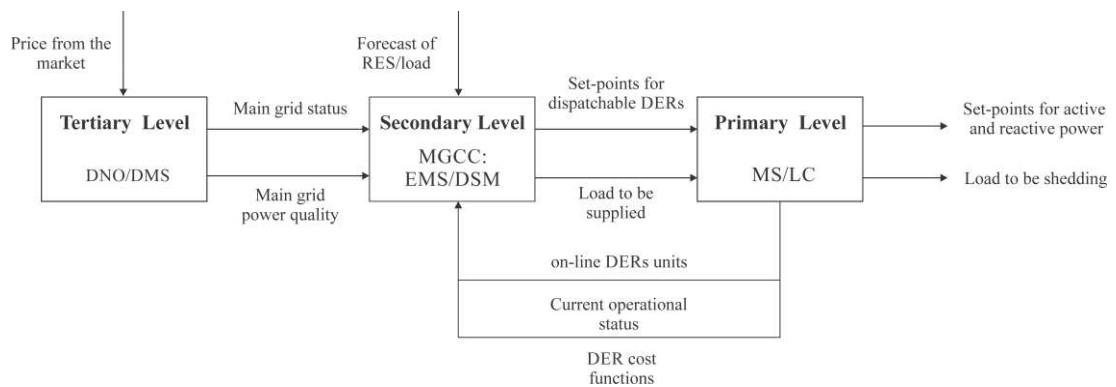


Figure 2. Information exchange between the primary, secondary and tertiary control level.

### 2.1.1 PRIMARY CONTROL

The primary control corresponds to the control with the fastest response, capable to respond to suddenly changes in loads and in the energy provided by the RESs. The main objective of this level is to control voltage and frequency in real-time operation, according to the operational set-points provided by the secondary control (EMS). Within their functions it

can be found: islanding detection, maintaining voltage and frequency stability, provide active and reactive power sharing controls [30], among others. This primary control is implemented at the local controllers (LC) of DG units, and it can operate autonomously, without communication data from others DERs units.

In conventional grids, when an power unbalance occurs, it is instantly balanced by the inertia in the rotatory generators, and as consequence a change in the frequency is observed [10]. However, this control is not feasible for MGs due that most of the DG sources are based on renewable energy, which are inertia-less and requires an electronically inverter to be suitable to a direct connection to the electrical network. Based on this, the control of all inverters is a main concern in the MG's operation, being found two different control strategies: PQ droop control and Voltage Source Inverter (VSI) control [31].

In the PQ droop control the inverter is used to supply a given active and reactive power (set-point provided by the EMS). In this control strategy, the inverter operates injecting into the grid the power available at its inputs. As it can be seen in Figure 3, a power variation in the micro-source induces a DC-link voltage error, which is corrected via a PI controller by adjusting the magnitude of the active and reactive current to balance voltage and frequency [31], [32]. One of the advantages of this control is that no communication is required, allowing the implementation of a decentralized primary control level.

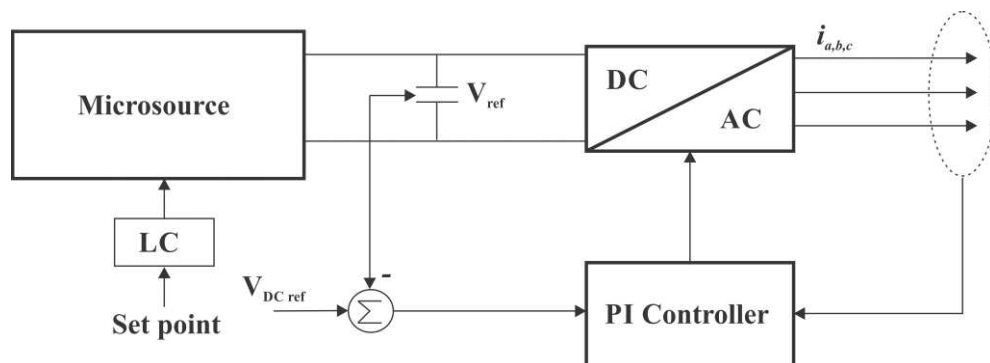


Figure 3. PQ inverter controller structure.

In the VSI control, the inverter is controlled to feed the load with pre-defined values for voltage and frequency, acting as a voltage source. Depending on the load, the VSI active and reactive power output is defined. The VSI emulated the behavior of a synchronous machine, thus controlling voltage and frequency on the AC system through droops [31]. The basic principle of droop characteristic is that, frequency decreases with the increase of output active power, and voltage amplitude decreases with increase of reactive power [28], as is shown in Figure 4.

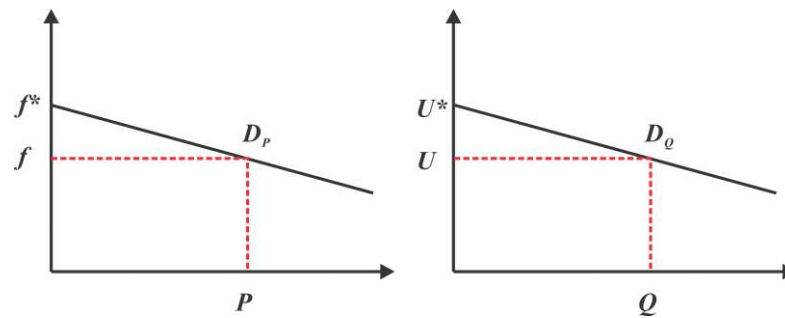


Figure 4. Frequency/active power and voltage/reactive power droop characteristics [28].

Although control approaches of stand-alone and grid connected mode are well known and described in literature, microgrid's control require a new approach capable to manage the transition between these two operation modes. According to [33], two approaches can be developed: (1) in the first approach it can be developed a method to switch from one mode of control to other when necessary, and (2) in the second approach it is possible to merge the two control algorithm in a unique one, based on the fact that one mode of operation could be seen as a disturbed expression of the other, increasing the reliability of the control scheme.

In this sense, two control schemes have been proposed to control electronically power interface units: a Single Master Operation (SMO) and a Multi-Master Operation (MMO) [32]. In the SMO an inverter acting as a master is controlled as a VSI and it is used as a voltage and

frequency reference, emulating that the main grid and all the others inverters are operated in PQ mode. On the other hand, in the MMO approach it is used several inverters in a VSI mode with pre-defined frequency and voltage characteristics. In this approach the secondary control can modify the operational set-points to regulate frequency and voltage.

### **2.1.2 SECONDARY CONTROL**

Generally, the secondary control level, in the control proposed structure, is more known as Energy Management System (EMS) (or Power Management System, PMS). This control level is the main focus of this master dissertation, and it will be further discussed in Section 2.2.

### **2.1.3 TERTIARY CONTROL**

The main function of the tertiary control is to coordinate the operation with the MV grid and the Distribution Network Operator (DNO), communicating to the secondary control information such as power quality required at the PCC, possible islanding operation due to maintenance, possible instability and low power quality in the main grid, etc. This coordination with the DNO is mainly done through the Distribution Management System (DMS).

As part as an incoming future, the tertiary control will have the objective of coordinating its operation with multiples MGs, all aggregated in a Virtual Power Plant (VPP). In this sense, the VPP coordinator will be responsible for supervision, balancing control, ancillary services and market interface of all aggregated MGs aiming to improve economic long-term dispatch and operation [34].

## 2.2 ENERGY MANAGEMENT SYSTEMS

An EMS can be defined as a comprehensive automated and real-time system used for optimal scheduling and management of energy, providing data management, grid information, monitoring, control and dispatch of units [3], [4], [35]. To provide an optimal schedule, the EMS requires information about load consumption, RES forecast, price of electricity and heat, cost of fuel, environmental regulations, etc. This will allow the microgrid to be properly operated in order to guarantee benefits such as enhancement of power quality and reliability of supply to the customers, reduction of network losses and emissions, and efficiency increase [20]. Some of the main functions of an EMS are [2], [36]:

- Maximize customer's power availability, increase system's reliability.
- Minimize energy losses, operational cost, green gas emissions, and fuel consumption.
- Maximize the use of renewable energy and minimize the energy purchased outside the MG.
- Determine the power set points of DER units to balance power, control voltage and frequency.
- Resynchronization of the microgrid with the main grid, if required.

In Figure 5 some common inputs and outputs of an EMS are shown. Input information such as forecasting of non-dispatchable generation, forecasting of electrical/thermal load, forecast of energy price, State-of-Charge (SOC) of the ESSs, operational limits, security and reliability constraints and information provided by the main grid, is used to estimate and provide operational set points and load management to the MSs and LCs. Accordingly, the

EMS needs to provide output information at the utility level (import/export power from/to the main grid), at the DER level (operational set-points) and at load level (shedding schedule managed by the Demand Side Management (DSM)) [37].

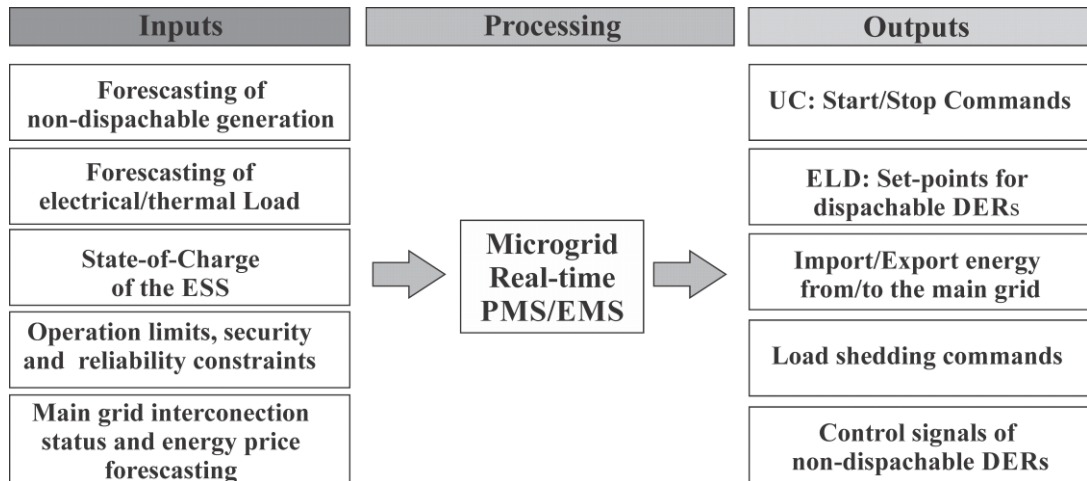


Figure 5. Information flow (inputs/outputs) of a general EMS.

Once all input information is collected, an optimization algorithm can be executed to obtain the optimal scheduling by solving an UC problem and an a ELD problem [38]. In general, UC is the process of deciding when and which generating units needs to start-up or shut-down subject to load and generation forecast over a planning horizon and taking into account running/stop time constrains of each unit and ramping time limit. Meanwhile, ELD is the process of estimating power outputs schedule for the on-line units [39]. Both problems can be considered as a very challenging optimization problem [26], [40], especially in MGs with high renewable energy penetration, in which the search space is large, exists uncertainty in some variables and it is necessary to consider some strict operational constrains [41], [42].

In literature, the most extended structure for the EMS uses a decomposition approach combined with a Model Predictive Control (MPC) or Rolling Horizon (RH) strategy. This

strategy allows the solution of the UC and ELD problems within a pre-defined time window, in order to make the EMS more suitable for real-time applications [26], [43], [44].

In general, this decomposition approach is composed of two stages of scheduling: a long-term and a short-term optimization stage. In the long-term stage, is considered an optimization horizon of one or two days in discrete time-steps, and it is solved an UC and ELD problem, obtaining an optimal schedule of the dispatchable units considering the constraints that have a high impact in the lifecycle and the operation of the generation systems.

Once the long-term schedule is obtained, the short-term stage considers only the on-line units to solve an ELD problem for the next operation hour in short time-steps, looking to manage active and reactive power balance due to suddenly variations in loads and in the RES generation, increasing the robustness of the EMS to manage uncertainty. In this MPC approach, only the first control action of the long-term schedule is implemented, as shown in Figure 6. Then, the EMS recalculates the operation strategy using the current operational status of the microgrid as the initial state, repeating this procedure continuously. One of the most important advantages of this operational strategy is that the EMS is more robust to manage the forecast error of the load demand and RES generation.

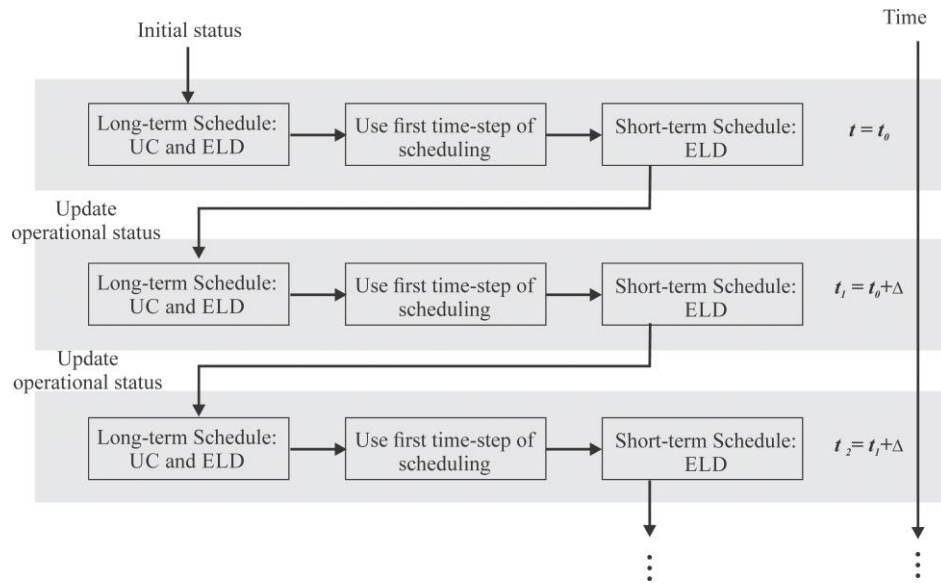


Figure 6. MPC/RH Strategy in an EMS.

As discussed before, to obtain an optimal schedule the EMS needs to solve two complex optimization problems. In literature, the current trend to solve the energy management problem corresponds to metaheuristics, mainly because this optimization techniques can obtain highly accurate solutions regardless of the type of evaluation function or constrains [45]–[47]. Inside the metaheuristics, the evolutionary algorithms such as Genetic Algorithms (GA) are the most preferred because it can handle the nonlinear, non-convex and non-smooth characteristics of the energy management problem [46], allowing to obtain near-optimum solutions in a low computational time. On the other hand, if the energy management problem is formulated as a multi-objective optimization problem, evolutionary algorithms can provide in one execution a set of solutions of the Pareto front, in contrast with the classical solutions techniques. However, if metaheuristics are not properly customized for the specific problem, they can perform poorly too.

In particular, in [48] it is developed an EMS for a standalone microgrid with RESs, a diesel generator and a lead-acid battery system for a remote island in China. In the proposed

optimization model it is included the battery Life Loss Cost (LLC), the operation and maintenance cost, fuel cost and environmental cost and it is used the Non-dominated Sorting Genetic Algorithm II (NSGA-II), considering as optimization objectives the operational cost and the battery LLC, finding results aiming to operate the microgrid with a low generation cost while maintaining the batteries in healthy working conditions, considering that the lead-acid battery requires a high investment due to transportation cost. However, in this work is a simplified model of the diesel generator is considered. Also, heuristic rules are defined to dispatch the diesel generator based on the current value of the SOC of the battery system.

In [49] it is proposed and developed a centralized EMS for a microgrid using a RH strategy considering the EMS as a finite state machine. To define the transitions rules for the next stage are defined priorities for the generation systems, given the higher priority to the wind system, then the PV system, and the lowest to the fuel-cell generation system. As a quality and reliability measure it is used the Loss of Power Supply Probability (LPSP) criteria to define the probability that the load cannot be supplied by the generation systems considering operation in islanding mode. The main drawback of this EMS state-machine is that the wind and PV generation system are switched off in some states given more priority to the batteries or the fuel-cell system, reducing the benefits of the available renewable resources.

Considering the execution time of the optimization algorithm and taking into account that the implementation of the EMS is envisioned to be in real-time, in [50] it is introduced and validated experimentally an EMS based on a new metaheuristics denominated as Multi-period Gravitational Search Algorithm (MGSA) for a microgrid composed of a PV and wind system, an energy storage system and a diesel and micro-turbine generator, taking as the optimization objective the operational cost. The performance of the algorithm is compared with classical PSO showing promisor results related to the execution time proving to be a feasible

implementation of a real-time EMS. Similarly, in [51] the EMS proposed is intend to operate in real-time, defining an control scheme depending on the wind forecast generation and the current SOC of the ESS. Although these EMS based on heuristic algorithms do not guarantee a global optimum, generally they have a low execution time, what make them a more suitable algorithm to implement in a real-time environment. Related to metaheuristics, other research papers have implemented algorithms such as Particle Swarm Optimization (PSO) [52] and Chaotic Differential Evolution [53]. In almost all of these research papers, it is not evaluated technically the impact of the management in the electric grid. This is due that simulations are performed using simplified models and the distribution feeder is not considered in the optimization problem.

Aiming to increase the robustness of the EMS and reduce its dependence of the forecast error of the load demand and RES generation, in [54] it is developed and EMS capable to handle uncertainty for a microgrid composed of residential loads, RES, a storage facility, connected to the main grid via a transformer. The objective of the EMS developed is to plan the battery schedule in order to increase the utilization rate of the battery during high demand and the utilization rate of the renewable generator for local use. To accomplish this, it is used a MPC framework considering noise disturbance and variation in the renewable generator output observing that the EMS can handled this disturbances satisfactorily. On the other hand, in [55] the uncertainty is handled using Robust Optimization (RO) and Prediction Intervals (PIs) of the RES generation and load demand obtained analyzing available statistical data.

Concerning the classical optimization techniques, as the energy management problem is a Mixed-Integer Non-Linear Programing problem (MINLP), in [26], [44] it is used CPLEX software to solve the optimization problem. Also, it is proposed an MPC framework composed of a short- and long-term optimization stage for both research works. The main

contribution of [26] is related to the highly detailed mathematical formulation of the energy management problem including a detailed modeling of the distribution system. Similarly, in [43] the energy management problem is proposed as an MINLP and is used CPLEX as the optimization tool. Here, the EMS is developed to control a diesel generator, an ESS, a water supply system and loads, managing uncertainty in the forecasted load and generation using an RH strategy.

### **2.3 STRUCTURE OF THE PROPOSED ENERGY MANAGEMENT SYSTEM**

Considering all the previous discussion, in this section it is presented the structure of the proposed Energy Management System (EMS) proposed, shown in Figure 7. This EMS is framed in a three-level control structure, as previously described, composed of two optimization stages: a long-term and a short-term stage. The long-term stage has to schedule all the dispatchable units for the next 24-h in time-steps of 15-min. To do this, the long-term stage state the energy management problem as a UC and ELD problem, deciding when to start-up or shut-down the dispatchable units and the charging/discharging schedule of the ESSs. Once these schedules are defined, the long-term stage has to define the power output profile of all the dispatchable systems considering load consumption and the RES generation.

Considering that one of the most important function of an EMS is to provide operational set points of DERs units and ensure a power balance at the PCC, an EMS require a fast and accurate response. Based on this, the main function of the short-term stage is to re-calculate the power output of all dispatchable units to match microgrid's generation with load consumption. For this, the short-term stage has to solve an ELD problem in time-steps of 5-min, considering the UC and the charging/discharging schedule of the ESS provided by the long-term optimization stage. As in the MPC/RH strategy, this management strategy is

applied continuously, using the long-term state to define the next day schedule, once are updated the new load consumption and RES generation. The short-term stage runs on-line, operating every 5-min. Here it is not considered a fault scenario, where a unit can unexpectedly shut-down or the grid become unavailable.

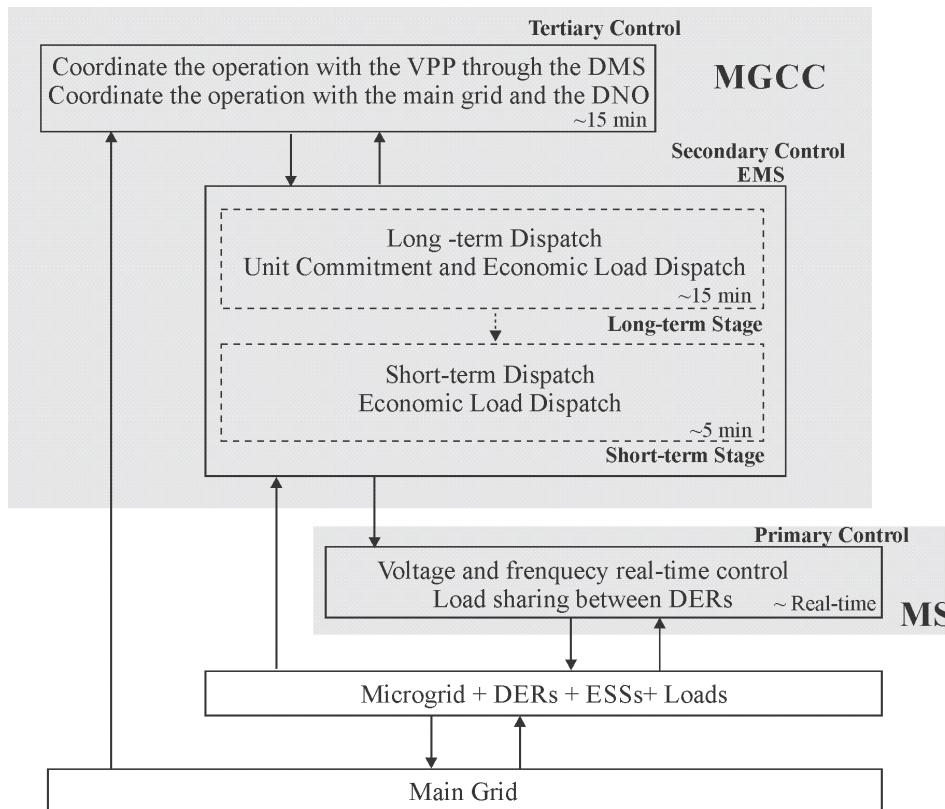


Figure 7. Proposed Hierarchical Control Structure of a LV Microgrid.

The idea behind the use of these two optimization stages, developed to solve the energy management optimization problem, is to perform this task with the lowest computational time, trying to achieve energy management in real-time, and reduce the impact of the forecast error. The real-time processing is required to ensure that power balance is maintained during real-time operation at the PCC. Thus, if load or generation varies from the expected value, the EMS must deviate from the original optimization schedule and estimate new operational set points, communicating to the primary control the new operation scheme.

Although it is not the focus of this thesis to develop a forecast module for the proposed EMS, it is important to highlight that the accuracy of the forecast load demand and RES generation plays an important role in the energy management problem [56]. If load or RES generation values are underestimated the grid operation and stability can be in risk, due to the insufficient active power reserve or low capacity to respond due to the low number of on-line units. On the other hand, if load or RES generation values are overestimated, too many units will be operating, increasing operational cost.

For the proposed EMS, the forecast module has to provide load consumption and RES generation with two different resolutions, a 15-min resolution for the long-term stage and 5-min resolution for the short-term stage. One important difference between load and weather forecast is that load forecast has a strong dependency on behavioral patterns, which are tightly linked to loads characteristic and calendar data, while weather forecast has a more stochastic behavior [40]. Due to this, load and weather forecast accuracy is limited and prediction errors achieved by the best forecast solutions are in the order of 5 to 15%, depending on the resolution and the time-window prediction [40]. Therefore, an EMS should be robust against these forecast errors.

The main contribution of this master dissertation is related to the hierarchical framework developed for the Energy Management System which re-dispatches the controllable units and the energy storage systems to reduce the impact of the forecast error. Also, to state and solve the energy management problem, it is proposed a disaggregation approach where the binary variables are defined by a MOGA and the continuous variables solving a QP problem using MATLAB as solver. Finally, a more detailed model for the diesel generator was considered. In this model, operational constraints as down-rate and up-rate limit and total in-line and off-line operational time were included in the optimization problem.

---

## 3 SYSTEM MODELING AND STATEMENT OF THE PROBLEM

---

### 3.1 RESIDENTIAL FEEDER

As previously discussed, the LV microgrid considered in this work was developed in GridLabD software. GridLabD is an open-source power distribution system simulator, developed by the Pacific Northwest National Laboratory (PNNL) [57], which allows users to study and quantify the impact of distributed generation technologies in conventional power systems. Within the most interesting features about GridLabD it can be found: *(i)* the user is allowed to include its own weather data and quantify the operation of the system under on-site weather conditions, *(ii)* it can be analyzed three-phase unbalanced distribution systems, *(iii)* it can be studied new control load algorithms (demand response).

In addition, GridLabD includes a highly detailed residential model, in which the operation schedule of equipment such as refrigerators, water heaters, microwaves, lights, freezers, and the operational set-points (cooling and heating set-points) of HVAC systems can be specified deterministically or randomly [58]. In this thesis the operational schedule of all the equipment are randomly defined.

The considered microgrid corresponds to a residential LV feeder composed of 45 residential consumers connected to the MV grid through three single-phase distribution transformers, as it can be seen in Figure 8. The LV microgrid also include three wind turbines and a diesel generator, both connected to the MV grid through a three-phase MV transformer.

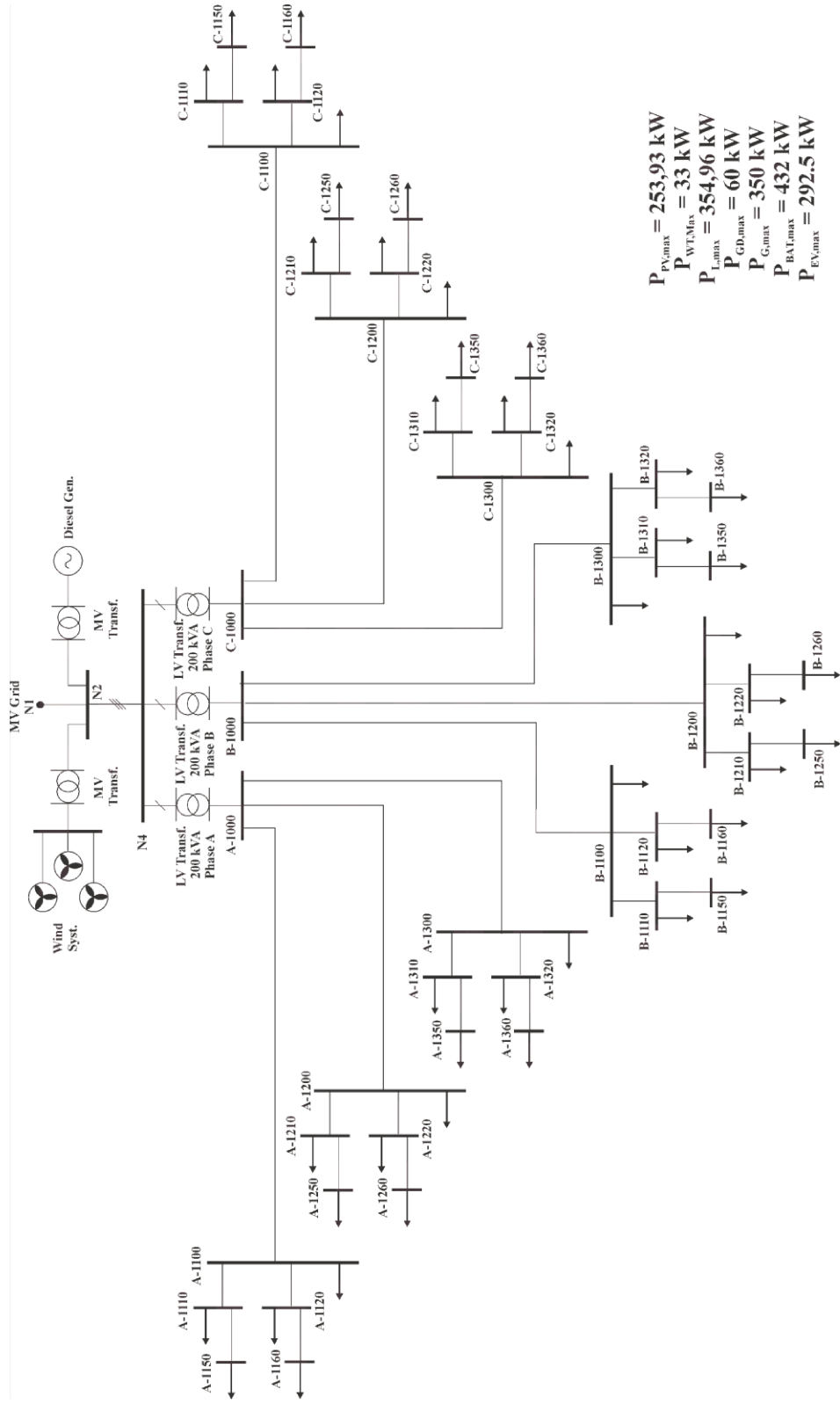


Figure 8. Residential LV microgrid developed in GridLabD.

All the parameters used in GridLabD to define the electric and physical model of transformers and lines are described in Appendix A.

In this LV microgrid, every residential consumer has integrated its own battery and solar system coupled to an inverter. Also it is considered an Electric Vehicle (EV) for every consumer. Aiming to simulate the random behavior in the three single-phase distribution transformers, the residential consumers are classified in five different types depending on its consumption and PV nominal installed capacity.

Considering this, in Table 1 it is shown some characteristics that define the level of consumption of a residential consumer, such as floor area, heating and cooling set-point and nominal capacity of the solar system. The Type 5 house corresponds to the consumer with the lowest consumption and the lowest PV nominal installed capacity, and the Type 1 house corresponds to the consumer with the highest consumption and the highest PV nominal capacity. Furthermore, it is added a ZIP load model in for every residential consumer to model an appliance commonly used in Brazil, the electric shower.

Table 1. Characteristics of the five type of residential consumers implemented in GLD.

House Type	Floor area [m <sup>2</sup> ]	Heating set-point [°C]	Cooling set-point [°C]	Power Inverter [kW]	Photovoltaic System Area [m <sup>2</sup> ]
Type 1	280	16	20	15	80
Type 2	260	17	23	15	80
Type 3	240	18	23	13	70
Type 4	200	18	24	13	70
Type 5	180	20	24	10	50

According to GridLabD, the structure of a house is shown in Figure 9, within it, an inverter to properly connect the solar system, the batteries to storage electrical energy, the EV and the thermodynamic and electric model of the house are included. In the node where the house and

the inverter are connected, triplex-line meters (TM) to properly measure variables such as voltage, current, and active power are installed.

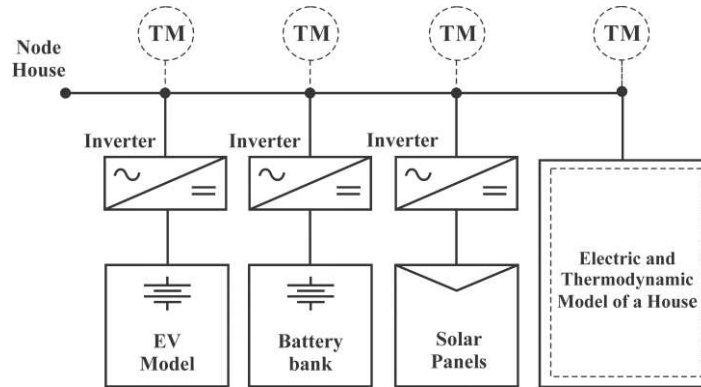


Figure 9. Structure of a house in GridLabD, composed of four Triplex Meter (TM), a solar system, a battery bank, an EV and a thermodynamic and electric model.

### 3.2 PV AND WIND SYSTEM

For the PV system, it is assumed that this always operates at the maximum power point, which is a reasonable assumption, for most of grid connected PV inverters operating with Maximum Power Point Tracking (MPPT) control, and therefore its operation is independent of the EMS. To model the PV generation Equation (1) is used.

$$P_{PV}^t = A_s \cdot \eta_{STC} \cdot \eta_{INV} \cdot G_A^t \cdot \left[ 1 + K_p \cdot (T_A^t - T_{STC}) \right] \quad (1)$$

Where,  $A_s$  corresponds to the area of the PV system in  $m^2$ ,  $\eta_{STC}$  is the efficiency of the PV panel at the Standard Test Conditions (STC),  $\eta_{INV}$  is the inverter's efficiency, assumed to be constant;  $G_A^t$  corresponds to the irradiance in  $W/m^2$  at hour  $t$ ,  $K_p$  is the temperature coefficient for the active power,  $T_A^t$  is the ambient temperature in K, and  $T_{STC}$  corresponds to the STC temperature in K.

Similar to the PV system, the power produced by the wind turbine is independent of the EMS. To model the wind system generation a piecewise power curve model is used to give the output power as a function of the wind velocity, as is shown in Equation (2).

$$P_{U,WT}^i = \begin{cases} 0 & v \geq v_{CO} \\ P_N & v_N \leq v \leq v_{CO} \\ p_1 \cdot v^3 + p_2 \cdot v^2 + p_3 \cdot v + p_4 & v \leq v_N \end{cases} \quad (2)$$

Where,  $P_{U,WT}^i$  corresponds to the active power output of the wind turbine in kW,  $v_{CO}$  is the cutoff velocity in m/s,  $v_N$  is the nominal velocity in m/s, and  $p_1, p_2, p_3, p_4$  correspond to the active power coefficients of the power curve model. The values of the active power coefficient are obtained after a characterization of the wind turbine generation model used by GridLabD.

The parameter values used for the PV and wind system generation model are listed in Table 2. As previously discussed, every residential consumer has its own PV system. However, for the power balance, an aggregated model considering the total PV system area is used. The maximum output power of the aggregated PV system ( $P_{PV,Total}$ ) is approximately 253.93 kW, estimated at STC conditions.

Table 2. Parameters of the PV and Wind system model.

Parameter	Value	Units
$A_s$	1485	m <sup>2</sup>
$P_{PV,max}$	253,93	kW
$\eta_{STC}$	0.18	-
$\eta_{INV}$	0.95	-
$K_p$	-0.000233	K/W
$T_{STC}$	248.16	K
$v_{CO}$	10	m/s
$P_{U,WT}^i$	11	kW

$P_{WT,max}$	33	kW
$v_N$	5	m/s
$p_1$	0.050037	kW/(m/s) <sup>3</sup>
$p_2$	0.36592	kW/(m/s) <sup>2</sup>
$p_3$	-0.52584	kW/(m/s)
$p_4$	0.068178	kW

### 3.3 ENERGY STORAGE SYSTEM

The inclusion of the energy-storage system in the microgrid can mitigate the impact of the uncertainty of renewable energy sources. Generally, batteries are the most common choice for short-term storage. However, for longer-term storage of energy, their application might be inappropriate owing to their low energy storage density and unavoidable self-discharge [59].

For the microgrid considered, the ESS is composed of a bank of lead-acid batteries distributed through the distribution feeder located at every consumer's house. This type of battery corresponds to the more common choice in PV-Battery systems. The main function of the ESS is to reduce the variability of the RES. Also, the battery system is used to store energy when the local generation is higher than the load demand. This energy is then used in periods when the energy has a higher cost.

The battery model used allows to estimate the output power as the difference between the stored energy of two consecutive time-steps, measured by the State of Charge (SOC), as is shown in Equation (3).

$$SOC^t = SOC^{t-1} + \frac{P_{BAT}^t \cdot \Delta t \cdot \eta_{BAT}}{C_{BAT} \cdot V_{BAT}} \quad (3)$$

Where,  $SOC^t$  corresponds to the SOC of the ESS at time  $t$ ,  $\eta_{BAT}$  is the battery efficiency,  $C_{BAT}$  is the nominal capacity of the battery bank in  $Ah$ , and  $V_{BAT}$  corresponds to the nominal voltage of the battery.

In this model it is assumed that if  $P'_{BAT} > 0$ , then the battery is in charging mode, and if  $P'_{BAT} < 0$  the battery is in discharging mode. To increase the lifespan of the battery, the available battery bank capacity is limited according to the manufacturer specification, as in Equation (4).

$$SOC_{\min} \leq SOC^t \leq SOC_{\max} \quad (4)$$

Where,  $SOC_{\min}$  and  $SOC_{\max}$  correspond to the minimum and maximum values allowed for SOC. Also, it is assumed that the maximum input/output battery power is equal to 20% of the nominal capacity ( $C_{BAT}$ ), defined in Equation (5) as the down-rate ( $RD_{BAT}$ ) and up-rate ( $RU_{BAT}$ ) constrains. Hence, the battery power ( $P'_{BAT}$ ) is limited by a minimum ( $P'_{BAT,\min}$ ) and a maximum power ( $P'_{BAT,\max}$ ), as is shown in Equation (6).

$$RU_{BAT} = RD_{BAT} = 0.2 \cdot V_{BAT} \cdot C_{BAT} / \Delta t \quad (5)$$

$$P'_{BAT,\min} \leq P'_{BAT} \leq P'_{BAT,\max} \quad (6)$$

The minimum power ( $P'_{BAT,\min}$ ) is limited by the available energy stored in the battery and the  $SOC_{\min}$  restriction. Similarly, the maximum power ( $P'_{BAT,\max}$ ) is limited by the  $SOC_{\max}$  restriction, as is shown in Equation (7).

$$P'_{BAT,\min} = -\max \left\{ 0, \min \left[ RU_{BAT} / \Delta t, V_{BAT} \cdot C_{BAT} \cdot \left( (SOC^{t-1} - SOC_{\min}) / \Delta t \right) \right] \right\} \quad (7)$$

$$P_{BAT,max}^t = \max \left\{ 0, \min \left[ RD_{BAT} / \Delta t, V_{BAT} \cdot C_{BAT} \cdot \left( (SOC_{max} - SOC^{t-1}) / \Delta t \right) \right] \right\}$$

To measure the costs associated with the battery system usage, the Life Loss Cost (LCC) is calculated through Equation (8). According to [48], the LLC can be defined in terms of the  $SOC$  and the initial investment cost ( $C_{ini}$ ) of a battery unit, where  $k$  and  $d$  corresponds to empirical parameters, estimated by [48] for a lead-acid battery type.

$$C_{Life}^t = \frac{N_{BAT} \cdot C_{ini}}{390} \cdot \left[ k \cdot (SOC^t)^2 + d \cdot SOC^t \right] \quad (8)$$

All the values used for the battery model are listed in Table 3. As the ESS is distributed through the distribution feeder, an aggregated model is used for all batteries for the power balance problem. The maximum output power of the ESS in the aggregated model ( $P'_{ESS,Total}$ ) is limited by Equation (5), namely 432 kW for every time-step ( for the long-term stage).

Table 3. Parameters of the battery model.

Parameter	Value	Units
$\delta$	0.005	-
$\eta_{BAT}$	0.98	-
$C_{BAT}$	400	Ah
$V_{BAT}$	120	V
$SOC_{min}$	0.5	-
$SOC_{max}$	1	-
$N_{BAT}$	45	-
$RU_{BAT}$	9.6	kW
$C_{ini}$	500	USD\$
$k$	-1.6	-
$d$	2.1	-
$P'_{ESS,Total}$	432	kW

### 3.4 DIESEL GENERATOR

In grid-connected microgrids, the diesel generator can be used to provide ancillary services, increase reliability of the grid or support local generation. To model the fuel consumption of the diesel generator (l/h), the information provided by the manufacturer for a 60 kW unit is used and is shown in Table 4.

Table 4. Fuel consumption of a 60 kW diesel generator unit

Nominal Power [kW]	60
Fuel consumption at ¼ Load (l/h)	6.81
Fuel consumption at ½ Load (l/h)	10.98
Fuel consumption at ¾ Load (l/h)	14.38
Fuel consumption at Full Load (l/h)	18.17

The fuel consumption is modeled as a quadratic function, as shown in Equation (9), where  $FC(\cdot)$  corresponds to the fuel consumption in l/h as a function of the output power  $P_{GD}^t$ . In order to increase the generator lifespan, the EMS needs to consider operational constraints such as minimum and maximum capacity, as is given by Equation (10), where  $P_{GD,\min}$  corresponds to the minimum output power and  $P_{GD,\max}$  to the maximum output power,  $U_{GD}^t$  is the operational state of the diesel generator at time  $t$ , where  $U_{GD}^t = 0$  means that the diesel generator is off-line, and if  $U_{GD}^t = 1$  means that the unit is on-line.

$$FC(P_{GD}^t) = g_2 \cdot (P_{GD}^t)^2 + g_1 \cdot P_{GD}^t + g_0 \cdot U_{GD}^t \quad (9)$$

$$P_{GD,\min} \cdot U_{GD}^t \leq P_{GD}^t \leq P_{GD,\max} \cdot U_{GD}^t \quad (10)$$

Also, the up-rate and down-rate limits given by Equation (11) are considered, and the continuous running/stopping time is given by Equation (12), where  $RD_{GD}$  and  $RU_{GD}$  are the

down-rate and up-rate limit of the diesel generator, respectively;  $T_{GD,ON}^t$  and  $T_{GD,OFF}^t$  corresponds to the total on-line and off-line operational time at period  $t$ , and  $MUT_{GD}$  and  $MDT_{GD}$  corresponds to the minimum running and down time. All the parameters for the diesel generator model are listed in Table 5.

$$RD_{GD} \leq P_{GD}^t - P_{GD}^{t-1} \leq RU_{GD} \quad (11)$$

$$\begin{aligned} [T_{GD,ON}^{t-1} - MUT_{GD}] [U_{GD}^{t-1} - U_{GD}^t] &\geq 0 \\ [T_{GD,OFF}^{t-1} - MDT_{GD}] [U_{GD}^{t-1} - U_{GD}^t] &\geq 0 \end{aligned} \quad (12)$$

Table 5. Parameters of the diesel generator model.

Parameter	Value	Units
$P_{GD,min}$	25	kW
$P_{GD,max}$	60	kW
$g_2$	-0.000422	1/(kW) <sup>2</sup>
$g_1$	0.28153	1/(kW)
$g_1$	2.74	1
$RD_{GD}$	10	kW
$RU_{GD}$	20	kW
$MUT_{GD}$	180	min
$MDT_{GD}$	120	min

### 3.5 DEMAND-SIDE MANAGEMENT

Demand Side Management (DSM) is an important function in energy management in microgrids, created to provide support to smart grid functionalities, reduce peak load, operational cost, power losses and improve efficiency [60]. In general, a DSM program involves actions carried out by the consumers to manage its electrical consumption, usually by shifting load or postpone its use, modifying the final load shape in the distribution system.

This is based on a response of a smart pricing scheme, power saving technologies, electricity tariff, monetary incentives and government policies to mitigate the peak load demand [61].

Different DSM has been proposed in literature, each developed based on specific load characteristics [62], [63]. For residential MGs, the control is applied at equipment level and two kind of load categories are commonly found [64]: (i) regular or non-controllable loads, which must be activated immediately at any time (as lighting, TV or computers), and (ii) burst or controllable loads, which operated for long time periods (as fridge, water heater, dryer or dishwasher). Considering the intrinsic characteristics of each equipment, it can be developed a load consumption schedule to optimize cost without causing discomfort to the consumer.

Considering that in GridLabD the operational schedule of all residential equipment are randomly defined, the DSM developed here does not control loads at equipment level. Instead, it is used the DSM proposed in [43], [65]. Thus, it is supposed that online signals are send to the consumers in order to modify its load consumption. The degree of modification is modeled by shifting coefficients  $S^t$ , which are defined by the EMS. Therefore, the load consumption can be defined as in Equation (13), where  $\tilde{P}_L^t$  correspond to the load demand in kW, after applying the DSM strategy and  $P_L^t$  is the expected load demand in kW.

$$\tilde{P}_L^t = S^t \cdot P_L^t \quad (13)$$

To take into account the maximum expected consumer response to the signals, which in a real operational case would depend on the consumer behavior, a maximum ( $S_{\max}$ ) and minimum ( $S_{\min}$ ) value for the shifting coefficients are defined using Equation (14).

$$S_{\min} \leq S^t \leq S_{\max} \quad (14)$$

Additionally, it is assumed that all the expected energy consumption has to be supplied during the day, as described in Equation (15). Finally, in this DSM it is not considered an explicit economic incentive for consumers and it is supposed that all residential consumers participate actively.

$$\sum_{t=1}^T S^t \cdot P_L^t \cdot \Delta t = \sum_{t=1}^T P_L^t \cdot \Delta t \quad (15)$$

### 3.6 ELECTRIC VEHICLE

The integration of Electric Vehicles (EV) into smart grids has been intensively studied during the last years [66]. These researches have been carried out into the concept of vehicle-to-grid (V2G), with EV batteries used as means of mass energy storage in the power grid [67]. This mean that EVs will be connected into the power system when they are not in use and batteries can charge during low demand times and discharge when power is in shortage, as common in peak time. However, this concept may arise other problems that needs to be addressed as the consumption and power quality impact of large EV penetration in the current electric grid, among others [68].

Related to the EV model used in this master dissertation, it will be considered the Nissan-Altra vehicle, which is composed of a Lithium-Ion (Li-Ion) battery, characterized by a high power and high energy density. The mathematical model for the EV battery used depend on the State-of-Charge ( $SOC_{EV}^t$ ), which gives the level of energy in the battery in each time-step. The  $SOC_{EV}^t$  of the EV considered can be modeled using Equation (16) when the EV is used for transportation purposes, where  $\gamma(v, C_i^s)$  is the amount of energy used in kWh, which depends on parameters as the velocity  $v$  in m/s and  $C_i^s$ , a seasonal coefficient [69].

$$SOC_{EV}^t = SOC_{EV}^{t-1} - \gamma(v, C_i^s) \cdot \Delta t \quad (16)$$

When the EV is connected to the power grid, the EV model for the battery is shown in Equation (17), where  $P'_{EV}$  corresponds to the value of charging or discharging power in kW and  $C_{EV}$  is the nominal capacity of the EV battery. It is assumed that the model in Equation (17) can be used to describe the charging and discharging process. Also, if  $P'_{EV} > 0$  the EV will be in charging process, and if  $P'_{EV} < 0$  the EV will be in discharging process. Finally, according to manufacturer, the  $SOC^t_{EV}$  should be limited to a minimum value, defined by the depth of discharge ( $DOD_{EV}$ ), given in Equation (18).

$$SOC^t_{EV} = SOC^{t-1}_{EV} + \frac{P'_{EV}}{C_{EV}} \cdot \Delta t \quad (17)$$

$$\begin{aligned} SOC_{EV,\min} &\leq SOC^t_{EV} \leq SOC_{EV,\max} \\ DOD_{EV} &= 1 - SOC_{EV,\min} \end{aligned} \quad (18)$$

In Figure 10 it is shown the real charging profile for the EV Nissan-Altra. Additionally, it is considered a maximum charging and discharging capacity, modeled using Equation (19). All the parameters for the EV Nissan-Altra model are listed in Table 6 [70].

$$-P_{EV,\max} \leq P^t_{EV} \leq P_{EV,\max} \quad (19)$$

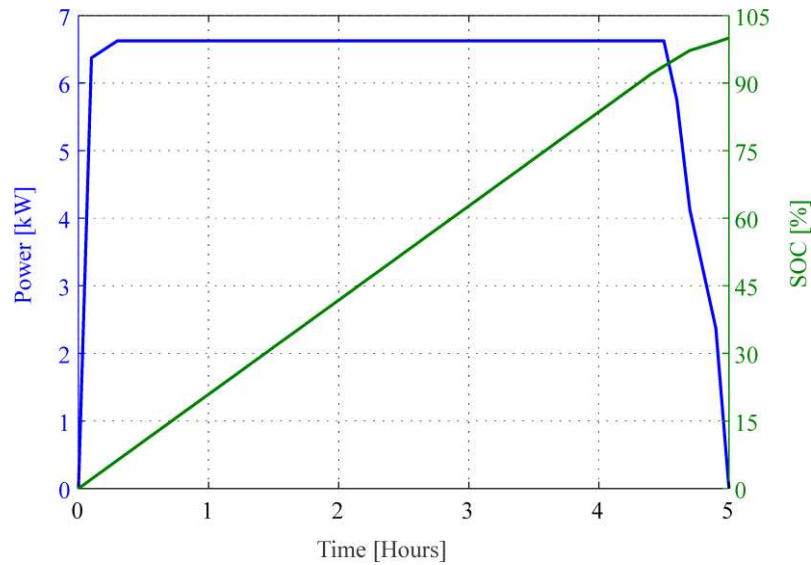


Figure 10. Charging profile of the Nissan Altra battery (lithium-ion) [71].

As for the ESS, for the EV model it is considered an aggregated model for the optimization problem in the power balance constraint. The maximum output power of the battery system is limited by Equation (19), and will depend on the number of EV ( $N_{EV}$ ) considered, which here corresponds to the number of residential consumers. Consequently, the maximum output power for the EV ( $P'_{EV,Total}$ ) aggregated model is 292.5 kW for every time-step (for the long-term stage).

Table 6. Parameters of the EV Nissan Altra.

Parameter	Value	Units
$C_{EV}$	29	kWh
$P_{EV,max}$	6.5	kW
$DOD_{EV}$	60	%
$N_{EV}$	45	-
$P'_{EV,Total}$	292.5	kW

### 3.7 LINES AND TRANSFORMERS POWER LOSS MODELS

Two kinds of power losses are considered, the power losses due to the efficiency of the distribution transformers and the power losses in the triplex lines of the distribution feeder. To model this, is performed a power losses characterization study in the residential microgrid using GridLabD.

The losses due to the efficiency of the distribution transformer ( $P_{DT,Loss}$ ) can be modeled using Equation (20), where the output power ( $P_{DT,out}$ ) can be estimated as a function of the input power ( $P_{DT,in}$ ) and the efficiency of the distribution transformer ( $\eta_{DT}$ ). This efficiency is obtained experimentally, using the estimated power losses given by GridLabD and the output power, as can be seen in Figure 11. Then, the efficiency can be obtained using the slope of the linear regression model, as in Equation (21) [72], where  $\eta_{DT} = 99.96\%$ . The model used for the MV and the distribution transformers uses the parameters defined by default for GridLabD, shown in the Appendix A.

$$P_{DT,out} = \eta_{DT} \cdot P_{DT,in} \quad (20)$$

$$\eta_{DT} = \frac{P_{DT,out}}{P_{DT,out} + P_{DT,Loss}} \quad (21)$$

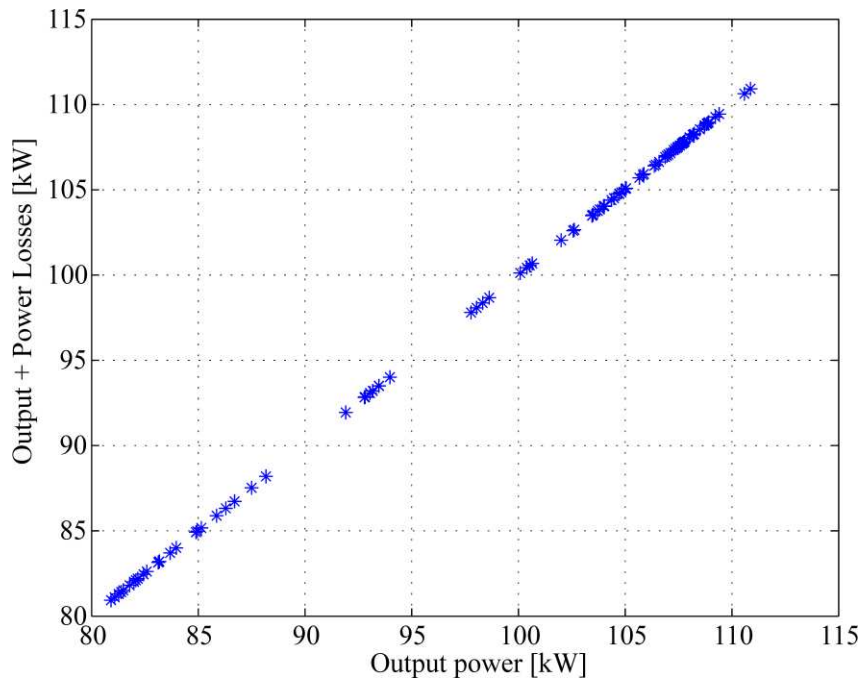


Figure 11. Power losses characterization of a distribution transformer (DT) in GridLabD.

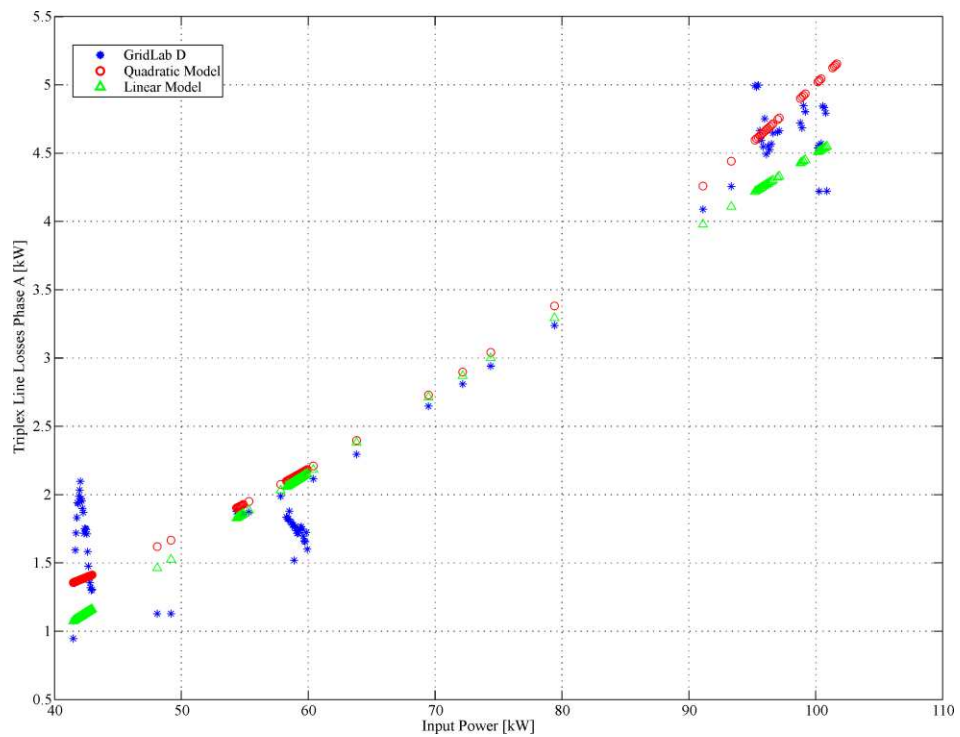


Figure 12. Triplex line power losses estimated by GridLabD, the linear model and the quadratic model as a function of the input power for a DT.

The power losses in the triplex line ( $P_{TL,Loss}$ ), are modeled as a function of the input active power of the distribution transformer. As can be seen in Figure 12, two models are considered: a linear and a quadratic model given by Equation (22) and (23), respectively. Both models are obtained using basic fitting techniques; the values of the parameters of the model are listed in Table 7. The validation and use of these two models is given in the next sections.

$$P_{TL,Loss}(P_{DT,in}) = tl_1 \cdot P_{DT,in} + tl_0 \quad (22)$$

$$P_{TL,Loss}(P_{DT,in}) = tlq_2 \cdot (P_{DT,in})^2 + tlq_1 \cdot P_{DT,in} + tlq_0 \quad (23)$$

Table 7. Parameters of the two line power loss models.

Parameter	Value	Units
$\eta_{DT}$	0.99	-
$tl_1$	0.0195	-
$tl_0$	-0.4507	kW
$tlq_2$	0.000145	1/kW
$tlq_1$	0.000198	-
$tlq_0$	0.1934	kW

### 3.8 STATEMENT OF THE ENERGY MANAGEMENT PROBLEM

In the next section the optimization objectives considered and the technical constraints that the EMS needs to attend to an optimal dispatch in the schedule horizon are presented. The structure of the EMS proposed in this master dissertation does not consider any contingency policy, i.e., the EMS has been developed to operate in regular operational conditions. Furthermore, none of generation systems have been penalized or favored, leaving the EMS to define the best operational schedule according to the optimization objectives.

In general, a multi-objective optimization problem can be defined as in Equation (24).

$$\begin{aligned}
& \underset{x}{\text{minimize}} && F(x) = (f_1(x), f_2(x), \dots, f_k(x)) \\
& \text{subject to} && g_i(x) \leq 0, \quad i = 1, \dots, m \\
& && h_j(x) = 0, \quad j = 1, \dots, p \\
& && x_q^l \leq x_q \leq x_q^u \quad q = 1, \dots, n
\end{aligned} \tag{24}$$

Where  $F(x)$  is the set of objective functions,  $g_i(x)$  is the set of inequality constraints,  $h_j(x) = 0$  is the set of equality constraints,  $x_q^l$  and  $x_q^u$  are the minimum and maximum values of each decision variable  $x_q$ , respectively. A multi-objective optimization problem consists in minimizing  $K$  objectives functions simultaneously, considering  $m$  inequality constraints and  $p$  equality constraints.

In this master dissertation, two objective functions are considered, the total operational cost ( $OC$ ) in USD\$, given by Equation (25) and the total power losses ( $PL$ ) in kW, given by Equation (26), for the total number of periods in the scheduling horizon ( $T$ ).

$$OC = \sum_{t=1}^T FC_{GD}^t \cdot C_{GD}^t \cdot \Delta t + \sum_{t=1}^T P_G^t \cdot C_G^t \cdot \Delta t \tag{25}$$

$$PL = \sum_{t=1}^T \left[ \sum_{j=1}^3 P_{DT, \text{Loss}}^t + P_{TL, \text{Loss}}^t \right] \tag{26}$$

Where,  $FC_{GD}^t$  corresponds to the fuel-diesel consumption in l/h at period  $t$ ,  $C_{GD}^t$  is the diesel cost in \$USD/l,  $P_G^t$  is the energy supply by the main grid at time  $t$  in kW, and  $C_G^t$  is the cost of the energy supply by the main grid in \$USD/kWh. Related to the power losses ( $PL$ ),  $P_{TL, \text{Loss}}^t$  represents the power losses in the triplex line in kW at time  $t$  and  $P_{DT, \text{Loss}}^t$  corresponds

to the power losses in the DT at time  $t$ . If in the operational cost ( $OC$ ) the LLC of the ESS is considered, then Equation (25) can be written as in Equation (27).

$$OC = \sum_{t=1}^T FC_{GD}^t \cdot C_{GD}^t \cdot \Delta t + \sum_{t=1}^T P_G^t \cdot C_G^t \cdot \Delta t + \sum_{t=1}^T C_{Life}^t \quad (27)$$

Also, it will be considered the time-of-use pricing scheme established recently by the ANEEL, where the price of electricity is tied to specific time periods, aiming to reduce the energy consumption in the peak hours and to encourage the demand side management. According to ANEEL's resolution, three different periods can be identified: peak (P), intermediary (I) and off-peak (OP), with the schedule and cost shown in Table 8. The used cost of energy corresponds to the price defined by one of the Sao Paulo's utilities (CPFL-Paulista). For the diesel cost a value of 1.10 \$USD/l is considered.

Table 8. Time-of-use pricing scheme used by the Sao Paulo's utility (CPFL-Paulista).

Period	Time	Energy cost (\$USD/kWh)
OP	00h00 to 17h00	0.0929
	22h00 to 23h00	
I	17h00 to 18h00	0.1241
	21h00 to 22h00	
P	18h00 to 21h00	0.1979

### 3.8.1 TECHNICAL CONSTRAINS

As a technical constraint, the EMS has to guarantee a power balance at the distribution transformers, matching the power from the main grid ( $P_G^t$ ), the EV power ( $P_{EV}^t$ ), the battery system ( $P_{BAT}^t$ ) and the diesel generator ( $P_{GD}^t$ ) with the load demand ( $\tilde{P}_L^t$ ), the power losses ( $PL^t$ ) and the RES generation ( $P_{PV}^t$  and  $P_{WT}^t$ ). Due to the fact that the PV system ( $P_{PV}^t$ ) and

the wind turbines ( $P_{WT}^t$ ) are non-dispatchable sources, their corresponding generation is subtracted to the load consumption, as is shown in Equation (28).

$$P_{GD}^t + N_{BAT} \cdot P_{BAT}^t + N_{EV} \cdot P_{EV}^t + PL^t + P_G^t = \tilde{P}_L^t - P_{PV}^t - P_{WT}^t \quad (28)$$

Furthermore, in the statement of the energy management problem a restriction related to the active power reserve ( $SR^t$ ) is considered. This restriction can be defined as in Equation (29).

$$R_{GD}^t + N_{BAT} \cdot R_{BAT}^t + R_G^t \geq SR^t \cdot \tilde{P}_L^t \quad (29)$$

The active power reserve of the diesel generator ( $R_{GD}^t$ ) is defined using Equation (30), where the active power reserve corresponds to the minimum value between the minimum up-rate constraint ( $RU_{GD}$ ) and the difference between the maximum output power ( $P_{GD,max}$ ) and the current output power ( $P_{GD}^t$ ). In Equation (31), the active power reserve of the main grid ( $R_G^t$ ), is defined as a function of the maximum power that can be extracted from the main grid ( $P_{G,max}$ ) and the current active power ( $P_G^t$ ). Finally, in Equation (32) the active power reserve of the battery system ( $R_{BAT}^t$ ) is defined, as a function of the up-rate output power ( $RU_{BAT}$ ) and the available energy defined by the current  $SOC$ . In Equation (29) the active power reserve of the EV is not included, since in a real operational case this system will not be available all the operating time.

$$R_{GD}^t = \min \{ RU_{GD}, P_{GD,max} - P_{GD}^t \} \quad (30)$$

$$R_G^t = P_{G,max} - P_G^t \quad (31)$$

$$R_{BAT}^t = N_B \cdot \min \left\{ RU_{BAT} / \Delta t, V_{BAT} \cdot C_{BAT} \cdot \left( (SOC^t - SOC_{min}) / \Delta t \right) \right\} \quad (32)$$

On the other hand, according to ANEEL, in the Module 8 (Power Quality) of the Procedures for Electricity Distribution in the National Electric System (PRODIST by its Portuguese acronym), the definitions used in Brazil by the utilities related to voltage unbalance, harmonics, power factor, steady-state voltage, among others are established [73]. This procedure is mandatory and regulates the quality of the power supply at the distribution level. As the LV microgrid operates in grid-connected mode, the EMS has to consider the voltage unbalance at the MV transformer. To measure the voltage unbalance ( $VU$ ), the indicator defined by ANEEL in the PRODIST is used and is shown in Equation (33).

$$VU(\%) = 100 \sqrt{\frac{1 - \sqrt{3 - 6\beta}}{1 + \sqrt{3 - 6\beta}}} \quad (33)$$

$$\beta = \frac{V_{ab}^4 + V_{bc}^4 + V_{ca}^4}{(V_{ab}^2 + V_{bc}^2 + V_{ca}^2)^2} \quad (34)$$

Where  $\beta$  is defined as in Equation (34), and  $V_{ab}$  corresponds to the phase-phase voltage between phase  $a$  and  $b$ . The reference values of the  $VU$  at the nodes of the MV transformer must be equal or less than 2% [73]. In addition, the voltage variation at the most remote nodes of the distribution system is considered. In these nodes, the voltage should be between 108 V (0.90 p.u.) and 127 V (1.05 p.u.), to be considered as in normal operational range.

For the ESS, as a technical restriction at the end of the schedule horizon, i.e., at the time-step  $T$ , the energy stored in the battery systems should be equal to the energy at the initial period. This constraint is given by the Equation (35), where a  $SOC^{t=0}$  of 80% is considered. However, during the operational day, the EMS can dispatch the battery system according to the optimization objectives, as long as constraint in Equation (4) is feasible. The main purpose

of this constraint is to ensure that there will be enough energy stored at the battery system for the next day of operation.

$$SOC^{t=0} = SOC^{t=T} \quad (35)$$

Finally, for the EVs some assumptions need to be made to state the energy management problem. First, it is assumed a deterministic behavior for the state of the EVs, i.e., it is defined the time schedule for the use of the EV as shown in Table 9 and in Figure 13. Second, it is established as technical constraint that the  $SOC_{EV}^t$  at 7:00 (time to go to work) and at 14:00 (time to go to work after lunch) should be equal to 100%. Also, it is established that  $SOC_{EV}^t$  at 00:00 should be 80%. This restriction is based on the scheduled for the next day.

Table 9. States of the EV during one day of schedule.

Time	State
00h00 to 7h00	Available for charging/discharging
07h00 to 12h00	EV in use/ Parking at work
12h00 to 14h00	Available for charging/discharging
14h00 to 17h00	EV in use/ Parking at work
17h00 to 24h00	Available for charging/discharging

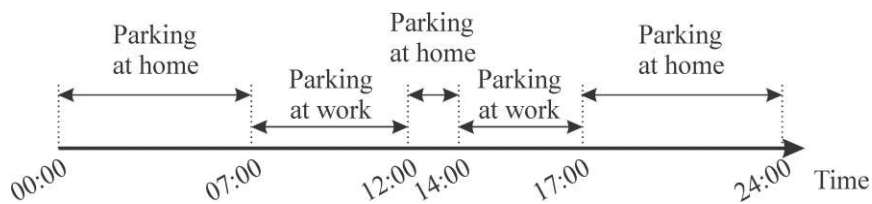


Figure 13. Schedule of the EV.

---

## 4 THE OPTIMIZATION STRATEGY

---

The algorithm used to solve the optimization problem for the long-term stage corresponds to the NSGA-II, complemented using a Quadratic Programming (QP) algorithm (denominated here as NSGA-II+QP), both developed in MATLAB. To understand how the NSGA-II works it is necessary to define the non-dominance concept used in multi-objective optimization. In a multi-objective optimization problem, given any two solution  $x_1$  and  $x_2$ , they can have one or two possibilities: one dominates the other or none dominates the other. In this sense, a candidate solution  $x_1$  is said to dominate the solution  $x_2$ , denoted as  $x_1 \preceq x_2$  (in a minimizing problem), if the following conditions are satisfactorily met:

- The solution  $x_1$  is better than solution  $x_2$  in all the  $k$  objectives. This is

$$f_k(x_1) \leq f_k(x_2), \text{ for all } k = \{1, \dots, K\}.$$

- The solution  $x_1$  is strictly better than solution  $x_2$  in at least one objective. This is

$$f_k(x_1) < f_k(x_2), \text{ for at least one } k \in \{1, \dots, K\}.$$

If any of the above conditions is not met, it is said that the solution  $x_1$  does not dominate the solution  $x_2$ . If  $x_1$  dominate the solution  $x_2$ , it is commonly referred as  $x_2$  is dominated by  $x_1$ . Here, it is important to highlight that the concept of ‘optimal solution’ in multi-objective optimization has a different meaning, because it cannot be found a unique solution that simultaneously optimizes objectives that are conflicting with each other. This means that

in multi-objective optimization is necessary to establish a compromise between objectives, so that the optimal set of final solutions represents a trade-off between objectives. The final optimal set corresponds to the non-dominated solutions, and are known as Pareto optimal set in the variable space and Pareto optimal front in the objective space [74].

From the above discussion, it is possible to point out that there are primarily two goals that a multi-objective optimization algorithm must achieve: (i) guide the search towards the global Pareto optimal regions and (ii) maintain population diversity in the Pareto optimal front.

The Non-dominated Sorting Genetic Algorithm or NSGA-II, was first introduced in [75]. This algorithm directly uses the concept of non-dominance to select the individuals for the next generation. To do this, the NSGA-II classify the population in non-dominating fronts or ranks. The individuals that belong to the first rank are denominated Pareto optimal individuals, since they are non-dominated. One advantage of selection based on dominance is that it is not necessary to set parameters a priori, as done in other algorithms [75].

To improve and maintain the diversity in the population, the NSGA-II uses the Crowding Distance (CD) concept. The CD can be seen as a density indicator, defined as the volume of the hypercube formed by the immediately preceding and following solutions for each objective [75]. To select the individuals for the next generations, the individuals of the first rankings are considered first (elitism). If the number of individuals for the next rank is greater than the maximum number of individuals to insert (and maintain the population size), it is calculated the CD for the individuals of this rank, and are selected those will the higher CD value. This procedure is repeated for all fronts until the number of selected individuals reaches the population size. The main drawback of this density metric is the computational time required to sort all the individuals for every objective to estimate its value.

Considering this and the intrinsic characteristics of the energy management problem, in the next section are presented the optimization algorithms developed to be implemented in the long- and short-term optimization stages.

#### 4.1 LONG-TERM OPTIMIZATION STAGE: NSGA-II+QP ALGORITHM

The computational flow of the proposed algorithm is given in Figure 16. The NSGA-II+QP algorithm can be described in the following steps:

- 1) First, some parameters of the NSGA-II are initialized, such as the size of the population ( $N_{pop}$ ), and the maximum number of generations ( $g_{max}$ ).
- 2) As an input, the algorithm requires the load and weather forecast. Here, it is assumed that these forecast values are provided by a one-day ahead forecast module. After this, it is estimated the RES generation using Equation (1) and Equation (2). It is not focus of this master dissertation develop and validate a weather and load consumption forecast module.
- 3) For the MOGA, solutions are codified as a 2-by- $T$  binary matrix, as is show in Equation (36), in which binary variables are defined using the heuristic procedure presented below. In Equation (36),  $U_{GD}^t$  is the operational status of the diesel generator and  $B_{BAT}^t$  is the battery status, which corresponds to  $B_{BAT}^t = 1$  when the battery is in charging mode, and to  $B_{BAT}^t = 0$  when it is in discharging mode. In this algorithm, the binary

variables ( $U_{GD}^t$  and  $B_{BAT}^t$ ) are defined using a heuristic procedure that can handle the minimum running and down time constraints of the diesel generator.

$$x_{1,GA} = \begin{bmatrix} U_{GD}^1 & U_{GD}^2 & \dots & U_{GD}^T \\ B_{BAT}^1 & B_{BAT}^2 & \dots & B_{BAT}^T \end{bmatrix} \quad (36)$$

---

```

If  $t_1 \leq t \leq t_2$ , Then  $U_{GD}^t = 1$ . Else  $U_{GD}^t = 0$ .
For  $t=1$  to  $T$ 
  If  $U_{GD}^t = 1$ 
    If  $U_{GD}^{t-1} = 0$ 
      If  $T_{GD,OFF}^t < MDT_{GD}$ , Then  $U_{GD}^t = 0$ , Endif
    Endif
  Elseif  $U_{GD}^t = 0$ 
    If  $U_{GD}^{t-1} = 1$ 
      If  $T_{GD,ON}^t < MUT_{GD}$ , Then  $U_{GD}^t = 1$ , Endif
    Endif
  Endif
Endfor

```

---

This heuristic procedure can handle the minimum up- and down-time constraint of the diesel generator, described in Equation (12), in which  $t_1$  and  $t_2$  are generated randomly using an uniform random distribution in the interval between 0 and  $T$ . For  $B_{BAT}^t$  is used a similar procedure, using randomly generated values for  $t_1$  and  $t_2$ . However, as there is not a constraint related to the charging and discharging time it is not applied the heuristic procedure described.

- 4) Once the binary variables are defined by the MOGA, the remaining continuous variables of the problem ( $P_{GD}^t, P_{BAT}^t, P_G^t, P_{EV}^t, S^t, SOC^t, SOC_{EV}^t$ ) are obtained formulating

and solving a one-objective QP problem. One advantage of this procedure is that it does not need the development of new and sophisticated genetic operators, which have to consider intrinsic characteristics of the energy management problem.

Considering this, a final solution for the energy management problem is defined as in Equation (37), where  $P_{GD}^t$  is the diesel generator power output,  $P_{BAT}^t$  is the battery input/output power,  $P_G^t$  is the power supply by the main grid,  $S^t$  is the shifting coefficient,  $P_{EV}^t$  is the EV power input/output,  $SOC^t$  is the State-of-Charge of the battery system and  $SOC_{EV}^t$  is the State-of-Charge of the EV.

$$x_1 = \begin{bmatrix} U_{GD}^1 & U_{GD}^2 & \dots & U_{GD}^T \\ B_{BAT}^1 & B_{BAT}^2 & \dots & B_{BAT}^T \\ P_{GD}^1 & P_{GD}^2 & \dots & P_{GD}^T \\ P_{BAT}^1 & P_{BAT}^2 & \dots & P_{BAT}^T \\ P_G^1 & P_G^2 & \dots & P_G^T \\ P_{EV}^1 & P_{EV}^2 & \dots & P_{EV}^T \\ S^1 & S^2 & \dots & S^t \\ SOC^1 & SOC^2 & \dots & SOC^t \\ SOC_{EV}^1 & SOC_{EV}^2 & \dots & SOC_{EV}^t \end{bmatrix} \quad (37)$$

To state the QP problem, the two-objective are combined in one-objective using the weight-sum method [38], as shown in Equation (38), where  $\eta$  is selected randomly using an uniform distribution function in the interval [0,1] and updated in every generation [38]. This is done to increase the searching capabilities of the NSGA-II+QP algorithm,  $OC(\cdot)$  and  $PL(\cdot)$  are defined as in Equation (25) and (26), respectively.

$$\min f = \eta \cdot OC(\cdot) + (1 - \eta) \cdot PL(\cdot) \quad (38)$$

- 5) The QP problem is solved with function *quadprog* in MATLAB, using an interior-point-convex algorithm. To use this function,  $PL(\cdot)$  in Equation (38) is written as a quadratic function of the diesel generator power output ( $P_{GD}^t$ ), and the power extracted from the main grid ( $P_G^t$ ), using the quadratic model described in Equation (23). Similarly, is used the linear model described in Equation (22) to model  $PL(\cdot)$  in the power balance constraint, shown in Equation (28).

These two models are used due to the characteristics of the *quadprog* function in MATLAB, which require a quadratic objective function and linear constraints. Considering this remarks, the QP problem can be formulated as in Equation (39), where  $P_{BAT}^t$  is decomposed in two new variables: battery power in charging mode ( $P_{CH}^t$ ), and battery power in discharging mode ( $P_{DCH}^t$ ). In Equation (39), the energy management problem is formulated as a QP problem, in which the objective is a quadratic function and the equality and inequality constrains are linear. Furthermore, as the GA defines the binary variables (ON/OFF schedule for the diesel generator and charging/discharging schedule for the battery system), the complexity of the final energy management problem is reduced.

$$\min \quad \eta \cdot OC(\cdot) + (1-\eta) \cdot PL(\cdot)$$

$$\begin{aligned}
s.t. \quad & P_{GD}^t + N_{BAT} \cdot P_{DCH}^t - N_{BAT} \cdot P_{CH}^t + N_{EV} \cdot P_{EV}^t + P_G^t - S^t \cdot P_L^t + P_{PV}^t + P_{WT}^t - PL^t = 0 \quad t = 1, \dots, T \\
& SOC^t - SOC^{t-1} \cdot (1-\delta) - \frac{\Delta t \cdot \eta_{BAT}}{C_{BAT} \cdot V_{BAT}} P_{CH}^t + \frac{\Delta t \cdot \eta_{BAT}}{C_{BAT} \cdot V_{BAT}} P_{DCH}^t = 0 \quad t = 1, \dots, T \\
& SOC^{t=1} - SOC^{t=0} - \frac{\Delta t \cdot \eta_{BAT}}{C_{BAT} \cdot V_{BAT}} P_{CH}^{t=1} + \frac{\Delta t \cdot \eta_{BAT}}{C_{BAT} \cdot V_{BAT}} P_{DCH}^{t=1} = 0 \\
& SOC^{t=T} - SOC^{t=T-1} - \frac{\Delta t \cdot \eta_{BAT}}{C_{BAT} \cdot V_{BAT}} P_{CH}^{t=T-1} + \frac{\Delta t \cdot \eta_{BAT}}{C_{BAT} \cdot V_{BAT}} P_{DCH}^{t=T-1} = 0 \\
& SOC_{EV}^t = SOC_{EV}^{t-1} + \frac{P_{EV}^t}{C_{EV}} \cdot \Delta t \quad t = 1, \dots, T \\
& P_{GD}^t + P_G^t + N_{BAT} \cdot P_{DCH}^t \leq N_{BAT} \cdot RU_{BAT} + P_{G,\max} + P_{GD,\max} - SR^t \cdot \tilde{P}_L^t \quad t = 1, \dots, T \\
& \sum_{t=1}^T S^t \cdot P_L^t = \sum_{t=1}^T P_L^t \quad (39) \\
& P_{GD}^{t+1} - P_{GD}^t \leq RU_{GD} \quad t = 1, \dots, T \\
& P_{GD}^t - P_{GD}^{t+1} \leq RD_{GD} \quad t = 1, \dots, T \\
& P_{GD,\min} \leq P_{GD}^t \leq P_{GD,\max} \quad t = 1, \dots, T \\
& 0 \leq P_{CH}^t \leq RU_{BAT} \quad t = 1, \dots, T \\
& 0 \leq P_{DCH}^t \leq RD_{BAT} \quad t = 1, \dots, T \\
& SOC_{\min} \leq SOC^t \leq SOC_{\max} \quad t = 1, \dots, T \\
& SOC_{EV,\min} \leq SOC_{EV}^t \leq SOC_{EV,\max} \quad t = 1, \dots, T \\
& 0 \leq P_G^t \leq P_{G,\max} \quad t = 1, \dots, T \\
& S_{\min} \leq S^t \leq S_{\min} \quad t = 1, \dots, T \\
& -P_{EV,\max} \leq P_{EV}^t \leq P_{EV,\max} \quad t = 1, \dots, T
\end{aligned}$$

6) The current population is classified in non-dominated fronts, applying the non-dominating concept described previously.

7) To create new solutions, tournament selection, crossover and mutation genetic operators are applied. For this, the one-point crossover and mutation genetic operators are adapted considering the operational constraints of the energy management problem. The genetic operators are used by the GA and applied only for the binary variables in Equation (36).

In the tournament operator, three solutions are selected randomly from the current population. Solutions with the highest rank in the non-dominating fronts are selected. If two solutions have the same rank, the selection is based on its CD, selecting the one with highest value. This procedure is repeated until create a mating pool with size of  $N_{pop}/2$ .

For mutation, one parent is selected randomly from the mating pool. Then, a random value  $\Delta$ , in the interval of  $-20 \leq \Delta \leq 20$ , is selected to move the schedule in the time to create the new solution, as is shown in Equation (40). Then, the heuristic algorithm described in Step 3 is applied to consider the minimum up- and down-time constraint for the diesel generator. A schematic example of crossover is presented in Figure 14.

$$x_{offsp}^{(t)} = x_p^{(t+\Delta)} \quad (40)$$

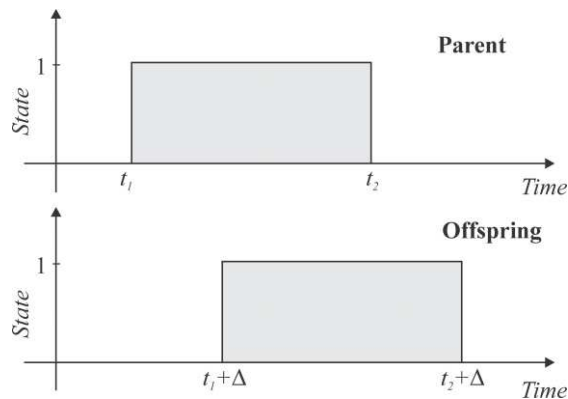


Figure 14. Schematic example of mutation.

For crossover, two parents ( $x_{p1}$  and  $x_{p2}$ ) are randomly selected from the mating pool. Then, it is randomly selected a crossover point ( $t_{\Delta}$ ) and the schedule are exchanged between the two parents to create the new two offspring, as it can be seen in Equation (41). Then, the heuristic algorithm described in Step 3 is applied to consider the

minimum up- and down-time constraint for the diesel generator. A schematic example of crossover is presented in Figure 15.

$$\begin{aligned}
 x_{offsp1}^{(t=1 \rightarrow t_{\Delta})} &= x_{p1}^{(t=1 \rightarrow t_{\Delta})} & x_{offsp1}^{(t_{\Delta} \rightarrow T)} &= x_{p2}^{(t_{\Delta} \rightarrow T)} \\
 x_{offsp2}^{(t=1 \rightarrow t_{\Delta})} &= x_{p2}^{(t=1 \rightarrow t_{\Delta})} & x_{offsp2}^{(t_{\Delta} \rightarrow T)} &= x_{p1}^{(t_{\Delta} \rightarrow T)}
 \end{aligned} \tag{41}$$

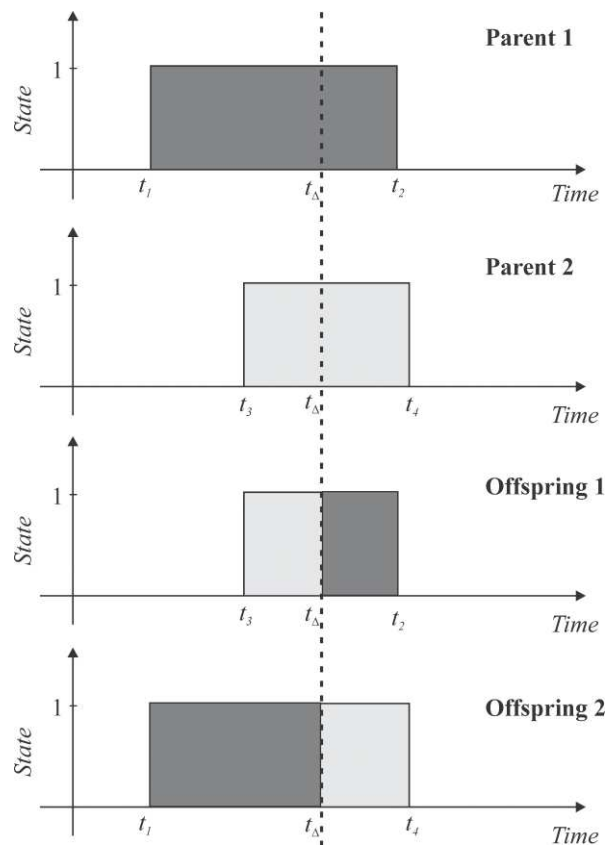


Figure 15. Schematic example of crossover.

- 8) Once the binary variables of the solutions are set, the continuous variables are defined solving the QP problem, as in Step 4 and 5.
- 9) Finally, non-dominating sorting is applied to the new population composed of parents and their offspring. To reduce the size of the current population it is used the CD and the ranking fronts, selecting those candidates solutions that belongs to the first fronts and with the higher crowding distance.

- 10) Once the NSGA-II+QP algorithm has converged, the objective functions of the solutions that belongs to the Pareto front are re-calculated using GridLabD, considering the technical constraints in Equation (33) and the voltage variations as is described in the PRODIST module.
- 11) To select the optimal solution from the Pareto front, the approach proposed in [36] is considered, where the Decision Maker (DM) is presented with one solution, selected as the Best Compromise Solution (BCS). To identify this solution in the Pareto front a membership function  $\mu^k$  is estimated as shown in Equation (42). The BCS is the one having the maximum value of  $\mu^k$ . In Equation (42),  $F_{\max}$  and  $F_{\min}$  is the maximum and minimum value for the objective  $i$  in the Pareto front, respectively, and  $N_{obj}$  is the number of objectives considered. This approach can be applied only if the final Pareto front is well covered.

$$\mu^k = \frac{\sum_{i=1}^{N_{obj}} \mu_i^k}{\sum_{k=1}^{N_{pop}} \sum_{i=1}^{N_{obj}} \mu_i^k} \quad \mu_i = \begin{cases} 1 & F_i = F_{\min} \\ \frac{F_{\max} - F_i}{F_{\max} - F_{\min}} & F_{\min} \leq F_i \leq F_{\max} \\ 0 & F_i = F_{\max} \end{cases} \quad (42)$$

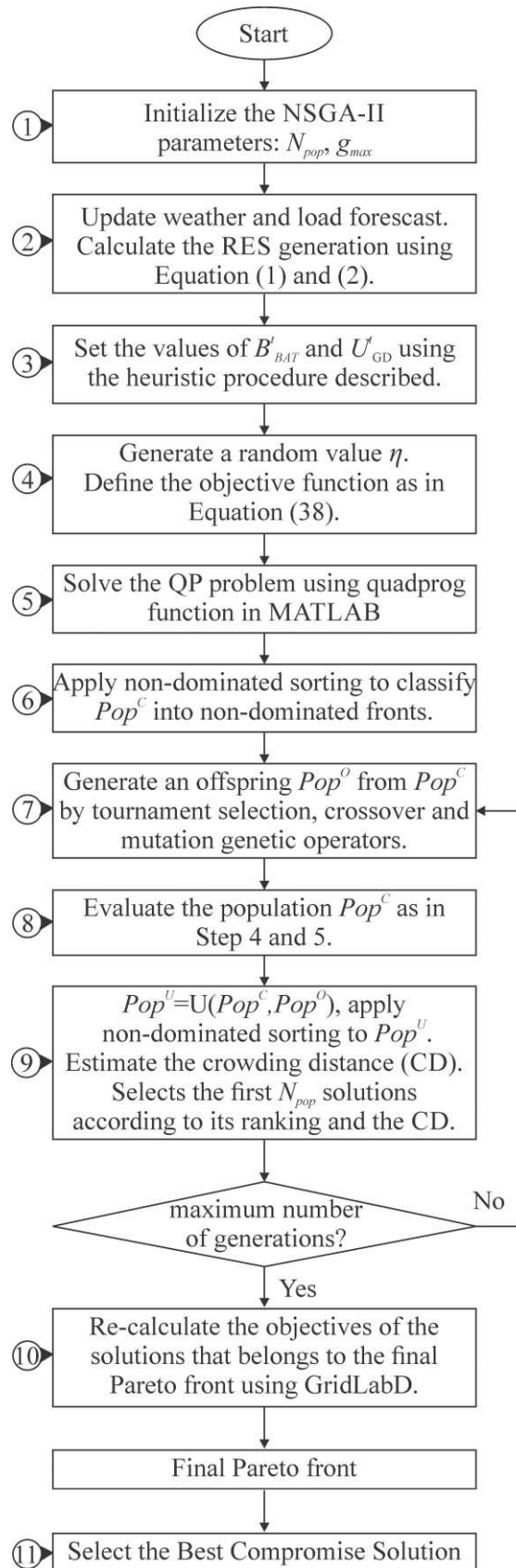


Figure 16. Computational flow of the proposed NSGA-II+QP algorithm.

## 4.2 SHORT-TERM OPTIMIZATION STAGE

As previously discussed, once the long-term optimization stage is solved, the ON/OFF and charging/discharging schedule of the diesel generator and battery systems are defined. The short-term optimization stage uses these previously defined information to state the energy management problem as an ELD problem, which is related to the QP problem described in Equation (39). However, in this short-term stage, the QP problem is stated considering an operational time of 1 hour, sub-divided in 12 periods of 5-mins. Thus, for an operational time of one day, in total the short-term stage has to solve 24 ELD problems independently, each one for an operational hour.

For each ELD problem, the short-term stage receive the initial and final SOC of the ESS, the shifting coefficients of the DSM, the state of the diesel generator (ON/OFF) and the mode of operation of the ESS (charging/discharging) from the long-term stage, and it is stated the energy management problem as in Equation (43), considering that  $\Delta t = 1/12$  hours (5-min time-step) and  $T = 12$ .

Regarding the DSM, the short-term stage considers the coefficients given by the long-term stage in time-steps of 15-min and use linear interpolation to define the DSM coefficients for the operational hour under consideration considering time-steps of 5-min. Here it is important to highlight that in a theoretical case, in which load consumption and RES generation forecast in time-steps of 5-mins corresponds to an interpolation of the forecast in time-steps of 15-mins, constraint described in Equation (15) will be fully satisfied for the 24 hours period. However, real operational cases does not have this requirement, and the shifting coefficients obtained using linear interpolation for the short-term stage will not satisfy constraint in Equation (15) once the 24 ELD problems have being solved. Nevertheless, load consumption

will be completely supplied due that the output power of the dispatchable units are defined solving the ELD problem under discussion considering every hour independently.

$$\begin{aligned}
& \min \quad \eta \cdot OC(\cdot) + (1-\eta) \cdot PL(\cdot) \\
s.t. \quad & P_{GD}^t + N_{BAT} \cdot P_{DCH}^t - N_{BAT} \cdot P_{CH}^t + N_{EV} \cdot P_{EV}^t + P_G^t - S^t \cdot P_L^t + P_{PV}^t + P_{WT}^t - PL^t = 0 \quad t = 1, \dots, T \\
& SOC^t - SOC^{t-1} \cdot (1-\delta) - \frac{\Delta t \cdot \eta_{BAT}}{C_{BAT} \cdot V_{BAT}} P_{CH}^t + \frac{\Delta t \cdot \eta_{BAT}}{C_{BAT} \cdot V_{BAT}} P_{DCH}^t = 0 \quad t = 1, \dots, T \\
& SOC^{t=1} - SOC_{ini} - \frac{\Delta t \cdot \eta_{BAT}}{C_{BAT} \cdot V_{BAT}} P_{CH}^{t=1} + \frac{\Delta t \cdot \eta_{BAT}}{C_{BAT} \cdot V_{BAT}} P_{DCH}^{t=1} = 0 \\
& SOC_{fin} - SOC^{t=T-1} - \frac{\Delta t \cdot \eta_{BAT}}{C_{BAT} \cdot V_{BAT}} P_{CH}^{t=T-1} + \frac{\Delta t \cdot \eta_{BAT}}{C_{BAT} \cdot V_{BAT}} P_{DCH}^{t=T-1} = 0 \\
& SOC_{EV}^t = SOC_{EV}^{t-1} + \frac{P_{EV}^t}{C_{EV}} \cdot \Delta t \quad t = 1, \dots, T \\
& P_{GD}^t + P_G^t + N_{BAT} \cdot P_{DCH}^t \leq N_{BAT} \cdot RU_{BAT} + P_{G,max} + P_{GD,max} - SR^t \cdot \tilde{P}_L^t \quad t = 1, \dots, T \\
& P_{GD}^{t+1} - P_{GD}^t \leq RU_{GD} \quad t = 1, \dots, T \\
& P_{GD}^t - P_{GD}^{t+1} \leq RD_{GD} \quad t = 1, \dots, T \\
& P_{GD,min} \leq P_{GD}^t \leq P_{GD,max} \quad t = 1, \dots, T \\
& 0 \leq P_{CH}^t \leq RU_{BAT} \quad t = 1, \dots, T \\
& 0 \leq P_{DCH}^t \leq RD_{BAT} \quad t = 1, \dots, T \\
& SOC_{min} \leq SOC^t \leq SOC_{max} \quad t = 1, \dots, T \\
& SOC_{EV,min} \leq SOC_{EV}^t \leq SOC_{EV,max} \quad t = 1, \dots, T \\
& 0 \leq P_G^t \leq P_{G,max} \quad t = 1, \dots, T \\
& -P_{EV,max} \leq P_{EV}^t \leq P_{EV,max} \quad t = 1, \dots, T
\end{aligned} \tag{43}$$

The computational flow of the algorithm used by the short-term optimization stage is given in Figure 17. This can be described in the following steps:

- 1) In the Step 1, all the information of the Best Compromised Solution (or the solution to implement), selected from the Final Pareto Front by the long-term optimization stage is loaded. This information include the shifting coefficient of the DMS, the ON/OFF

schedule of the diesel generator, SOC and the mode of operation (charging/discharging) of the ESS and the EVs.

- 2) It is read from the Best Compromise Solution the weight factor ( $\eta$ ), which defines the weight of the two objectives in the final QP problem. Then, the objective function can be defined as in Equation (43).
- 3) As an input, the algorithm requires the load and weather forecast for the next operational hour in time-step of 5-mins. Then, it is estimated the RES generation using Equation (1) and Equation (2).
- 4) The SOC of the ESS and the EVs are updated for the current and the next operational hour  $t$ . This SOC constraint are used as bounds constraint to limit the maximum deep of discharge or the energy extracted from the main grid in the charging mode of the ESS in one operational hour. The value of SOC is defined by the long-term optimization stage as was discussed previously.
- 5) The QP problem is solved with function *quadprog* in MATLAB, using an interior-point-convex algorithm, as in the long-term optimization stage in Step 5, Section 4.1.
- 6) The Final Operational Schedule for the current hour is obtained. This scheduled is executed by the EMS to operate the LV Microgrid.
- 7) Finally, this procedure is repeated continuously until the 24-hours are reached. Then, the short-term stage start over the optimization process, updating the new information related to the new Best Compromise Solution selected for the next operational day.

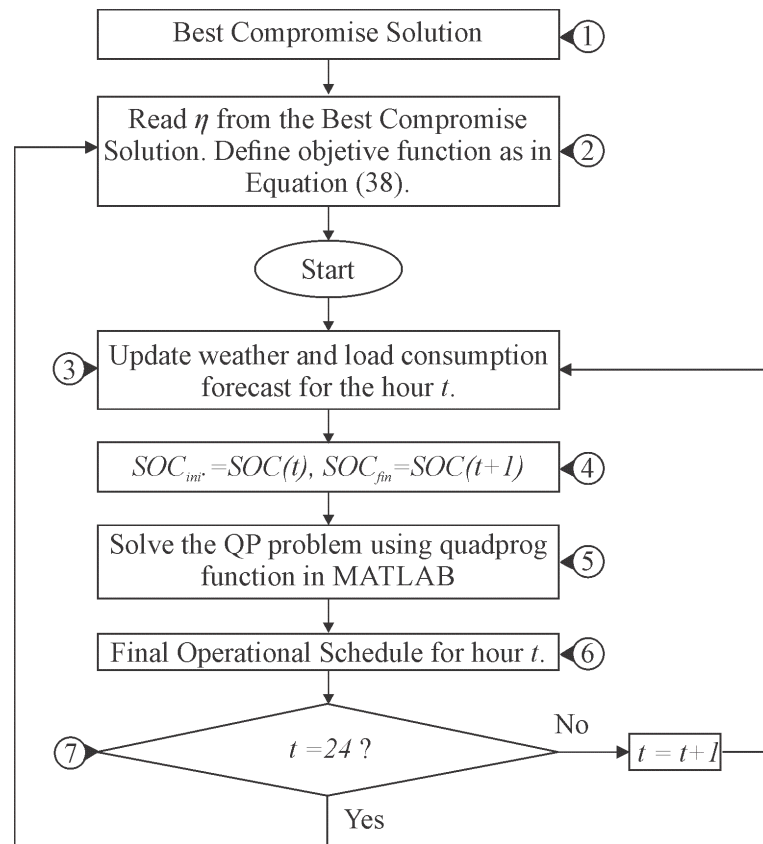


Figure 17. Computational flow of the short-term stage algorithm.

---

## 5 CASE STUDY I: BASIC MICROGRID

---

In this Chapter it is presented the first study scenario, in which it will not be considered the Demand Side Management (DSM) and the Electric Vehicle (EV) in the energy management problem. This first scenario intends to model a basic operational case considering the current development state of the Brazilian power distribution system.

This Chapter begins analyzing the weather data used to solve the energy management problem. Also, a validation of the RES models proposed in Section 3.2 is presented. Then, the two operational cases to be studied are described. A performance assessment of the final solutions provided by the long-term stage is presented. This assessment include a comparison and an evaluation of the impact of the forecast error in the final operational solution. Finally, it is presented an assessment of the short-term stage of the EMS system.

### 5.1 WEATHER DATA AND RES SYSTEM MODEL VALIDATION

For the weather data, 24-hours of November data of a typical meteorological year (TMY) for the state of São Paulo, Brazil is used. This information is composed of hourly weather data such as ambient temperature, wind speed, solar direct radiation, solar diffuse radiation, solar global radiation, humidity and pressure recorded by the SWERA Project near to the Congonhas Airport (São Paulo) (see Appendix B.). As these weather data is available in hour time-steps, for the long-term (15-mins time-step) and the short-term (5-mins time-step) stage linear interpolation techniques were used.

Considering this weather data, a simulation of the Solar and Wind system described in Equation (1) and (2) were performed. This simulation is compared to the models used by

GridLabD, obtaining the results shown in Figure 18. According to these simulations, both models shown a maximum Relative Error (RE) of 20% when compared with the GridLabD model, mainly due to their simplicity. However, they are considered to be accurate enough for the objectives of this dissertation.

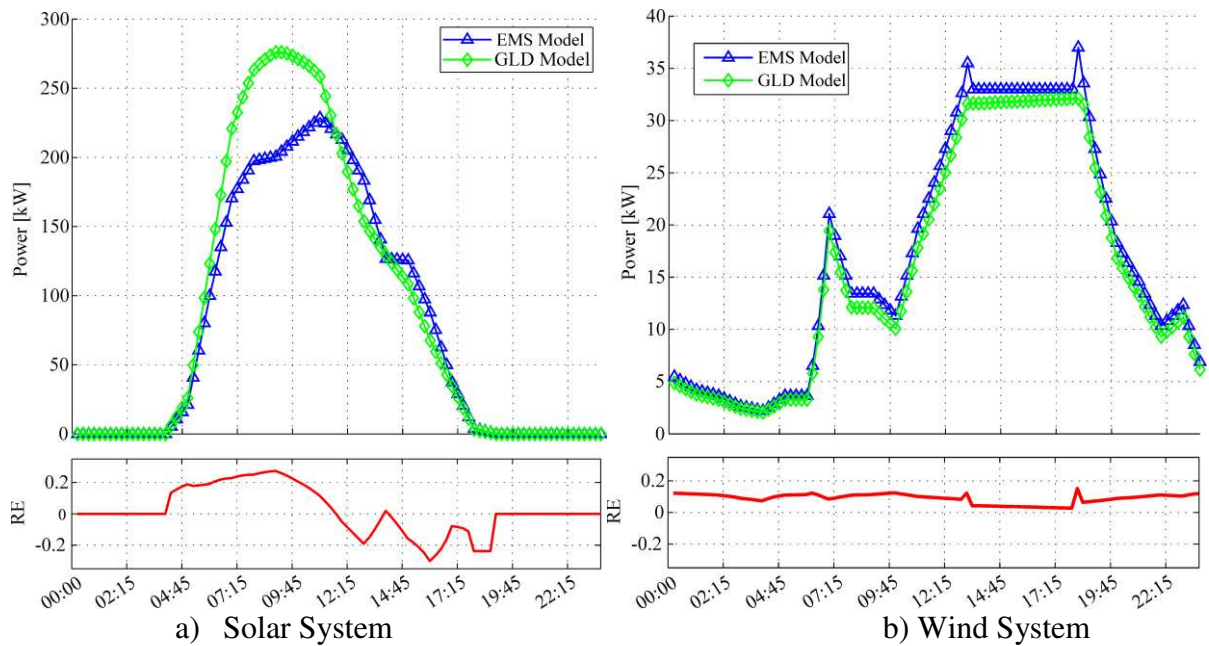


Figure 18. Solar and Wind System models compared to the GridLabD models.

## 5.2 CASES OF STUDY

Two main case of study will be used to assess the forecast error and evaluate the performance of the developed EMS. The first case is named as Perfect Forecast (PF) case, in which the EMS has a perfect knowledge of the load consumption and the RES generation for the next 24-hours. In the second case, named as Real Operational (RO) case, it will be used the RES models described in Section 3.2 in Equation (1) and (2), and a load consumption provided by a forecast module will be considered.

The load consumption used in the optimization problem for both case studies are shown in Figure 19. For the Real Operational case, the load consumption has been obtained using a

uniformly random distribution value  $\gamma \in U[0,1]$ , to obtain values with an RE (in %) in the interval  $[-5\%,+5\%]$ , as shown in Equation (44).

$$P_{L,RO}^t = P_{L,PP}^t + (-0.05 + 0.1 \cdot \gamma) \cdot P_{L,PP}^t \quad (44)$$

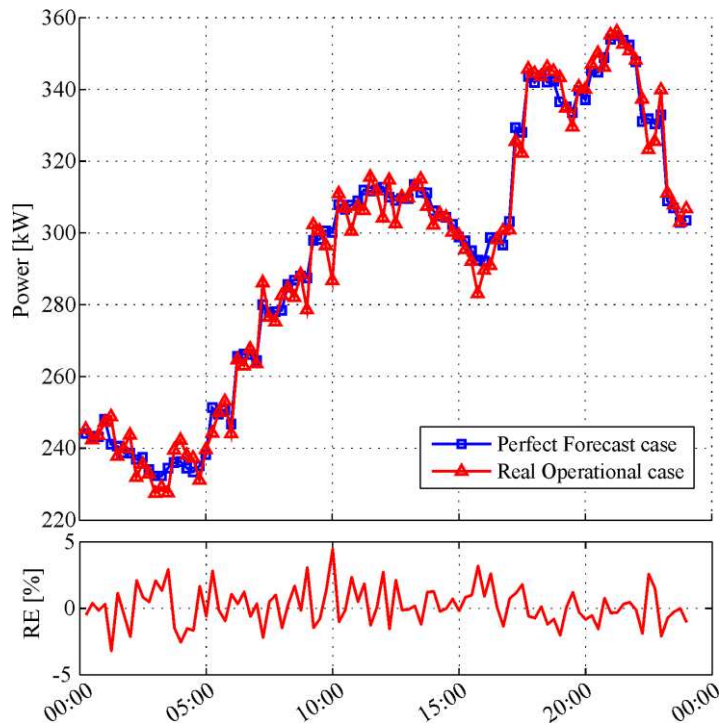


Figure 19. Load consumption used for the cases of study in Scenario I and II.

### 5.3 LONG-TERM STAGE

In this first Perfect Forecast case, the developed algorithm was executed using 200 individuals and 1000 generations, obtaining the Pareto front shown in Figure 20a). These values for the number of individuals and total generation are defined experimentally, aiming to ensure good convergence of the algorithm. Also, in this first case, the LCC of the battery system is not considered. In terms of quality of the final Pareto front, it is possible to conclude that the algorithm can provide a well-covered Pareto front, showing the conflict relation between the two considered objectives, i.e., a reduction in the OC implies an increase in the PL.

In addition, in Figure 20a) it is shown the final Pareto front once the objectives are re-calculated using GridLab-D, named as GLD-RPF. As expected, the GLD-RPF shows different values for the objective function compared to the RPF, under-estimating the PL. This is mainly due to the power losses models used in the optimization problem. Nevertheless, to validate the proposed front approach, a Relative Error (RE) obtained by the comparison of the two Pareto front is calculated and show in Figure 20b). According to these results, the maximum error for the OC objective is close to 0.3 % and for the PL objective, to 9.0 %. Considering the magnitude of the errors obtained, both errors can be considered small enough to be negligible, especially when the power losses are compared with the load consumption and the power supplied by the MV grid for all the time-step.

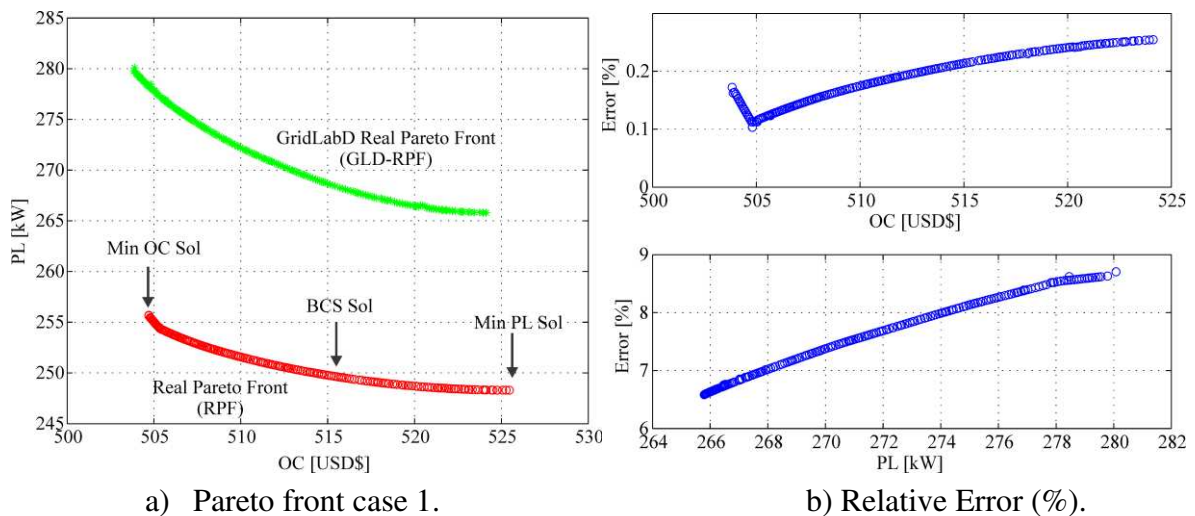
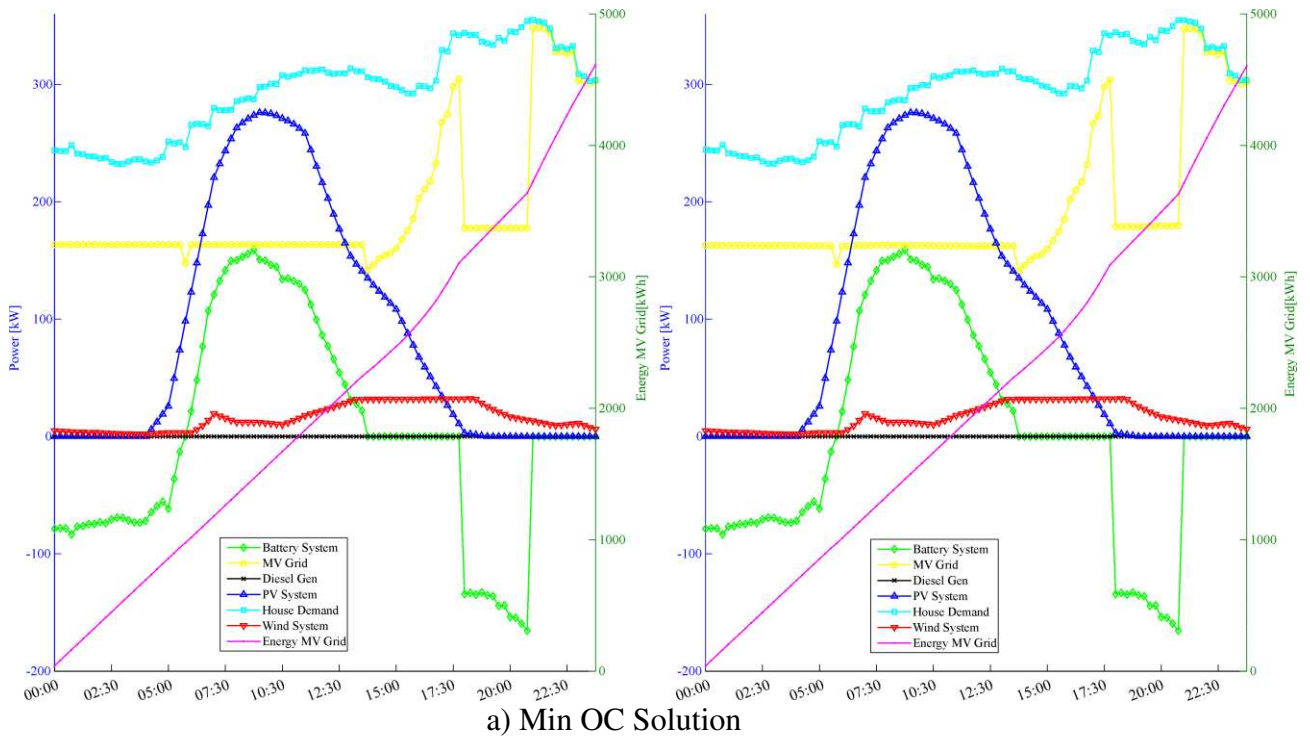


Figure 20. Scenario I: Pareto Front results obtained for the Perfect Forecast case.

To show the operational characteristics of the optimal schedules, three solutions are selected for analysis and comparison purposes: the minimum OC solution (Min OC Sol), the minimum PL solution (Min PL Sol) and the Best Compromise Solution (BCS Sol), all these shown in the Pareto front in Figure 20a) and its corresponding output power in Figure 21. For

every solution, in Figure 21 it is presented the optimal solution obtained executing the NSGA+QP algorithm (left) and the same solution once is simulated in GridLabD (right).

For the minimum OC solution, the long-term stage dispatches the battery system in discharging mode during the peak period, using the maximum power stored at the battery system, responding to the price-scheme proposed by the ANEEL. Similarly, for the minimum PL, the battery is dispatched in the peak and intermediary periods while trying to maintain constant the main grid power consumption. This is due to the fact that power losses in the distribution system are a function of the power extracted from the MV grid, and the energy stored in the battery system is used by the long-term stage to reduce power losses. Finally, the BSC solution shows operational characteristics similar to both extreme solutions, in which the battery system is discharged during the peak period but not at its maximum capacity. In this sense, the BCS do not prioritizes any of the considered objectives.



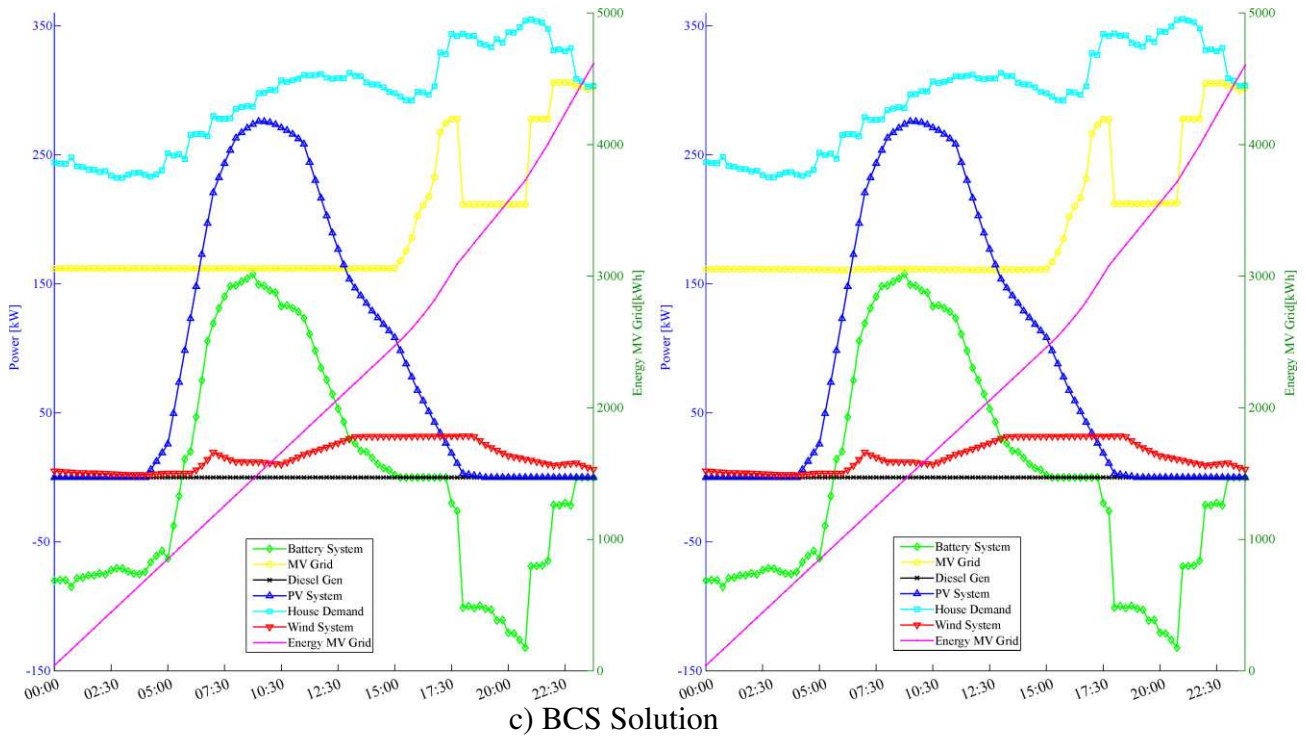
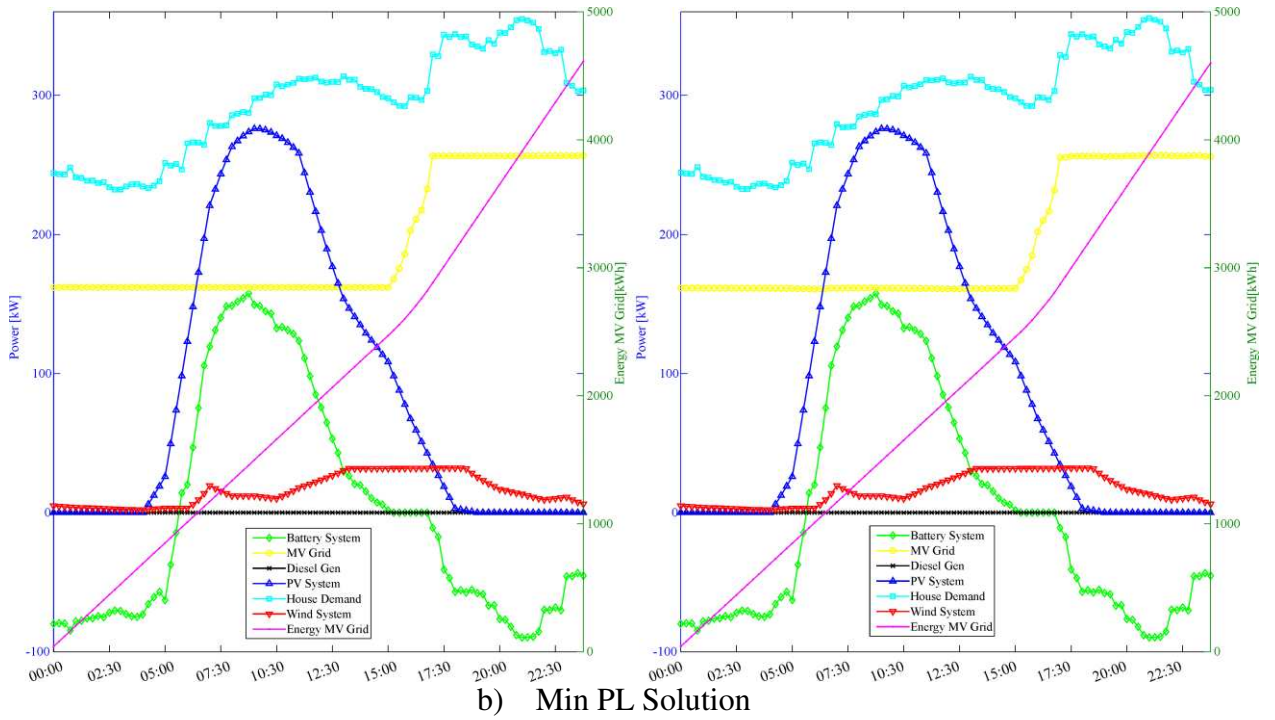


Figure 21. Scenario I: Output power for the battery system, PV and wind system, diesel generator and main grid for the Perfect Forecast case given by the long-term stage.

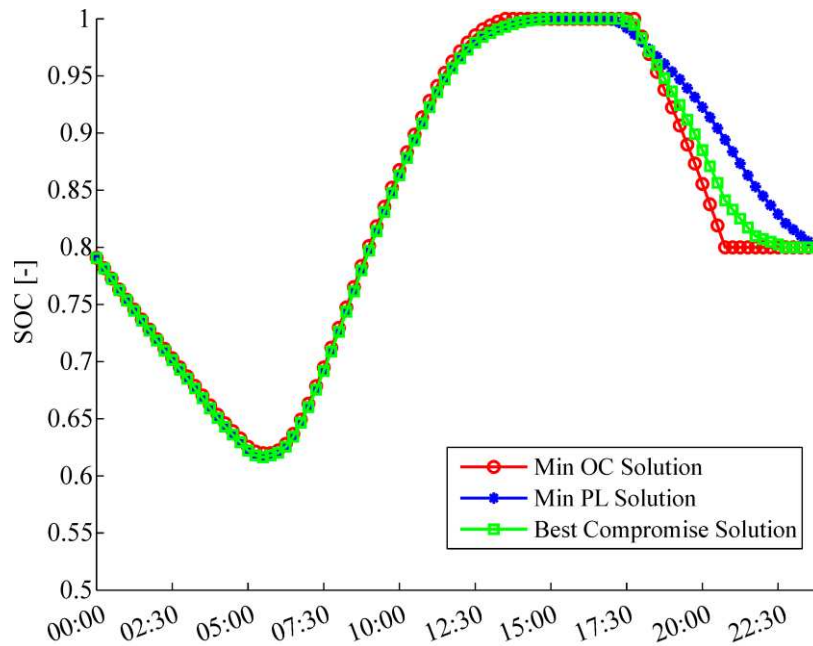


Figure 22. Scenario I: State-of-Charge (SOC) for the Perfect Forecast case.

Regarding the ESS, for the three solutions analyzed it is possible to observe that the long-term stage dispatches the battery system in charging mode at noon, and uses the energy generated by the PV and wind system to reduce the power extracted from the main grid. At this point, it is important to highlight that to reduce both objectives, the long-term stage uses the battery system to follow variations in the load consumption, maintaining the power extracted from the main grid constant.

In terms of the SOC, in Figure 22 it is observed the SOC for the three analyzed solutions. Here, for the Min OC Solution the long-term stage dispatches at its maximum capacity the battery system in discharging mode in the peak period until it reaches the final SOC condition (SOC at 80%). This final condition is reached before the Min PL and the BCS solution. The BCS solution corresponds to the solution with the lowest discharge rate. On the other hand, if the final SOC is not limited, i.e., if the technical constraint shown in Equation (33) is not considered, the long-term stage will use all the energy stored in the battery system to reduce

to the minimum the power extracted from the main grid during the peak period, reducing the final operational cost.

Table 10. Scenario I: OC, PL and Energy provided by the MV grid for different operational scenarios.

Scenario <sup>1</sup>	OC [USD\$]	PL [kW]	Energy [kWh]
MV	794.22	397.6	7138.24
MV+PV	592.20	258.57	4973.16
MV+PV+WT	550.26	258.57	4611.05
Min OC Sol	503.88	280.08	4604.54
Min PL Sol	521.12	265.79	4600.74
BCS Sol	511.58	270.96	4602.16

To compare and assess the impact of the long-term stage (and in general, the Energy Management System) in Table 10 it is presented comparative results for different operational scenarios. According to Table 10, when the PV and the wind system are considered, the final OC and the PL can be reduced 30.7% and 34.9%, respectively, mainly because the power consumption from the MV grid is reduced. Similarly, the power losses are reduced because the PV system is distributed through the distribution system, near to the residential loads. The wind system do not participate in the reduction of the PL because it is located near to the MV node, outside of the distribution system.

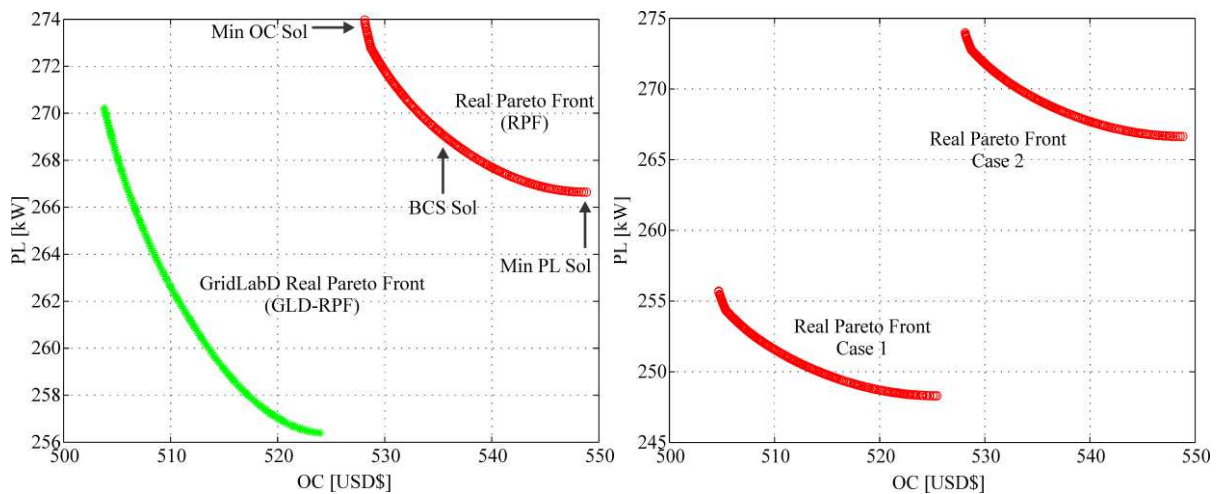
On the other hand, when the MV+PV+WT solution is compared with the Min OC Sol, the Min PL Sol and the BCS Sol a reduction in the final OC of 8.4%, 5.3% and 7.0% can be achieved, respectively. This reduction is a result of the management performed by the long-term stage in the MG. As for PL, the Min OC Sol, the Min PL Sol and the BCS Sol have a greater value than the MV+PV+WT solution. This increment in the PL is a result of the

---

<sup>1</sup> The scenario named as MV do not consider any distributed generation system, all the load consumption is provided by the MV grid. In the MV+PV only the PV system is considered. Finally, in the MV+PV+WT scenario, the PV and the wind system are considered.

battery system, which increase the power purchased from the MV grid when operate in charging mode. However, the inclusion of the battery systems allows the long-term stage perform energy management and reduce the final OC, as already discussed. In terms of the amount of energy provided by the MV grid, for the three analyzed solutions it is almost equal. However, its different OC and PL values are a consequence of its different operational characteristics defined by the main objective and the management performed by the EMS.

For the second study case, named as Real Operational case, the NSGA-II+QP algorithm was executed considering 200 individuals and 1000 generations, obtaining the PF shown in Figure 23a). These values for the number of individuals and total generation are defined experimentally, aiming to ensure good convergence of the algorithm.



a) Pareto front case 2.

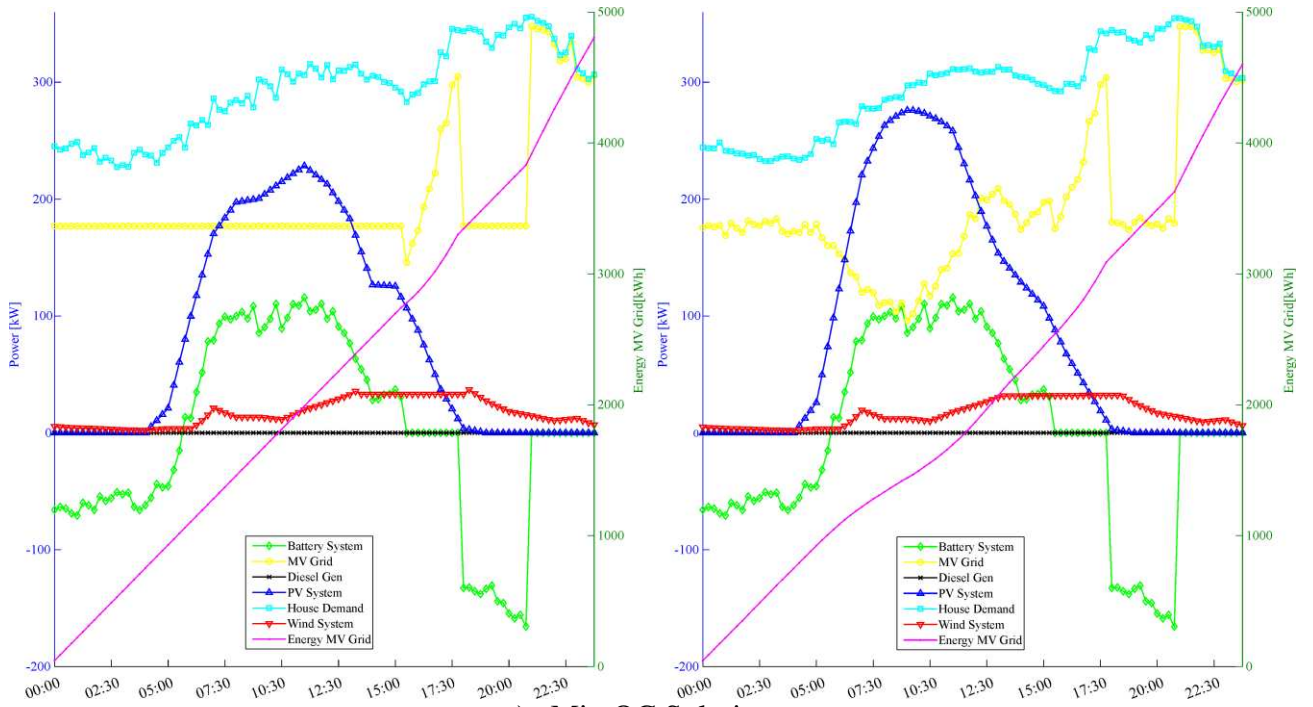
b) Pareto front for the two case study considered.

Figure 23. Scenario I: Pareto Front results obtained for the Real Operational case.

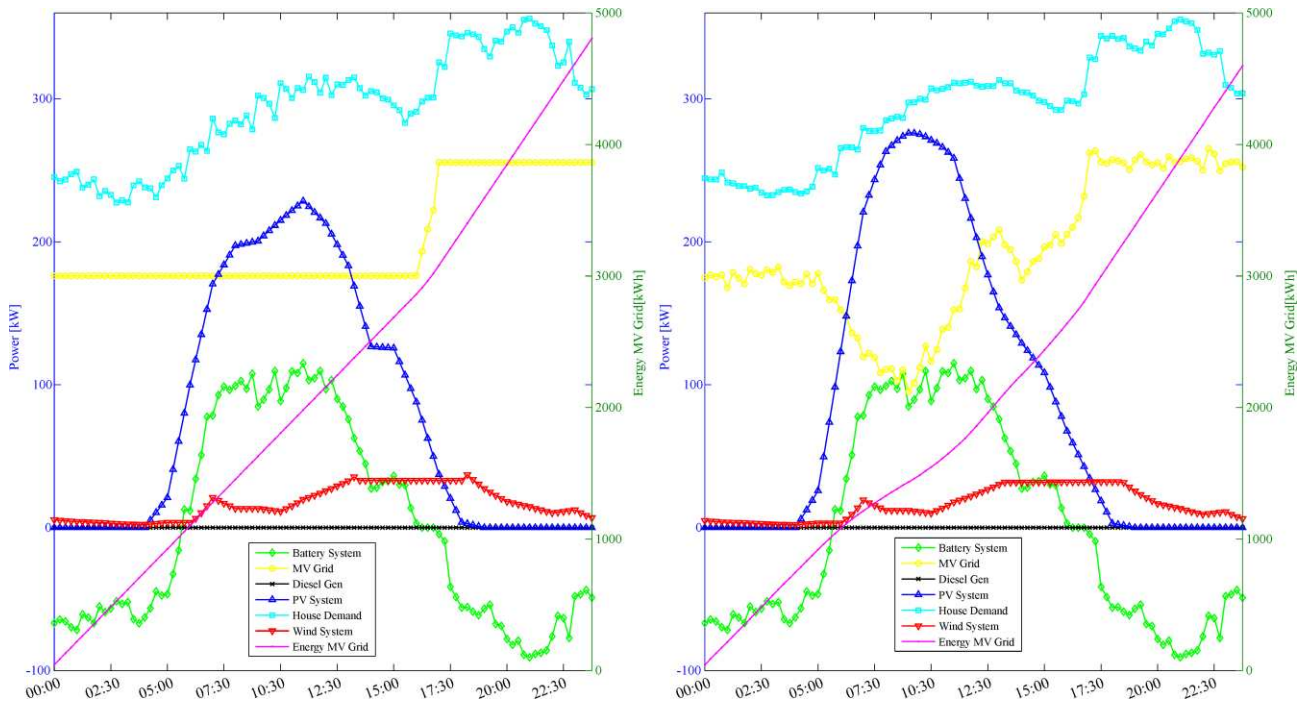
As in the Perfect Forecast case, the final Pareto front obtained re-calculating the objectives using GridLabD varies from the Final Pareto Front obtained using the NSGA-II+QP algorithm. However, in this second case of study the power losses were over-estimated. In case, the maximum RE is close to 4.8% and 4% for the OC and PL, respectively. Now, when the two Final Pareto Front for both case of study are compared, as in Figure 23b), it is

observed that the FPF for the second case have greater values for both objectives, as expected, considering that load consumption and the RES systems generation are not forecasted perfectly.

Related to the operational characteristics of the optimal solution, in Figure 24 are shown the output power for all the distributed generation systems and the MV grid for the Min OC, the Min PL and BCS Solution. According to Figure 24, the PV model estimates a PV maximum generation lower than the real one, and as a consequence the final amount of power provided by the MV grid is lower than the value expected by the long-term stage. For the Min OC Sol, the long-term stage dispatches the battery system at the intermediary and peak period, reducing the power supplied by the main grid, as in the Perfect Forecast case. Similarly, for the Min PL Sol, the long-term stage maintains the power extracted from the grid constant in order to reduce the power losses. However, as the load consumption and RES generation are not forecasted perfectly, the real operation schedule shows that the power extracted from the main grid changes constantly, increasing the power losses, when compared with the perfect forecast case. For all the solution analyzed, the long-term stage dispatch the battery system in charging mode at noon, when the PV generation is at its maximum.



a) Min OC Solution



b) Min PL Solution

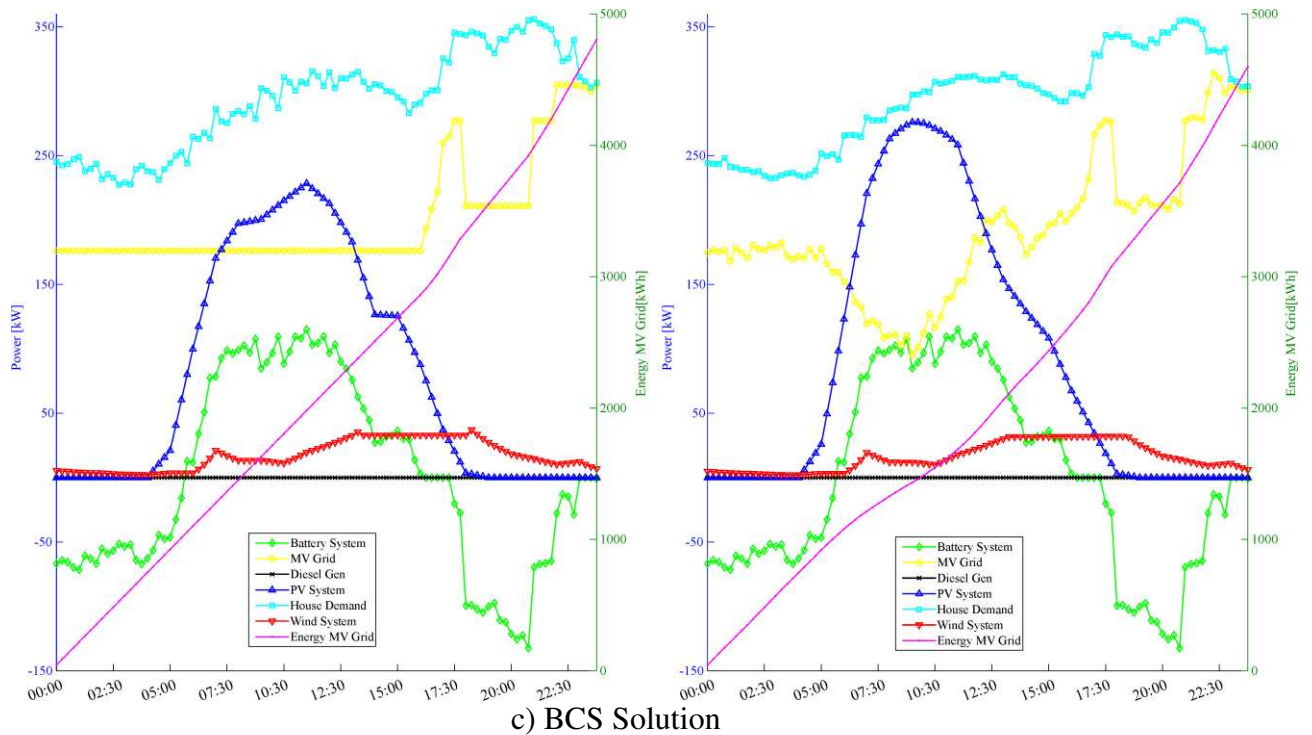


Figure 24. Scenario I: Output power for the battery system, PV and wind system, diesel generator and main grid for the Real Operational case given by the long-term stage.

Related to the ESS, the amount of power used by the battery system in charging mode at noon is lower than the value used in the Perfect Forecast case, this is a consequence of the lower expected PV generation value. In terms of the SOC, in Figure 25 it is shown the SOC for the three solution analyzed. As in the Perfect Forecast case, for the Min OC Solution the long-term stage dispatch the battery system in discharging mode in the peak period until it reaches the final SOC condition.

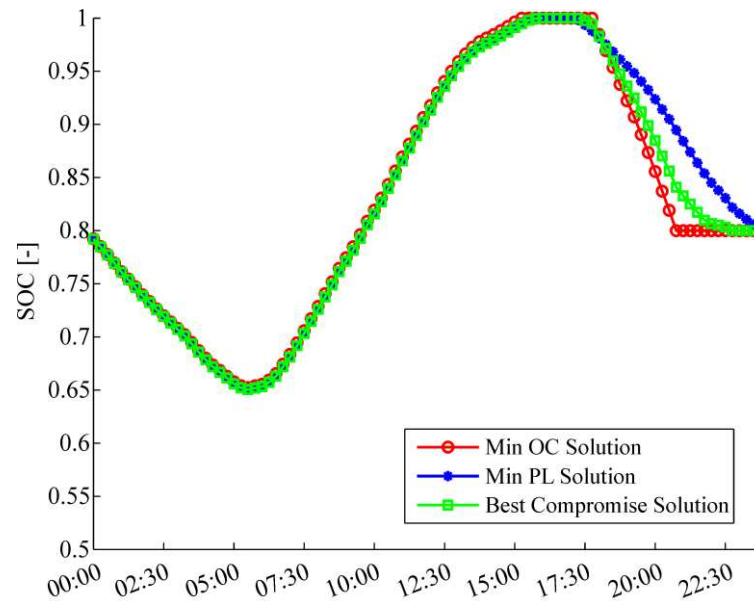


Figure 25. Scenario I: State-of-Charge (SOC) for the Real Operational case.

If the SOC of the battery system is compared for both operational cases, the three solutions reaches a minimum level of 61.99% for the Perfect Forecast case, 3.25% lower than the value reached in the Real Operational case. In addition, in Figure 27 it is shown the RE of the SOC for the three solutions when compared for both operational cases. According to Figure 27, the maximum RE for the three solutions is near to 6%, i.e., the forecast error has an impact in the final solution in almost 6% for the ESS. This means that, if the load consumption and the RES generation are not forecasted accurately, the long-term stage will not dispatch all the energy stored in the battery system, given more priority to the MV grid, which implies an increment in the final OC of the microgrid. However, it is important to highlight that the final shape of the SOC of the battery system remains similar for both cases considered, which means that the forecast error do not have a major impact, as long as the forecast system forecast accurately the trend (i.e., high and low periods) in the load consumption and the RES generation.

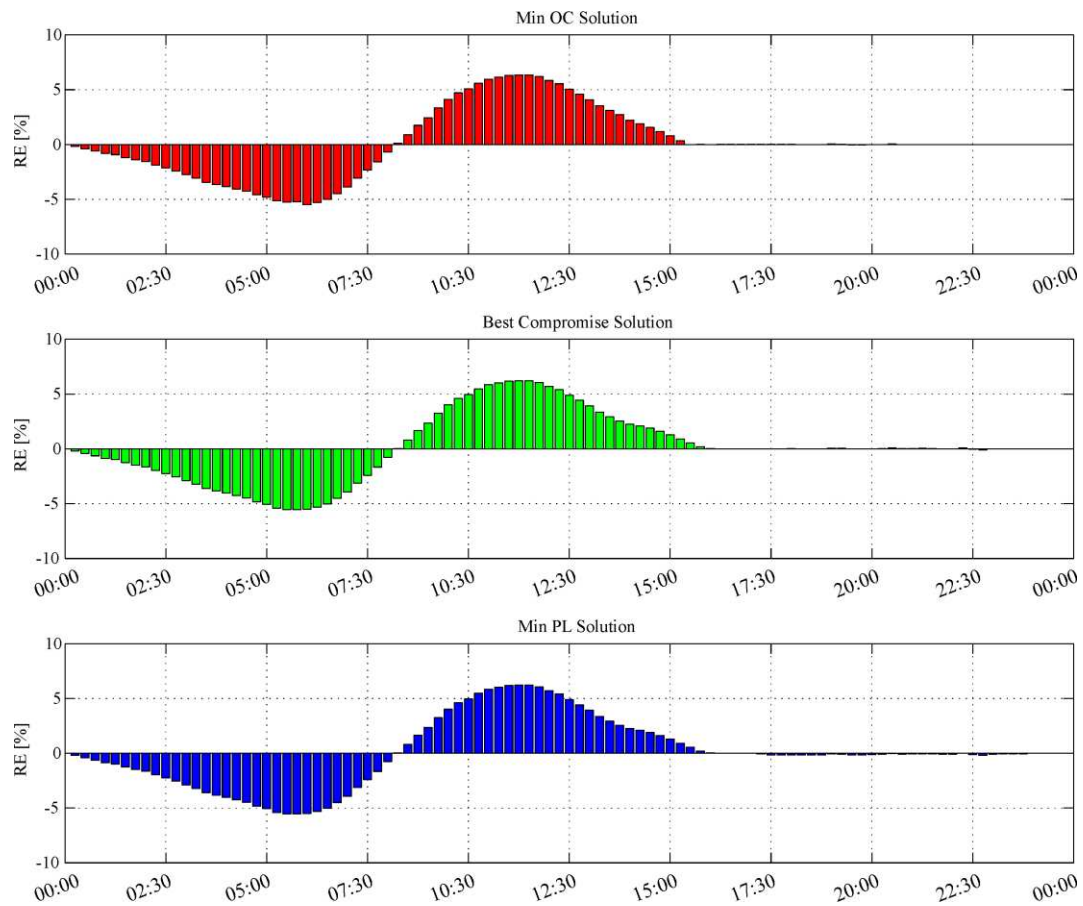


Figure 26. Scenario I: Relative Error (RE) for the SOC for both operational cases considered.

Furthermore, if the final optimal solutions analyzed are compared for both operational cases considered, as in Table 11, it is possible to conclude that the forecast error has an impact near to 5 % in the final OC and 7.5 % in the final PL. In addition, as previously discussed, the amount of energy dispatched by the battery system is lower for the Real Operational case compared to the Perfect Forecast case, near to 9%, and as a consequence, there is an increment in the energy supplied by the MV grid, near to 4.3%. This increment in the energy supplied by the MV grid can be considered small enough to be neglected for one day of operation. However, this error may have a major impact in the economic operation of the microgrid in an annual operation basis.

Table 11. Scenario I: Comparative results for the Min OC, the Min PL and the BCS Sol for the both operational cases considered.

Total	Case	Min OC	Min PL	BCS
$E_G$ [MWh]	PF	4.61	4.61	4.61
	RO	4.80	4.80	4.80
	RE[%]	<b>4.17</b>	<b>4.17</b>	<b>4.17</b>
$E_{CH}$ [kWh]	PF	820.0	827.5	827.5
	RO	750.0	755.0	755.0
	RE[%]	<b>-8.53</b>	<b>-8.76</b>	<b>-8.76</b>
$E_{DCH}$ [kWh]	PF	820.0	827.5	827.5
	RO	750.0	755.0	755.0
	RE[%]	<b>-8.53</b>	<b>-8.76</b>	<b>-8.76</b>
OC [USD\$]	PF	504.70	525.46	512.54
	RO	528.13	548.83	535.98
	RE[%]	<b>4.64</b>	<b>4.25</b>	<b>4.57</b>
PL [kW]	PF	255.70	248.29	250.55
	RO	273.96	266.64	268.88
	RE[%]	<b>7.14</b>	<b>7.39</b>	<b>7.31</b>

For both operational case considered, and shown in Figure 21 and in Figure 24, can be seen that the long-term stage does not dispatch the diesel generator. This is mainly due to the higher cost of the diesel fuel when compared with the cost of the energy that can be provided by the main grid. These results are also a consequence of the topology of the distribution system, in which the diesel generator is located near to the MV grid connection node. If the diesel generator were located near to the residential loads, this would be dispatched by the EMS to reduce power losses. However, according to the 482/2012 resolution, in Brazil it is not allowed to connect conventional generators in low voltage networks.

In both operational cases studied, the maximum power that the MV grid can supply is equal to the maximum load consumption, near to 350 kW. However, if this maximum power is limited, the EMS has to dispatch the diesel generator to meet all the operational constraints, especially the active power reserve constraint. To evaluate this scenario, in Figure 27 is

shown the schedule of the BCS solution given by the EMS when the users establish an agreement with the utility, limiting the amount of power purchased from the main grid to 250 kW.

As it can be seen in Figure 27, the diesel generator is dispatched at intermediary and peak periods, when the power supplied by the MV grid reaches its maximum value. In off peak periods, the diesel generator is still not attractive to the EMS. In Figure 27 it is important to highlight that, as the MV grid is dispatched at its maximum capacity, the active power reverse is guaranteed by the diesel generator and the battery system, while the power balance constraint is met. The diesel generator is not dispatched at its maximum capacity to reduce the final OC.

On the other hand, if the Life Loss Cost (LLC) of the battery system is considered in the energy management problem, the EMS will reduce the amount of power supplied by the battery system to reduce its life loss cost levels, as it can be seen in Figure 28. Thus, the diesel generator is dispatched at the peak period to supply load consumption, while the battery system operates with higher SOC values. In the BCS shown in Figure 28, the diesel generator is dispatched at its maximum capacity, this is due to the higher cost of operating the battery system with lower SOC values, compared to the diesel fuel cost.

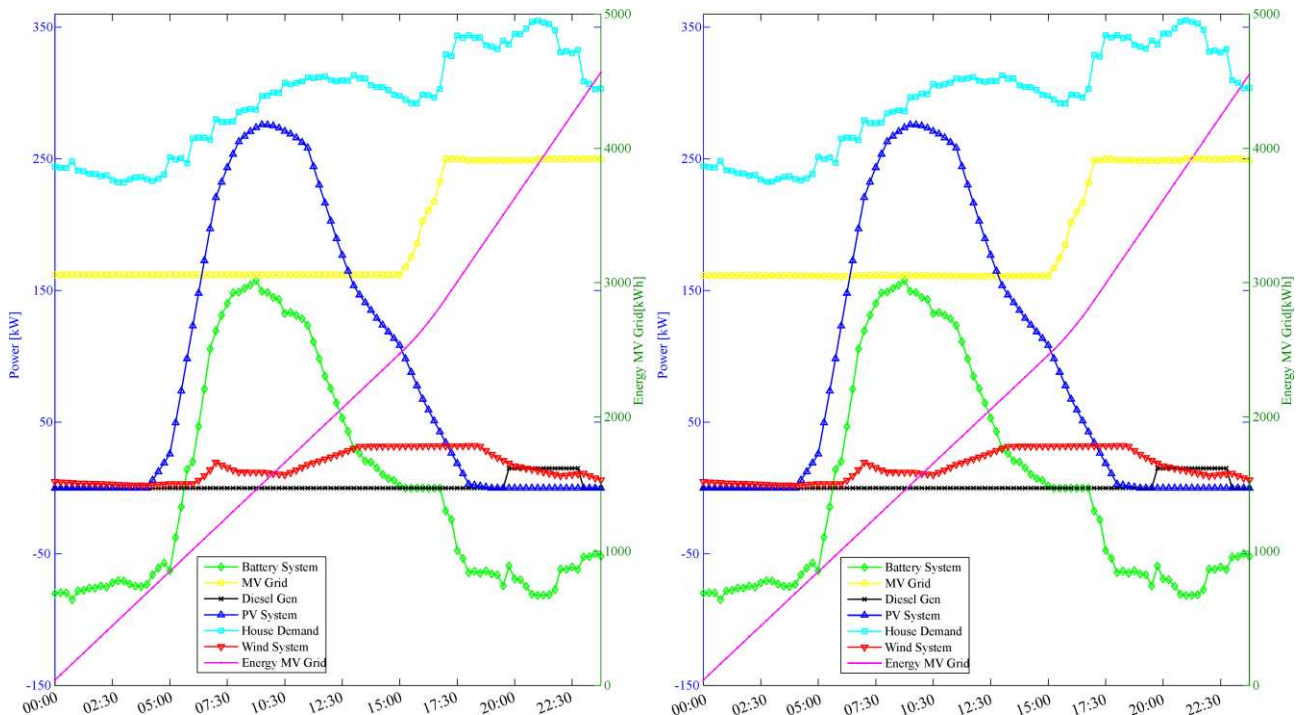


Figure 27. Output power for the battery system, PV and wind system, diesel generator and main grid for the Perfect Forecast case, limiting the power supplied by the MV grid.

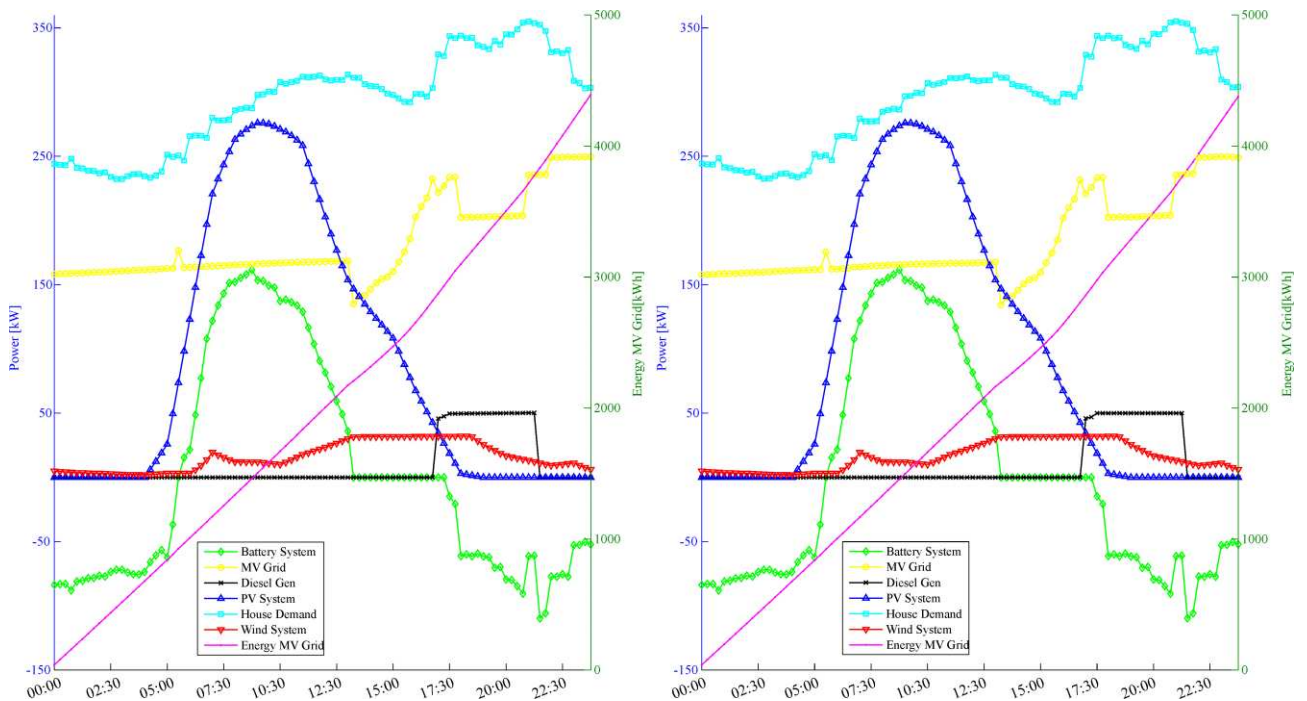


Figure 28. Scenario I: Output power for the battery system, PV and wind system, diesel generator and main grid for the Perfect Forecast case, considering the LLC of the battery system given by the long-term stage.

Table 12. Scenario I: OC, FC, PL and Energy provided by the MV grid for the cases where the diesel generator is more attractive.

Solution	OC [USD\$]	FC [l]	PL [kW]	Energy [kWh]
Min OC Sol	503.88	0	280.08	4604.54
Min PL Sol	521.12	0	265.79	4600.74
BCS Sol	511.58	0	270.96	4602.16
BCS limiting the MV grid power	548.65	28.94	265.31	4551.89
BCS considering the LLC of the ESS	605.34	109.06	268.96	4378.97

A comparison of the results for all the solutions and cases analyzed in this section is presented in Table 12, where it is possible to observe how the OC is increased when the diesel generator is dispatched, and consequently, the energy supplied by the MV grid is reduced. Finally, it is important to highlight that a case with higher values of energy cost was also considered. However, even considering the higher energy cost of all the utilities in the Brazilian market, the diesel generator was not attractive to be dispatched by the EMS. This is mainly due to the high value of the diesel cost, compared to the cost of the energy that the MV grid can provide.

#### 5.4 SHORT-TERM STAGE

As in the long-term stage, a Perfect Forecast and Real Operational case will be analyzed for the short-term stage. However, for the Perfect Forecast case, the load consumption and the RES generation used are obtained using linear interpolation techniques considering the same data as for the long-term stage. This means that even for the Perfect Forecast case there is not perfect knowledge of the load consumption and the RES generation.

As described in Section 4.2, the long-term solution selected to be implemented by the EMS (here will be analyzed also the Min OC and the Min PL solution), defines the SOC of the battery system for every hour of the next 24-hours of operation. Considering this SOC

information, the short-term stage define the power of the distributed generation systems and the MV grid. This is done solving 24 ELD problems independently.

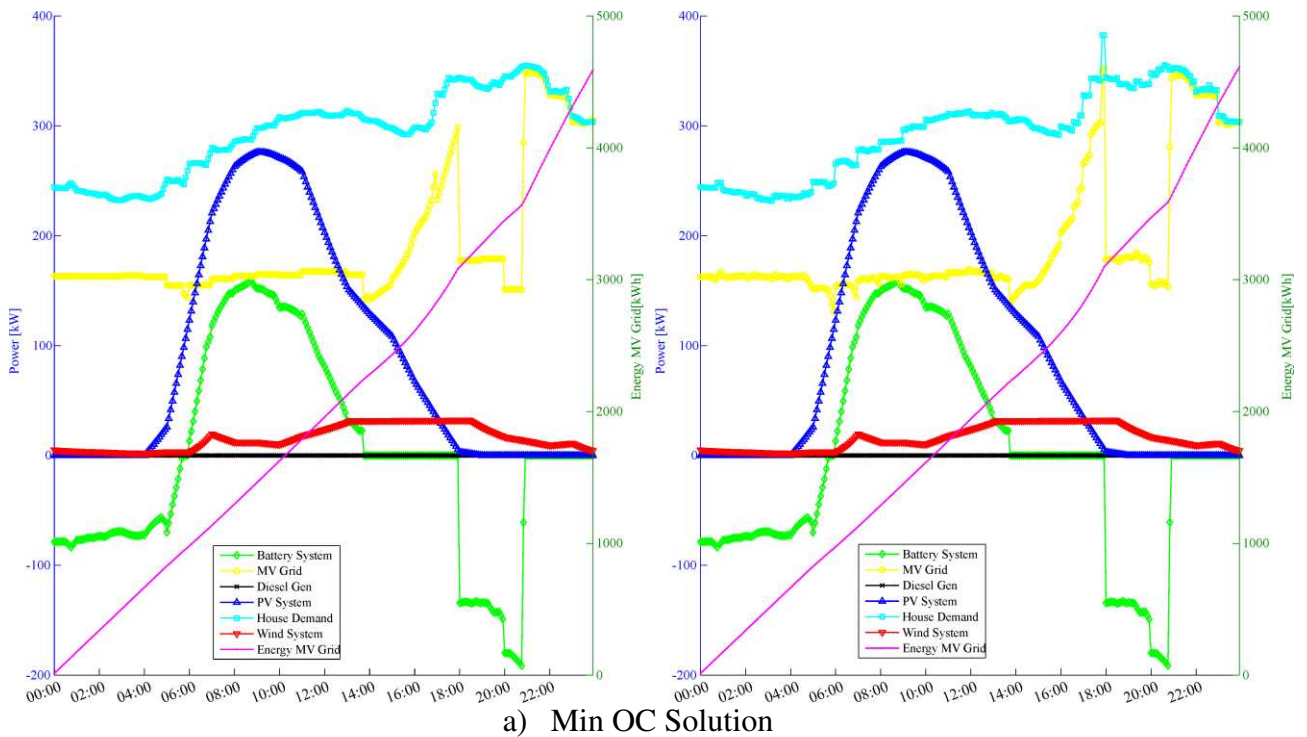
In Figure 29 it is shown the output power for all the distributed generation systems and the MV grid for the Min OC, Min PL and BCS Solution for the Perfect Forecast case. As it can be seen in Figure 29, the short-term stage of the EMS can follow sudden changes in load consumption successfully, defining the output power of the MV grid to match generation and consumption. Furthermore, as the initial and final condition of the SOC is previously defined by the long-term stage for every hour of operation, the charge/discharge profile of the battery system is in accordance with the dispatch profile estimated by the long-term stage (and shown in Figure 21), although the output/input power of the battery system are different. This strategy, in which the long-term stage defines the SOC for the operational day, allows the short-term stage to consider the intrinsic characteristics of the ELD problem in long-term, considering that the main function of the short-term stage is to reduce power unbalance.

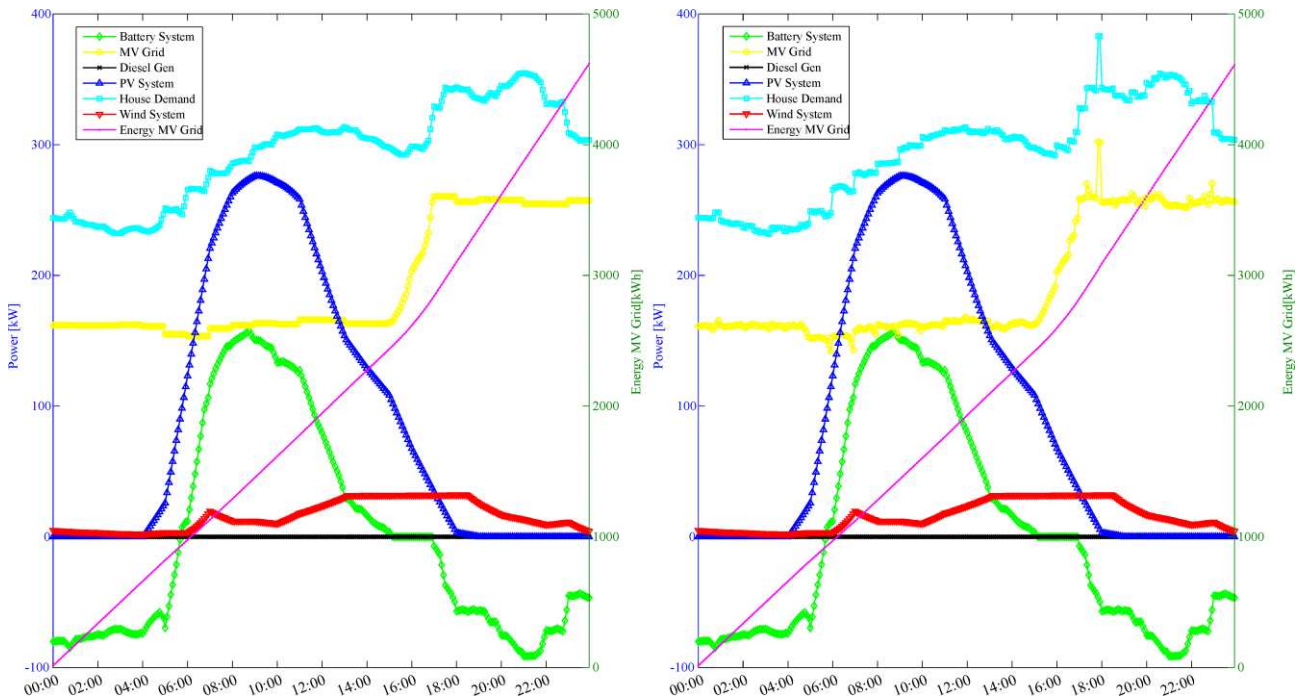
Finally, in Figure 29 the main difference between the solution obtained using the short-term stage of the EMS (left) and the solution implemented in GridLab-D (right) is related to the not perfectly knowledge of the load consumption and the PL models used, which increase the final OC and PL of the solution, as has been discussed through this Chapter. In Table 13 it is shown comparative results for the three solution analyzed obtained using the EMS and the simulation using GridLab-D. According to these results, the solution obtained using the short-term EMS has a RE near to 1% for the OC, 10% for the PL and 0.3% for the total Energy when compared with the solution obtained after simulate the optimal schedule in GridLab-D. In terms of OC, PL and total Energy is not possible to compare the solutions shown in Figure 29 and in Figure 21, mainly because the input information for both solution is not exactly the

same (load consumption and RES generation), although they represent the same operational case.

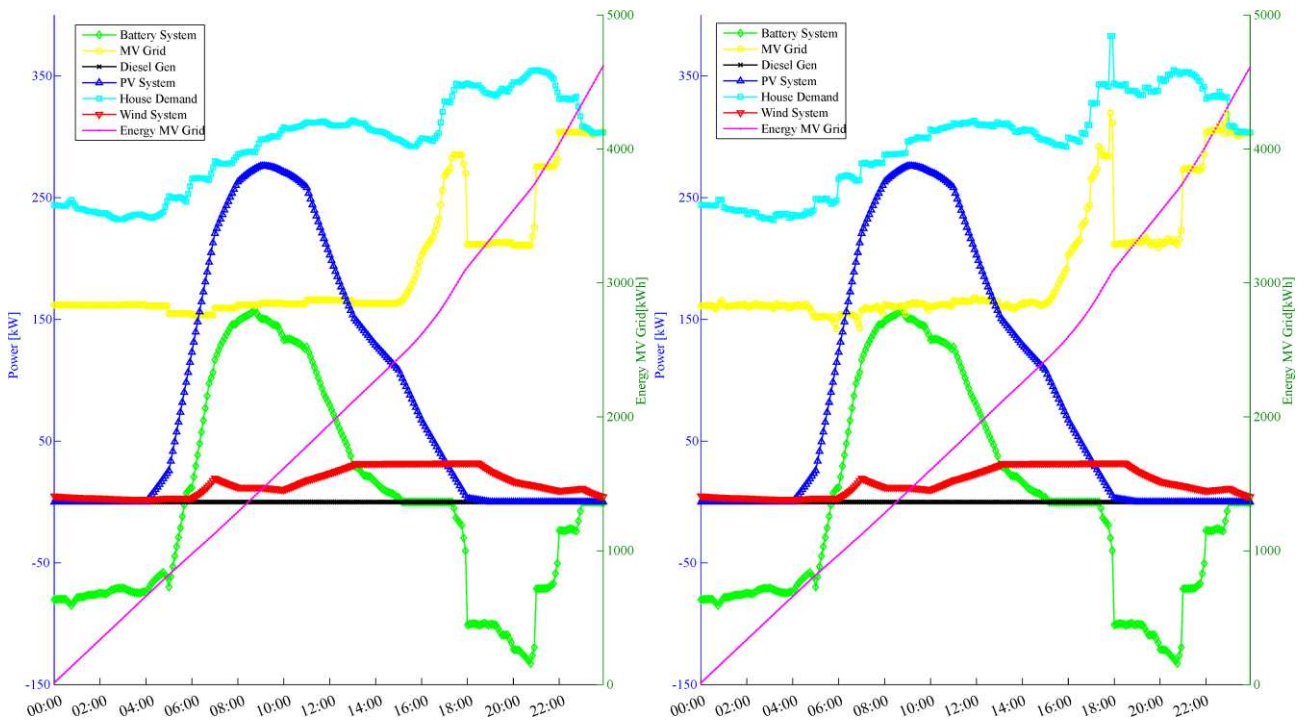
Table 13. Scenario I: Comparative results for the solution obtained using the EMS and the simulated solution in GridLab-D for the Perfect Forecast case.

		Min OC	Min PL	BCS
OC [USD\$]	Short-term EMS	501.30	526.35	513.66
	GridLab-D	505.31	525.83	513.51
	RE[%]	<b>-0.79</b>	<b>0.09</b>	<b>0.02</b>
PL [kW]	Short-term EMS	761.09	747.02	753.63
	GridLab-D	850.07	801.99	817.96
	RE[%]	<b>-10.46</b>	<b>-6.85</b>	<b>-7.37</b>
Energy [kWh]	Short-term EMS	4602.4	4602.4	4602.4
	GridLab-D	4614.0	4609.7	4611.2
	RE[%]	<b>-0.25</b>	<b>-0.15</b>	<b>-0.19</b>





b) Min PL Solution



c) BCS Solution

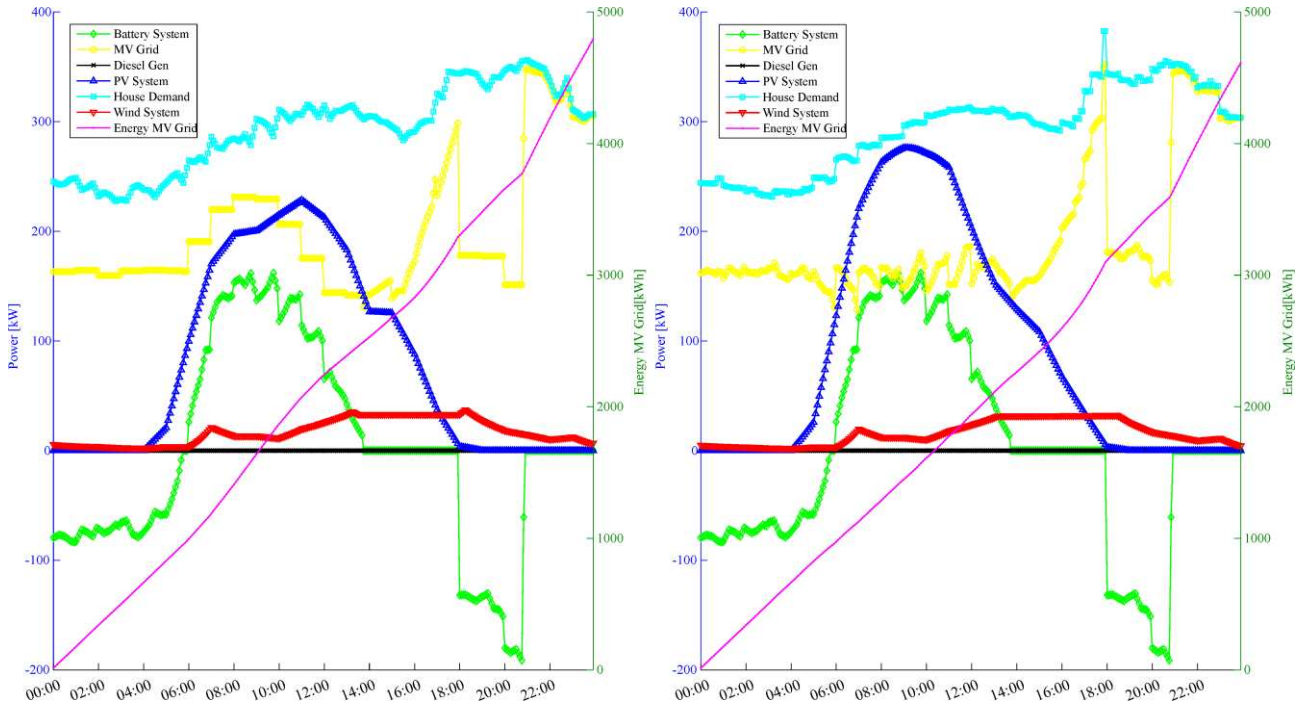
Figure 29. Scenario I: Output power for the battery system, PV and wind system, diesel generator and main grid for the Perfect Forecast case given by the short-term stage.

For the Real Operational case, the load consumption and the RES generation considered is provided by a forecast module, obtaining the output power schedule of the distribution

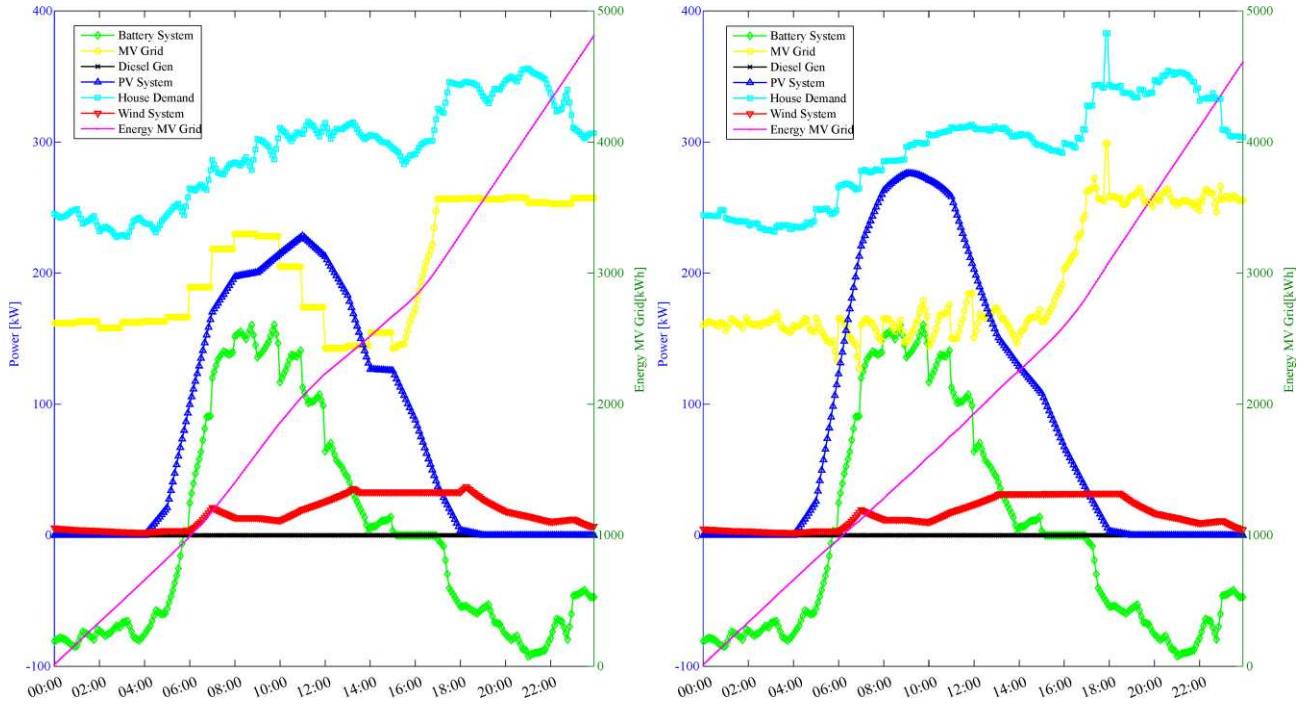
generation systems and the MV grid shown in Figure 30. As for the Perfect Forecast case, the solution obtained using the short-term stage varies from the solution simulated in GridLab-D as a result of the forecast error and the PL models used, with the RE shown in Table 14. However, it is possible to observe that the dispatch profile of the battery system remains similar to the Perfect Forecast case and to the long-term stage. This is a result of the predefined SOC that the long-term stage provides to the short-term stage, while the power supplied by the MV grid is defined to match the load consumption and the generation.

Table 14. Scenario I: Comparative results for the solution obtained using the EMS and the simulated solution in GridLab-D for the Real Operational case.

		Min OC	Min PL	BCS
OC [USD\$]	Short-term EMS	519.99	543.77	531.09
	GridLab-D	505.31	525.82	513.51
	RE[%]	<b>2.90</b>	<b>3.41</b>	<b>3.42</b>
PL [kW]	Short-term EMS	808.42	791.26	797.76
	GridLab-D	849.85	801.83	817.71
	RE[%]	<b>-4.87</b>	<b>-1.31</b>	<b>-2.43</b>
Energy [kWh]	Short-term EMS	4811.30	4811.30	4811.30
	GridLab-D	4613.90	4609.70	4611.11
	RE[%]	<b>4.27</b>	<b>4.37</b>	<b>4.34</b>



a) Min OC Solution



b) Min PL Solution

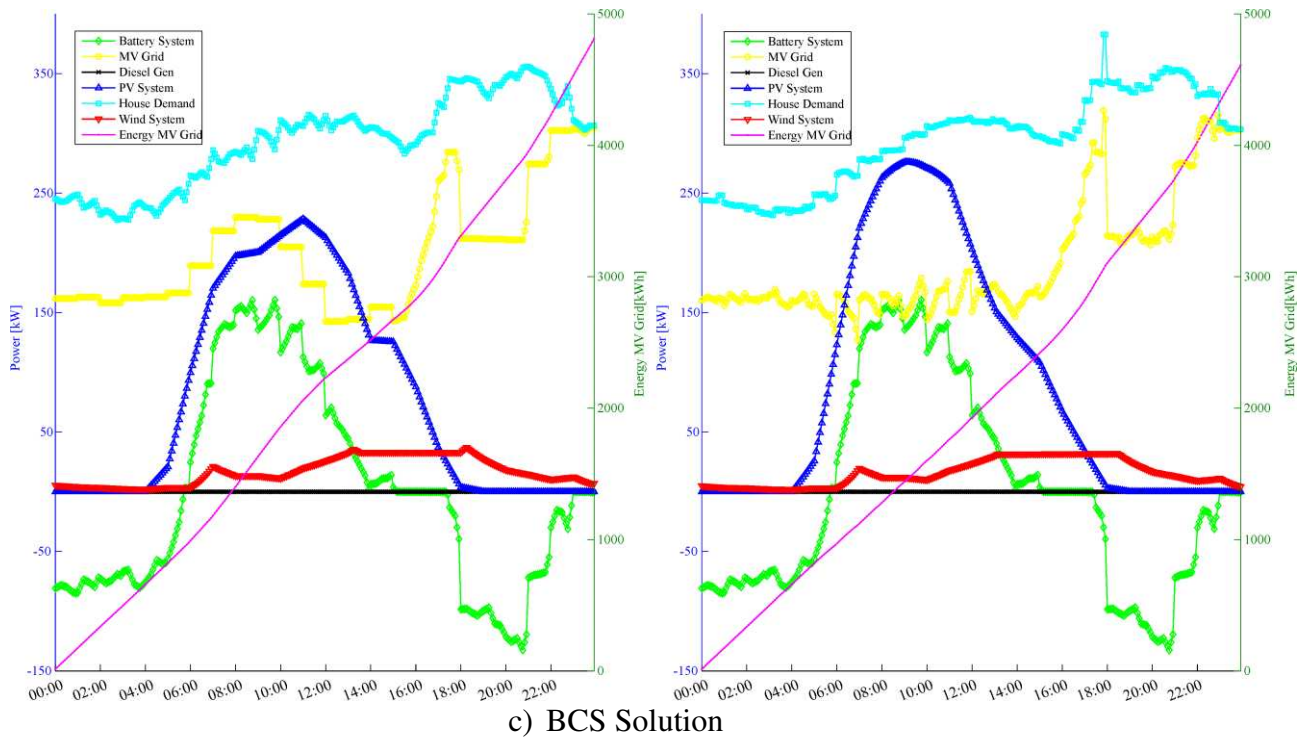


Figure 30. Scenario I: Output power for the battery system, PV and wind system, diesel generator and main grid for the Real Operational case given by the short-term stage.

Table 15. Scenario I: Comparative results for the Min OC, the Min PL and the BCS Sol for both operational cases considered.

Total	Case	Min OC	Min PL	BCS
OC [USD\$]	PF	501.30	526.35	513.66
	RO	519.99	543.77	531.09
	RE[%]	<b>3.72</b>	<b>3.30</b>	<b>3.39</b>
PL [kW]	PF	761.09	747.02	753.63
	RO	808.42	791.26	797.76
	RE[%]	<b>6.21</b>	<b>5.92</b>	<b>5.85</b>
Energy [kWh]	PF	4602.4	4602.4	4602.4
	RO	4811.30	4811.30	4811.30
	RE[%]	<b>4.53</b>	<b>4.53</b>	<b>4.53</b>

Finally, if the Min OC, the Min PL and BCS Sol for both operational cases considered are compared, as in Table 15, is possible to observe that due to the forecast error in the load consumption and the RES generation, there is an RE near to 4% for the OC and 6.5% for the

PL for the three solution analyzed. Similarly to the long-term stage, this error can be considered small enough to be neglected, especially considering that the short-term stage defines the output power for the next operational hour. However, in an annual basis this error can have a major impact in the economic operation of the microgrid.

---

## 6 CASE STUDY II: A MORE INTELLIGENT MICROGRID

---

In this Chapter it is presented a second study scenario, in which the Demand Side Management (DSM) system and Electric Vehicles (EV) are considered in the energy management problem. This second scenario intends to model a more intelligent operational case, in which residential users participate actively in a demand-side management program and all the users have an electric vehicle available to be used for the management of the LV Microgrid.

As in the first scenario presented in Chapter 5, in this Chapter it will be analyzed two operational cases: a Perfect Forecast and a Real Operational case. Also, a performance assessment of the final solutions provided by the long-term stage is presented, including a comparison and an evaluation of the impact of the forecast error in the final operational solution. Finally, it is presented an assessment of the short-term stage of the EMS system.

### 6.1 LONG-TERM STAGE

For the Perfect Forecast case, the algorithm of the long-term stage has been executed considering 200 individuals and 1000 generations, obtaining the Pareto Front shown in Figure 31a). These values for the number of individuals and total generation are defined experimentally, aiming to ensure good convergence of the algorithm. Also, in this first case it is not considered the LLC for the ESS, and for the DSM it is considered a maximum load shifting coefficient of 5%.

In terms of the quality of the final Pareto front, it is possible to conclude that the long-term stage can provide a well-covered Pareto front, even when the DSM and the EV are considered, showing the conflict relation between the objectives. This conflict relation has been discussed previously in Scenario I. The results shown in Figure 31 cannot be compared directly to the Pareto front obtained for the Scenario I, due to the inclusion of the EV as a load, which increase the load consumption from the MV grid and consequently increase the OC.

In Figure 31a), it is also shown the final Pareto front once the objectives are re-calculated using GridLab-D (and named as GLD-RPF), where it is possible to observe that the long-term stage over-estimates the final PLs, due to the error in the power losses models. According to the results obtained for this case of study, the algorithm estimates the OC objective with a maximum RE close to 0.3% and for the PL objective with a maximum error close to 15%. The sources of this modeling error has been previously discussed in Chapter 5.

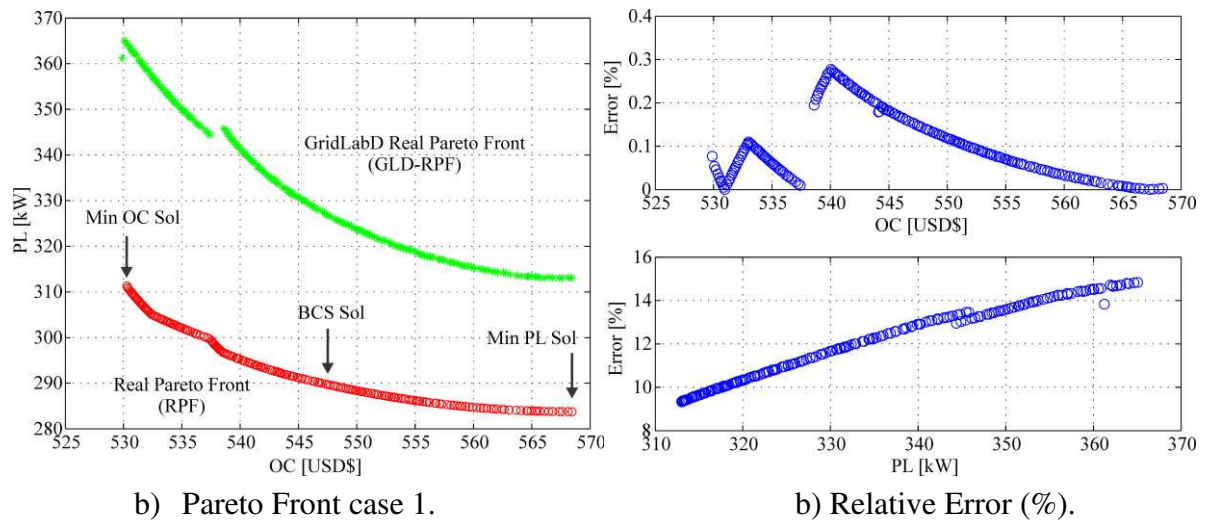
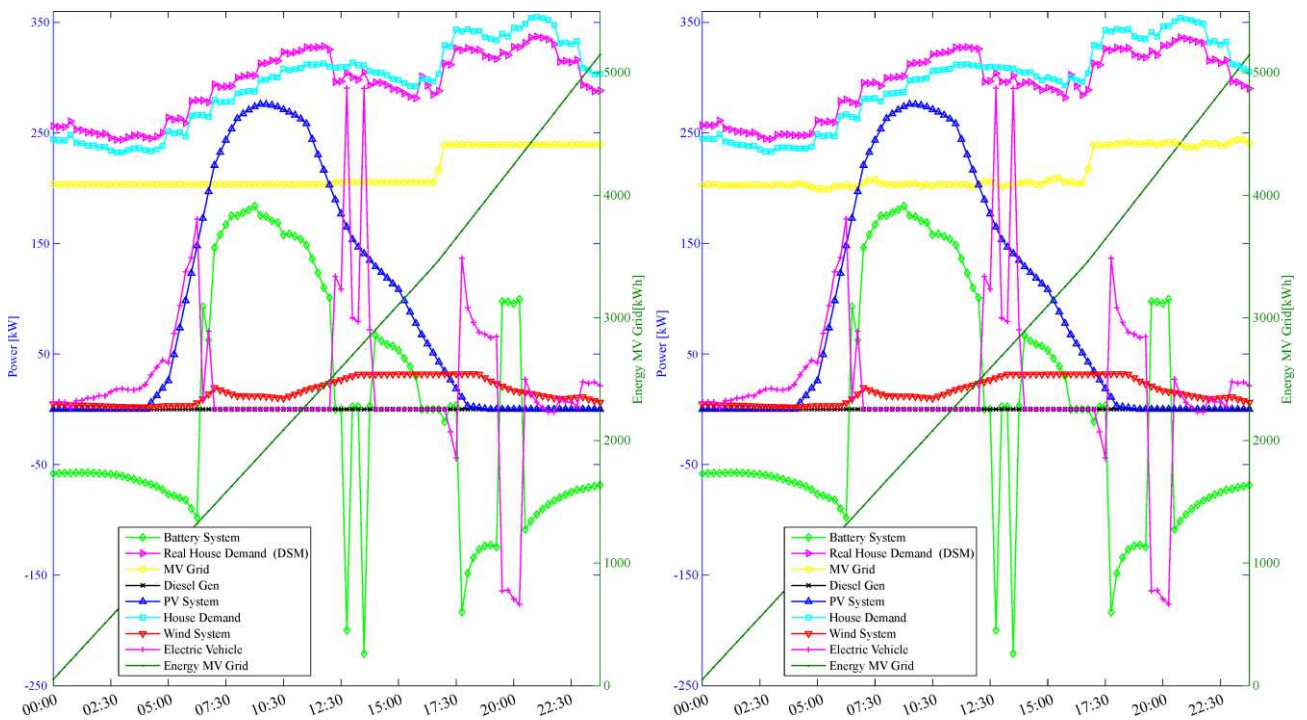
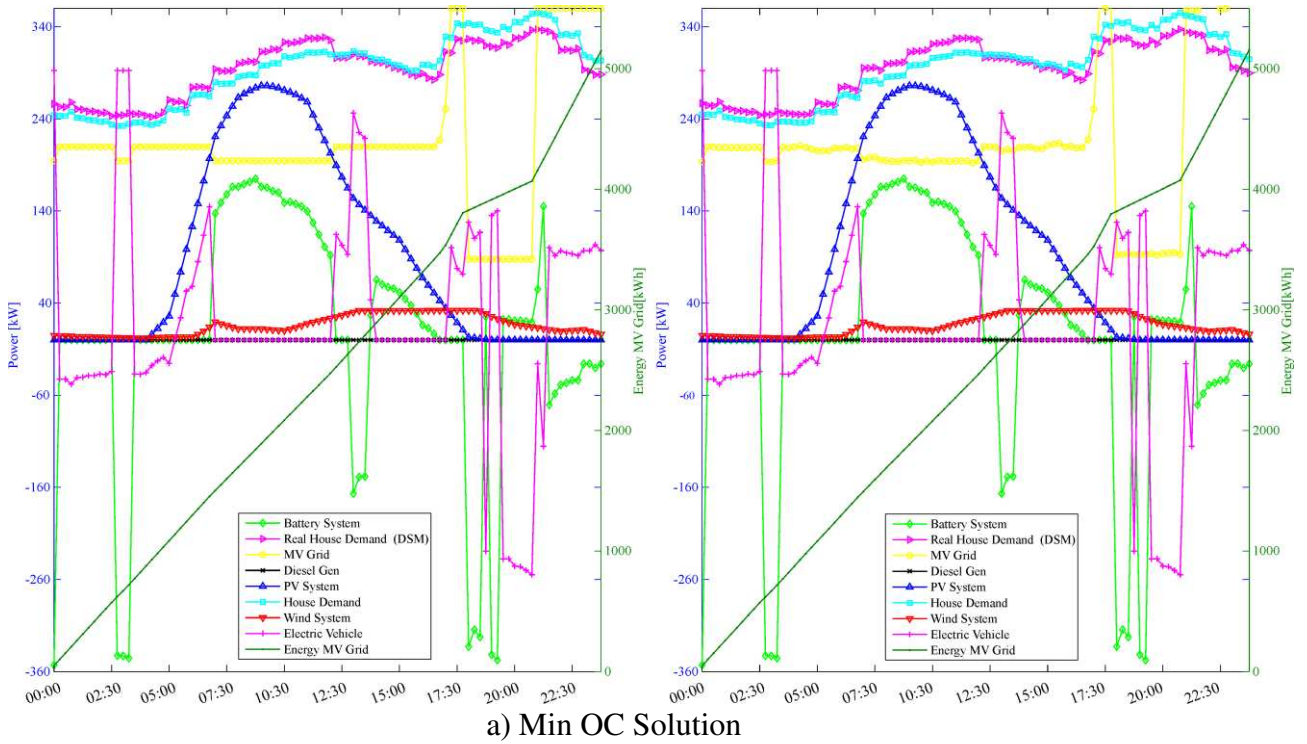


Figure 31. Scenario II: Pareto Front results obtained for the Perfect Forecast case.

Related to the operational characteristics of the optimal obtained schedule, in Figure 32 it is shown the output power of all the generation systems and the MV grid for the Min OC, the

BCS and the Min PL solution, located at the RPF as is shown in Figure 31a). For every solution, in Figure 32 it is presented the optimal solution obtained executing the NSGA+QP algorithm (left) and the same solution once is simulated in GridLabD (right).



b) Min PL Solution

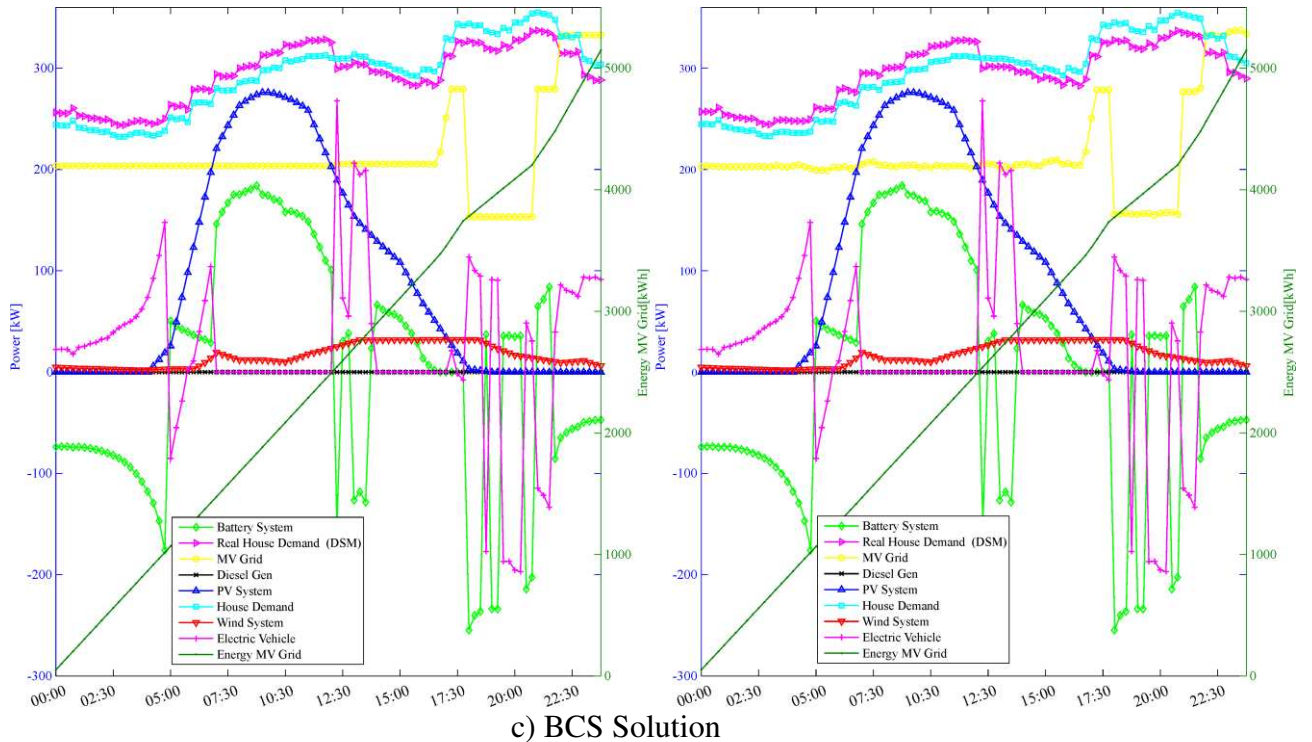


Figure 32. Scenario II: Output power for the battery and EV system, PV and wind system, diesel generator and main grid for the Perfect Forecast case given by the long-term stage.

For the three solution being analyzed, related to the DSM system it is possible to observe how the long-term stage increase the load consumption in 5% (its maximum allowed value) before and at noon, when the PV generation is at its maximum level and the cost of the energy provided by the MV grid is the lowest. As a result, the DSM reduce the load consumption in 5% after noon and until midnight. Also, all the load consumption expected during the day is supplied. According to these results it is possible to conclude that the statement of the DMS, as presented in Section 3.5, meets all its goals.

For the Min OC solution, regarding the ESS and the EV system, when the EV system is available for management in the distribution system, it seems to have a complementary behavior with the battery system and the PV system. For instance, from midnight to 2:00 am, part of the energy stored at the EVs and at the ESS is used to reduce the power extracted from

the main grid, operating both in discharging mode. On the other hand, near to 2:30 am, the long-term stage dispatches the EV in charging mode, purchasing energy from the battery system and not from the main grid. Similarly, before 5:00 am, when the PV system begins to generate power, the EVs uses this power to increase its SOC, while the battery system remains off-line. This is done to fulfill the constraint that the SOC of the EVs at 7:00 am should be equal to 100%. In Figure 33 it is shown the SOC for the battery system and for the EVs.

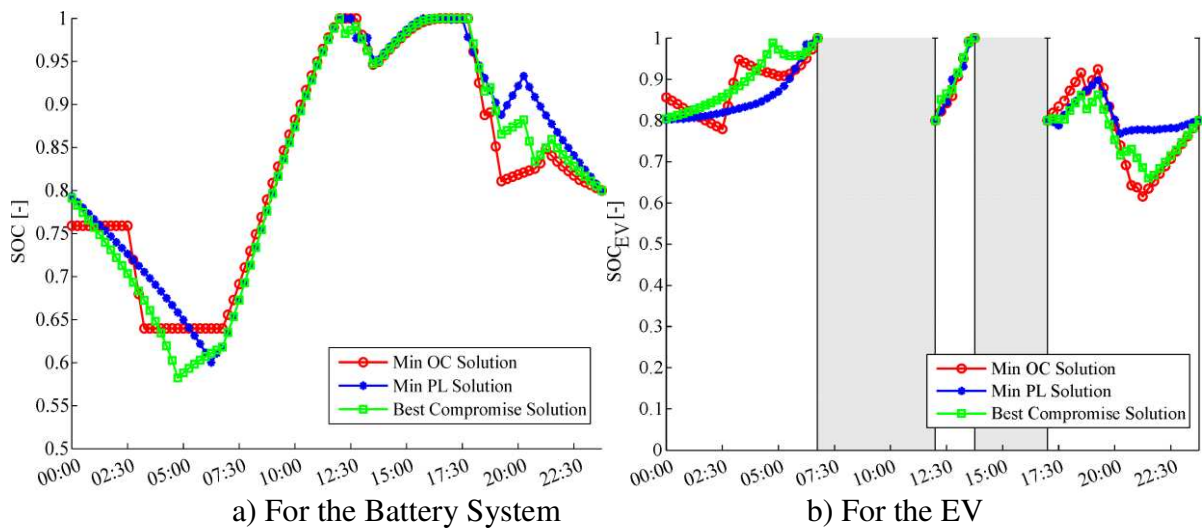


Figure 33. Scenario II: State-of-Charge (SOC) for the Perfect Forecast case.

Additionally, near to noon, and when the EVs is not available for management (from 7:30 am to 12:00 pm), the long-term stage dispatch the battery system in charging mode, using the energy generated by the PV system until it reaches a SOC of 100%. At noon, specifically from 12:00 pm to 2:00 pm, when the EV arrives at home from work, the energy stored at the battery system is used to charge at its full capacity the EVs, fulfilling the constraint that the SOC of the EV should be equal to 100% at 2:00 pm.

Lastly, after 17:00 pm, when the EV arrived from work at the end of the workday, the EV and the battery system are dispatched in discharging mode to reduce the amount of power purchased from the MV grid at the peak period. After the peak period, near to 21:00 pm, the

EV is dispatched in charging mode, purchasing energy from the battery system and from the MV grid. In this period, the MV grid is supplying more power than required by the residential consumers, due to the EV. Finally, as the wind system is not distributed through the distribution system, its output power is subtracted to the power supplied by the MV grid, not taking an important role in the management.

For the Min PL solution, to reduce power losses the long-term stage dispatches all the systems in such a way that the power supplied by the MV grid is maintaining constant. To do this, the EV and the ESS shown a complementary behavior in which, when the EV is in charging mode the battery system operates in discharging mode. The battery system is charged at its maximum capacity at noon when the PV system generates its maximum power. At the peak period and after this, the power supplied by the MV grid is maintain constant near to 250 kW, while the EV is purchasing energy from the battery system from 17:30 pm to 19:30 pm. On the other hand, between 19:30 pm to 21:00 pm, the EV is dispatched at discharging mode and the battery system at charging mode. Finally, after 20:00 pm, the ESS operated in discharging mode. For this solution the EVs and the ESS are the main systems that follows the variation in the load consumption.

For the BCS solution, shown in Figure 32c), the complementary behavior between the EVs and the ESS can be observed during all the operational day. This solution represents a compromise between the two objectives considered, characterized by dispatching the EV and the ESS to reduce the amount and variation of the power purchased from the MV grid simultaneously.

As the ESS and the EV system has shown a complementary behavior, the nominal capacity of these two systems will play a key role in the performance of the EMS. In this sense, if the nominal capacity of the ESS is lower that the capacity of the EV system, the ESS will not be

able to supply all the energy that the EV system will require to have an SOC of 100%. This will increment the operational cost of the final solution because more power will be purchased from the MV grid to fulfill this constraint.

Complementary, the nominal capacity of the ESS and the PV system is also important. As it can be seen in Figure 32, almost all the energy that the EV requires to reach a SOC of 100% comes from the ESS, which reach a SOC of 100% using the energy generated by the PV system. Considering this, all the energy generated by the PV system is used to charge the EV system and the ESS to perform management.

To assess the long-term impact in the operation of the LV MG, in Table 16 it is presented comparative results for different operational scenarios. According to Table 16, the inclusion of the DSM can reduce the OC in 0.81% when comparing to the MV case. Similarly, when the DSM is considered for the MV+PV+WT case, the OC can be reduced in 1.17%.

On the other hand, when the MV+PV+WT+DSM is compared with the Min OC Sol a reduction in the final OC of 2.55% can be achieved. However, the Min PL Sol shows an increment of 17.01% in the PL when compared to the MV+PV+WT+DSM case. This increment is a result of the inclusion of the EVs and the ESS, which increases the power purchased from the MV grid when operates in charging mode. Also, an increment of approximately 12% in the total energy provided by the MV grid can be observed.

Finally, it is important to highlight that the inclusion of the ESS allows the long-term stage perform energy management and reduce the final OC, as was already discussed for the Min OC Sol. Similarly, the final OC of the Min PL Sol and the BCS Sol is not significantly higher, when compared to the MV+PV+WT+DSM case, considering that the EVs operates as a load. This is a consequence of the management performed by the EMS.

Table 16. Scenario II: OC, PL and Energy provided by the MV grid for different operational scenarios.

Scenario <sup>2</sup>	OC [USD\$]	PL [kW]	Energy [kWh]
MV	794.22	397.6	7138.24
MV+DSM	787.76	397.6	7138.24
MV+PV	592.20	258.57	4973.16
MV+PV+WT	550.26	259.80	4611.05
MV+PV+WT+DSM	543.79	259.80	4611.04
Min OC Sol	529.87	361.25	5156.30
Min PL Sol	568.43	313.05	5143.60
BCS Sol	544.55	331.17	5148.40

For the second case of study, named as Real Operational case, the NSGA-II+QP algorithm was executing considering 200 individuals and 100 generations, obtaining the results shown in Figure 34a). In addition, in Figure 34a) it is shown the Final Pareto Front once the objectives are re-calculated using GridLabD. Comparison results of the Final Pareto Front for both operational cases considered is also shown in Figure 34b).

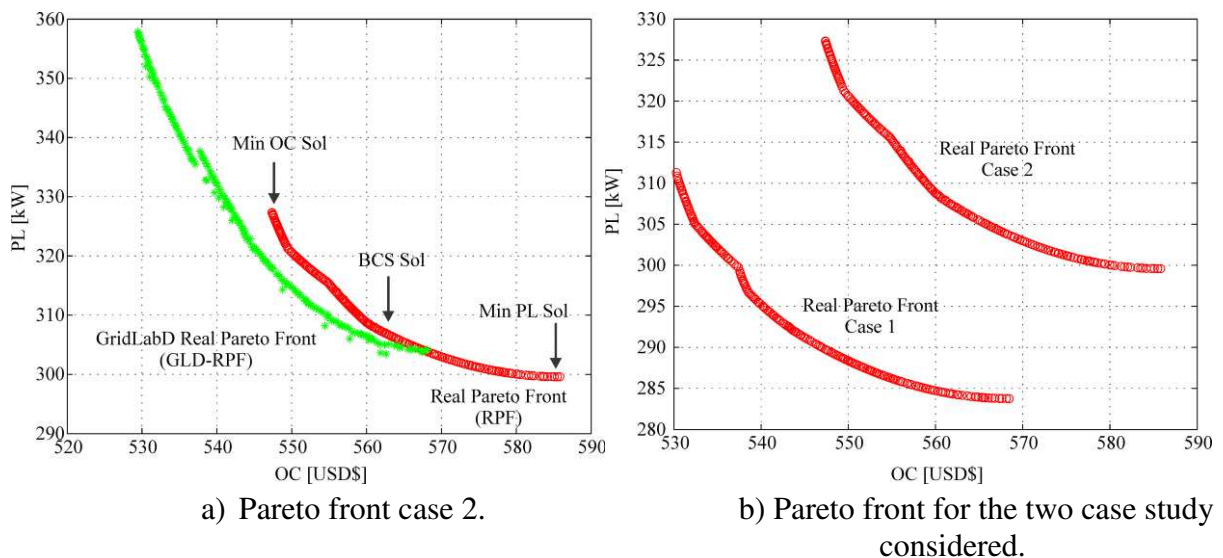


Figure 34. Scenario II: Pareto Front results obtained for the Real Operational case.

<sup>2</sup> The scenario named as MV do not consider any distributed generation system, all the load consumption is provided by the MV grid. In the scenario MV+DSM is considered the Demand Side Management system. In the MV+PV only the PV system is considered. Finally, in the MV+PV+WT, the PV and the wind system are considered.

As expected, the GLD-FPF varies from the FPF obtained using the NSGA-II+QP algorithm due to the power losses models. In this case, the used power losses models underestimate the real power losses in the distribution system, obtaining a maximum RE of 10% for the PL objective and 3.5% for the OC objective. On the other hand, when the FPF of the Perfect Forecast and Real Operational case are compared, it is observed that the FPF for the second case have greater values for both objectives, considering that load consumption and the RES generation are not forecasted perfectly. As it can be seen in Figure 34b), the main impact of the forecast error is that the FPF provided by the NSGA-II+QP algorithm do not reaches the ideal solution (FPF for the Perfect Forecast case), which has an impact in the final economic operation of the LV microgrid.

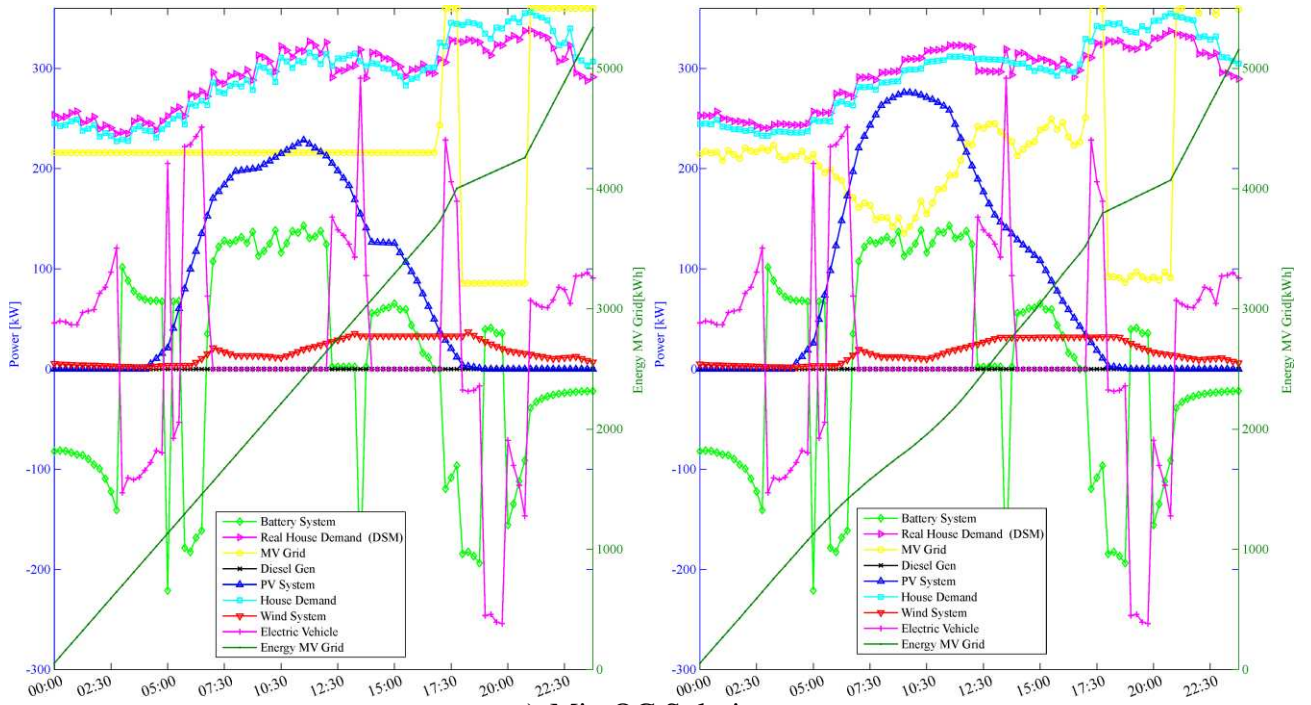
To show the operational characteristics of the solutions of the Final Pareto Front for this case of study, in Figure 35 it is show the output power of the generation systems and the power supplied by the MV grid for the Min OC Sol, Min PL Sol and the BCS Sol.

As it is shown in Figure 35, the PV model estimates a PV generation lower than the real one, and as a consequence the final amount of power provided by the MV grid is lower than the value expected by the long-term stage. For the DSM system, this reduce the load consumption before the intermediary and peak periods and increase it at noon when the PV generation has its maximum. Considering this, the DSM strategy implemented for the Real Operational case, when compared to the Perfect Operational case, does not varies significantly. This means that the DSM as proposed in this work is not affected significantly by the forecast error. This is mainly because the trend in the load consumption is forecasted accurately, i.e., the load consumption at night is higher than at noon.

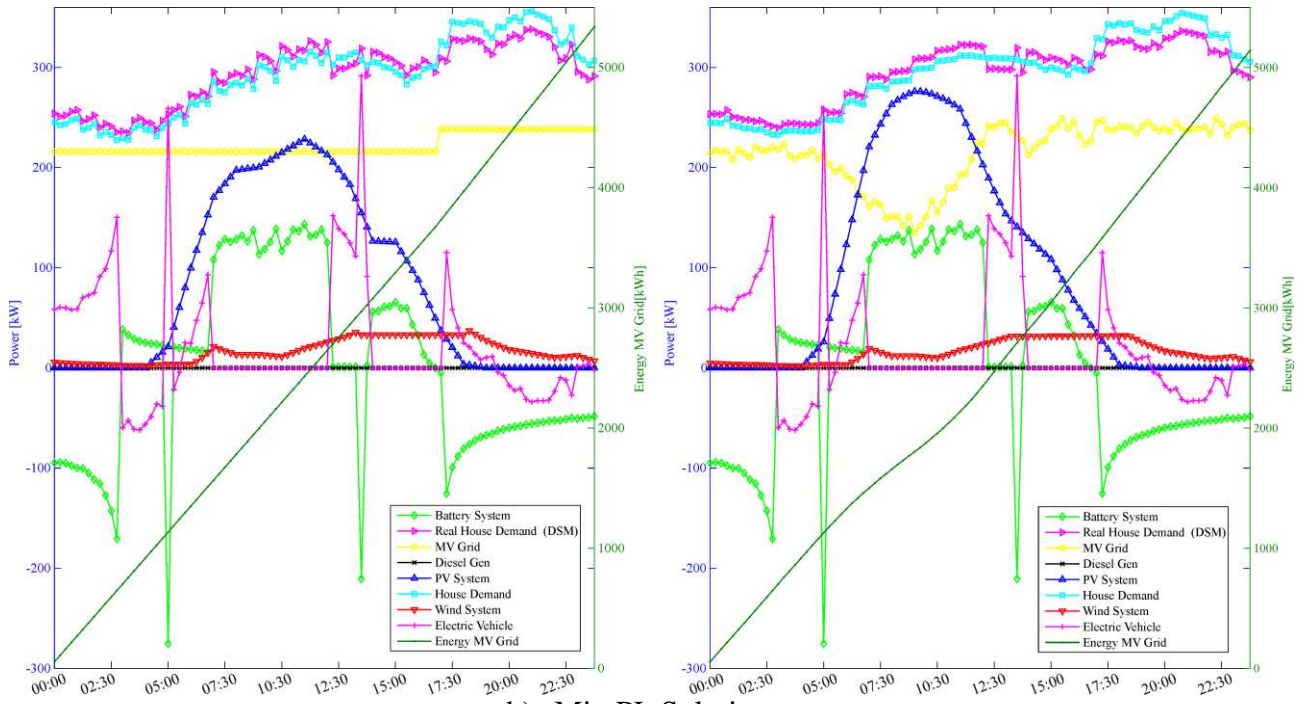
In general, for the three solution being analyzed in Figure 35, the long-term stage of the EMS addapts the operational schedule of all the generation systems and the MV grid to the

PV generation predicted by the PV model. Considering this, if the Min OC Sol for both operational cases are compared, it is possible to observe that the EV system and the ESS shown the same complementary behaviour. However, in the Real Operational case, as the PV generation is under-estimated, the EV systems is dispatched in charging mode from 00:00 am to 2:30 am, purchasing more energy from the ESS. Similarly, near to the peak periods, the EMS dispatches the battery system in discharging mode to reduce the amount of power purchased from the MV grid. However, in the Real Operational case the amount of power supplied by the ESS is lower than in the Perfect Forecast case. As a consequence, the final OC of the solution increases.

The major impact of the forecast error can be seen in the Min PL Sol. To reduce the final amount of power losses, the long-term stage of the EMS has to maintain constant the amount of power purchased from the MV grid. To do this, the ESS and the EV system follows the variations in the load consumption. However, as the load consumption and the RES generation are not forecasted perfectly, the final Min PL Sol shows how the MV grid follows the variations in the load consumption and in the RES generation, increasing the final PL. Nevertheless, this problem is reduced when the short-term stage of the EMS is considered.



a) Min OC Solution



b) Min PL Solution

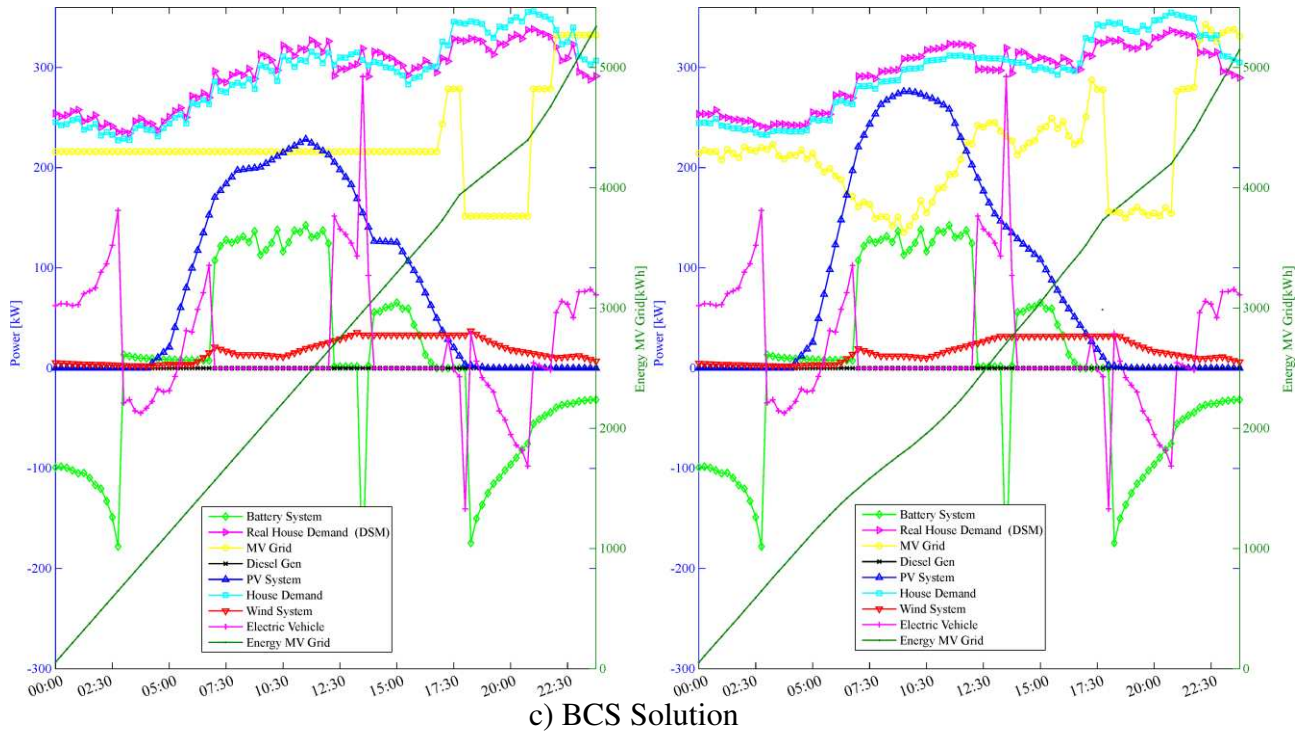


Figure 35. Scenario II: Output power for the battery and EV system, PV and wind system, diesel generator and main grid for the Real Operational case given by the long-term stage.

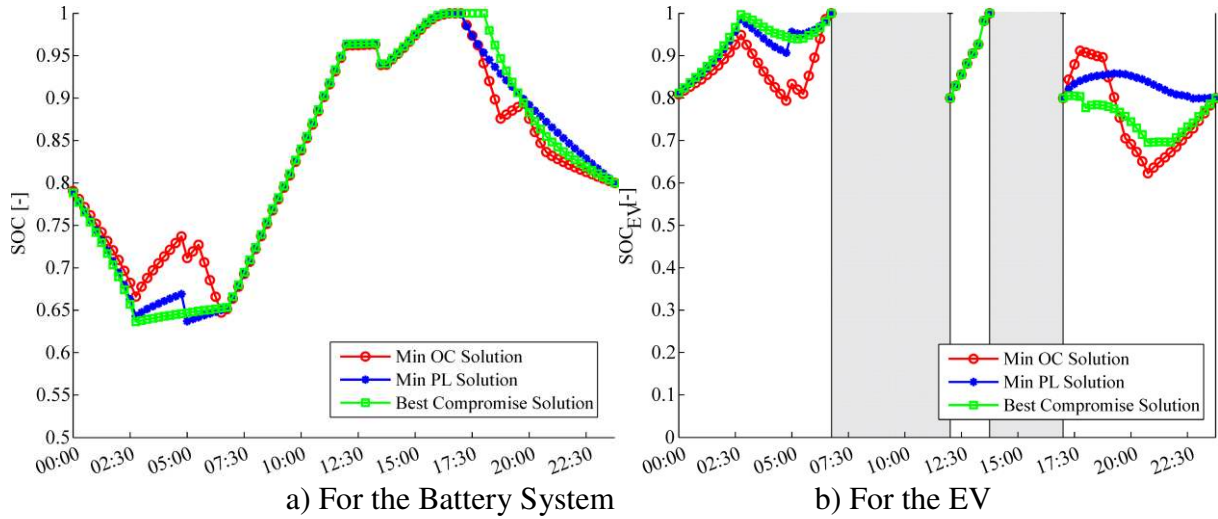


Figure 36. Scenario II: State-of-Charge (SOC) for the Real Operational case.

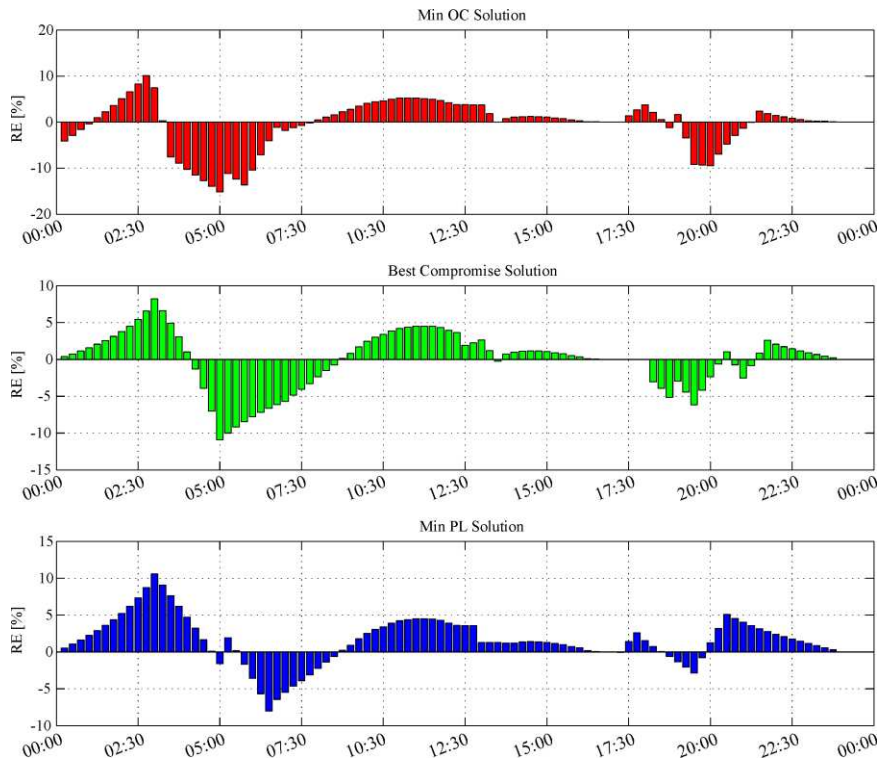


Figure 37. Scenario II: Relative Error (RE) for the SOC of the ESS for both operational case considered.

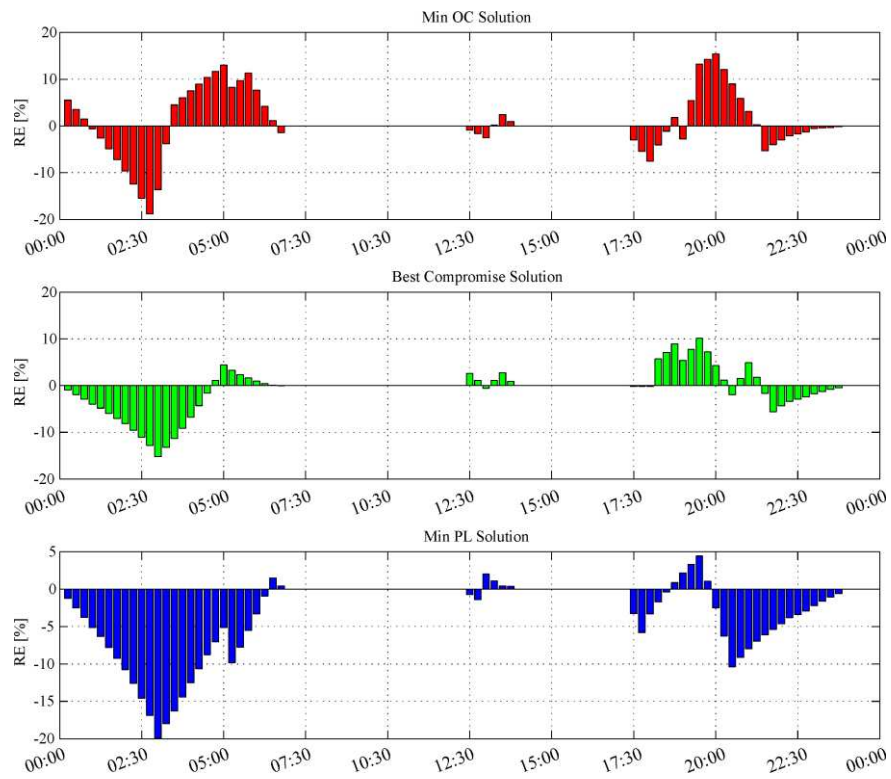


Figure 38. Scenario II: Relative Error (RE) for the SOC of the EV for both operational case considered.

For the BCS Sol, the major impact of the forecast error can be seen in the difference of both operational schedule at peak periods. In the Real Operational case, the EVs and the ESS shown a more smooth behavior when compared to the Perfect Forecast case. This behavior can be seen when the SOC of the EV and the ESS for both operational cases are compared. In Figure 36 it is shown the SOC of the EVs and the ESS for the Real Operational case.

According to Figure 36a), for the BCS solution, the minimum SOC of the ESS reaches a value of 63.63%, 5.4% greater than the value reached for the same solution in the Perfect Forecast case. In addition, in Figure 37 it is shown the RE for all the solutions when both operational cases considered are compared, showing a maximum RE near to 12%. Related to the EVs, in Figure 38 it is shown that the SOC of the EV system has a maximum RE near to 20%. These errors means that, if the load consumption and the RES generation are not forecasted accurately, the long-term stage will not dispatch all the energy stored in the battery system. Consequently, the long-term system will purchase more power form the MV grid to maintain power balance. The impact of the forecast error in the SOC of the ESS is important considering that the SOC corresponds to the main information that the long-term stage provides to the short-term stage.

Furthermore, if the final optimal solutions (Min OC Sol, Min PL Sol and BCS Sol) are compared for both operational cases considered, as in Table 17, it is possible to conclude that the forecast error has an impact near to 3.3% for the OC objective and 5.6% for the PL objective. According to Table 17, the amount of energy purchased form the MV grid in the Real Operational case is 3.7% greater than the energy purchased in the Perfect Forecast case. This increment is a consequence in the reduction of the amount of energy provided by the ESS, directly related to the low PV generation that the EMS expects.

As highlighted before, the increment in the power supplied by the MV grid can be considered small enough to be neglected for one day of operation. However, this error may have a major impact in the economic operation of the microgrid in an annual operation basis.

Table 17. Scenario II: Comparative results for the Min OC, the Min PL and the BCS Sol for both operational cases considered in the scenario II.

Total	Case	Min OC	Min PL	BCS
$E_G$ [MWh]	PF	5.14	5.14	5.14
	RO	5.33	5.33	5.33
	RE[%]	<b>3.69</b>	<b>3.69</b>	<b>3.69</b>
$E_{CH}$ [kWh]	PF	981.53	1067.74	1133.11
	RO	1039.27	892.08	837.97
	RE[%]	<b>5.88</b>	<b>-16.45</b>	<b>-26.01</b>
$E_{DCH}$ [kWh]	PF	981.53	1067.74	1133.11
	RO	1039.27	892.28	837.97
	RE[%]	<b>5.88</b>	<b>-16.45</b>	<b>-26.04</b>
OC [USD\$]	PF	530.28	568.44	543.54
	RO	547.37	585.81	560.76
	RE[%]	<b>3.22</b>	<b>3.05</b>	<b>3.16</b>
PL [kW]	PF	311.30	283.76	292.15
	RO	327.32	299.59	308.10
	RE[%]	<b>5.14</b>	<b>5.57</b>	<b>5.45</b>

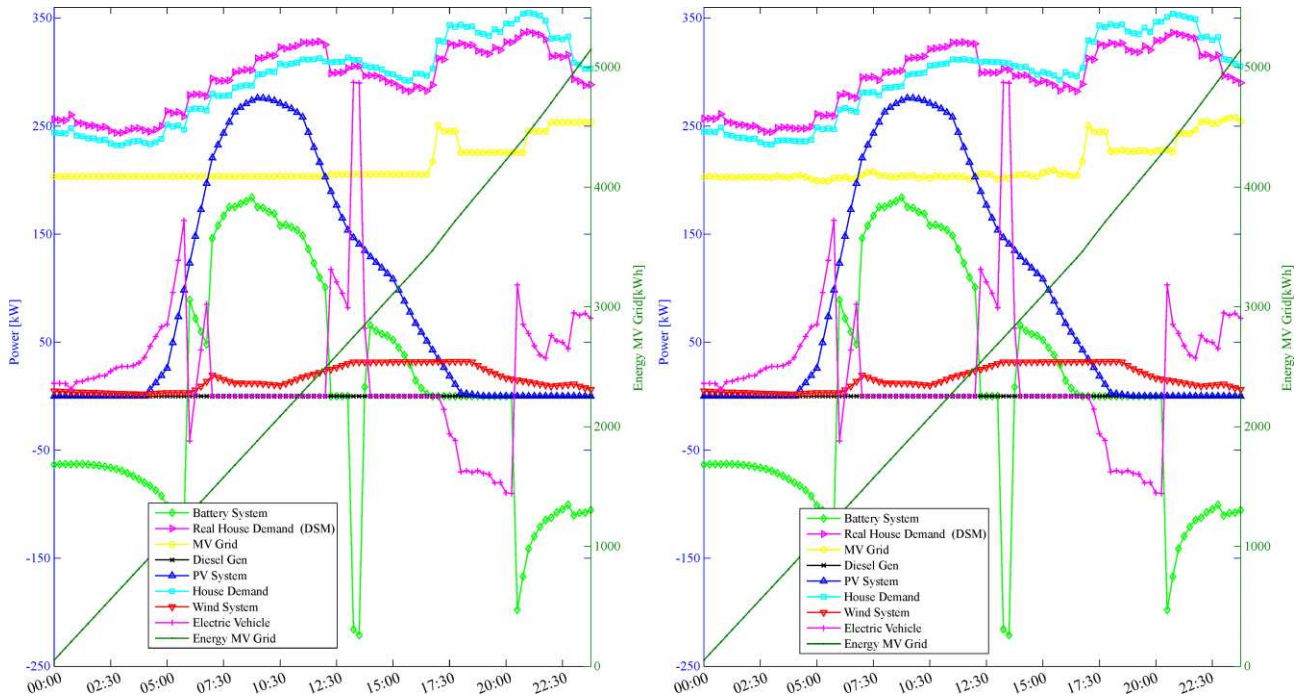
As expected, considering the results obtained in Chapter 5, for all the solutions analyzed the long-term stage does not dispatch the diesel generator. This is a consequence of the high diesel cost and the low energy cost of the power supplied by the MV grid. As discussed in Chapter 5, this is also a consequence of the topology of the distribution system and the localization of the diesel generator.

For both operational cases studied, the maximum power that the MV grid can supply is equal to 360 kW. If this maximum power is limited, the EMS has to dispatch the diesel generator to meet all the operational constraints. To evaluate this scenario, the long-term stage

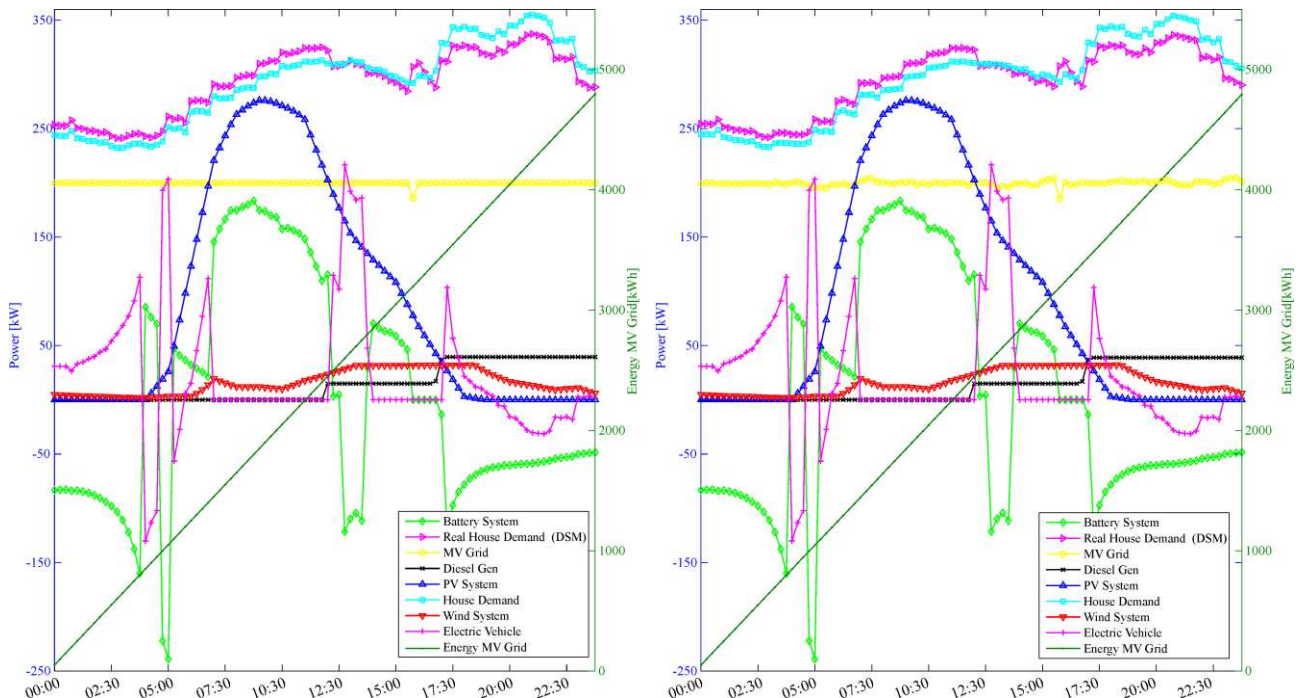
has been executed considering that the maximum power of the MV grid is limited to 260 kW. The results are shown in Figure 39a).

According to Figure 39a), under this operational scenario, the long-term stage does not dispatch the diesel generator, even when the maximum power of the MV grid is limited to 260 kW. This is due to the energy stored at the EVs, which is used at the intermediary and peak periods, from 17:00 pm to 20:30 pm to supply load consumption. Also, as the MV grid power is limited, the EV use the energy stored at the battery system to fulfill all its operational constraints (and supply the load consumption), showing the complementary behavior discussed before. This complementary behavior reduces the amount of power purchased from the MV grid, because the ESS is charged using the energy generated by the PV system during the day.

To consider a second operational scenario in which the diesel generator can be more attractive for the long-term stage, the NSGA-II+QP algorithm has been executed considering that the maximum MV grid power is limited to 200 kW. The results are shown in Figure 39b). According to these results, the long-term stage dispatches the diesel generator after 11:30 am until midnight. This is done dispatching the diesel generator at its minimum output power (20 kW), from 11:30 am to 17:30 pm. After 17:30, just before the peak period begins, the diesel generator is dispatched at its maximum output power, 60 kW. As in all the analyzed cases, the EV and the ESS have shown a complementary behavior to reduce the amount of power purchased from the MV grid. Finally, as the power supplied by the MV grid is maintained constant at its maximum value, the variations in the load consumption are followed by the EV and the ESS systems.



a) Maximum MV power: 260 kW



b) Maximum MV power: 200 kW

Figure 39. Scenario II: Output power for the battery and EV system, PV and wind system, diesel generator and main grid for the Perfect Forecast case, limiting the maximum MV power given by the long-term stage.

Now, if the LLC of the ESS is considered the long-term stage reduces the output power of the battery system to reduce the final OC, as it can be seen in Figure 40 and in Figure 41. At the beginning of the operational day, the EMS dispatches the EV in discharging mode to reduce the power supplied by the main grid. Near to 6:00 am, when the PV starts to generate power, the EMS dispatches the EV in charging mode to fulfill its SOC constraint (100% at 7:30 am). After this, the EMS dispatches the battery system in charging mode to increase its operational SOC near to 100%, maintaining this value in almost all the operational day. This behavior is a consequence of the inclusion of the LLC cost in the OC objective, which has a major impact compared to the cost of the power purchased from the MV grid and the fuel diesel cost.

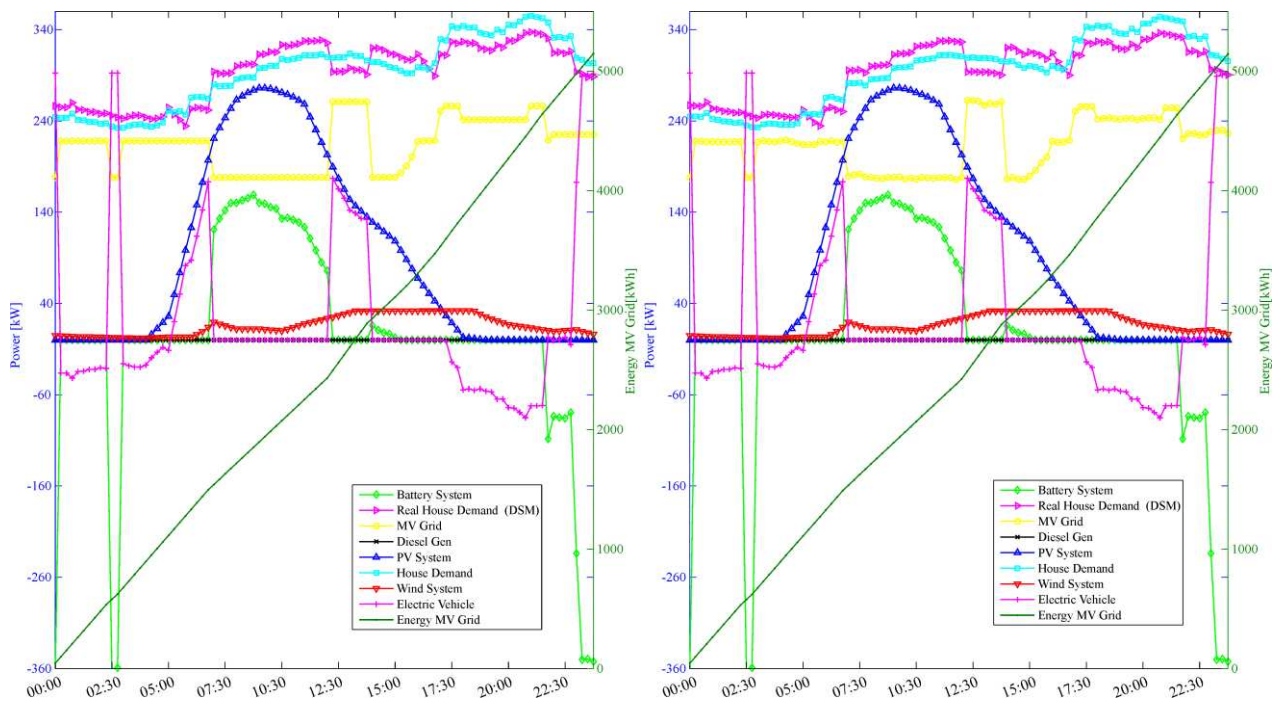


Figure 40. Scenario II: Output power for the battery and EV system, PV and wind system, diesel generator and main grid for the Perfect Forecast case, if the LLC is considered.

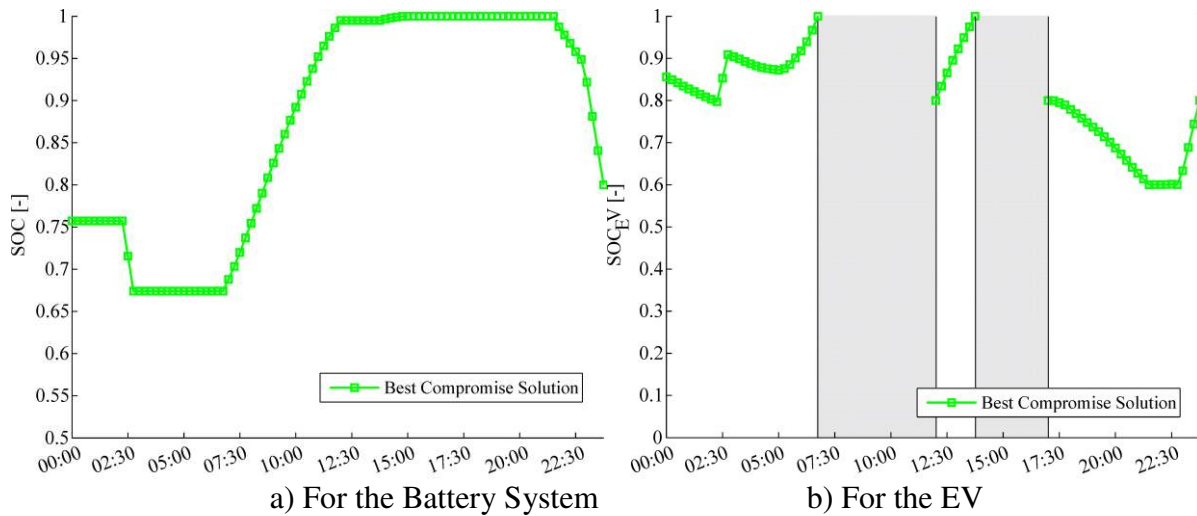


Figure 41. Scenario II: State-of-Charge (SOC) for the Real Operational case, if the LLC is considered.

In addition, it is important to highlight that in this case the EMS does not dispatch the diesel generator, as in the case studied in the Chapter 5. This is mainly due to the inclusion of the EV system, which is dispatched in discharging mode at peak periods to reduce the power supplied by the main grid. Finally, the battery system is used to charge the EV at the end of the operational schedule to fulfill the SOC constraint of the ESS system (SOC equal to 80% at the end of the operational day). If this constraint is not considered, the EMS will not dispatch the ESS, maintaining its SOC at its maximum value.

In Table 18 it is shown the final PC, FC, PL and energy provided by the MV grid for all the cases studied in this section, showing that when the diesel generator is dispatched the final BCS solution increases its final OC. The OC when the LLC is considered is higher due to the cost of operating the battery system.

Table 18. Scenario II: OC, FC, PL and Energy provided by the MV grid for the cases where the diesel generator is more attractive.

Solution	OC [USD\$]	FC [l]	PL [kW]	Energy [kWh]
Min OC Sol	529.87	0.0	361.25	5156.30
Min PL Sol	568.43	0.0	313.05	5143.60
BCS Sol	544.55	0.0	331.17	5148.40
BCS limiting the MV grid	564.57	0.0	313.41	5143.69

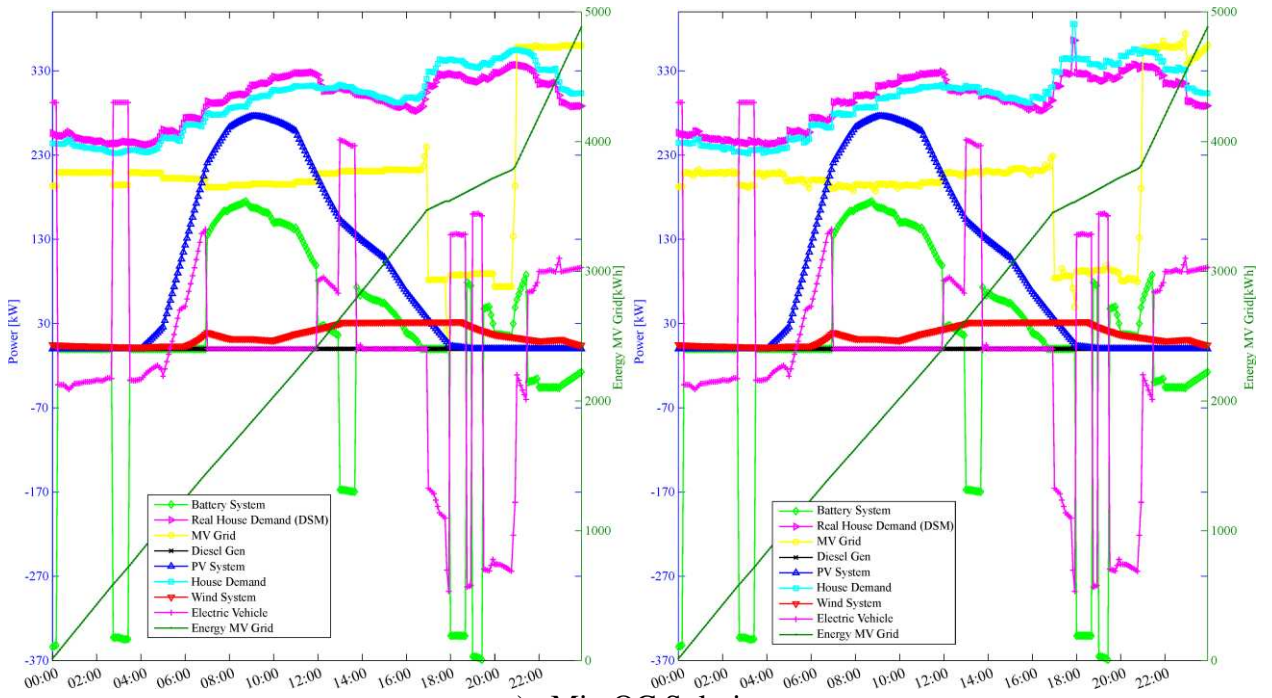
power to 260 [kW]				
BCS limiting the MV grid power to 200 [kW]	658.75	125.21	313.53	4795.79
BCS considering the LLC of the ESS				
	669.78	0.0	286.35	5143.74

## 6.2 SHORT-TERM STAGE

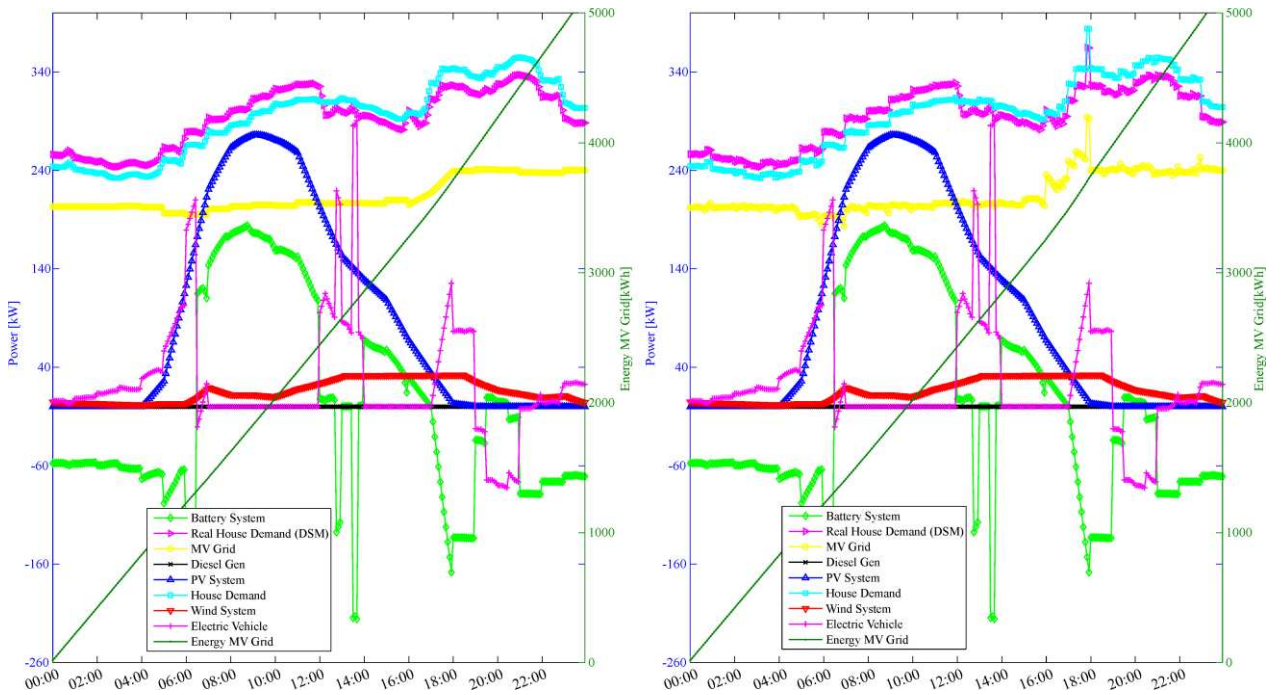
As in Section 5.4, the load consumption and the RES generation considered here is obtained using linear interpolation techniques considering the same that as for the long-term stage. On the other hand, and as already discussed, once the EMS selects the BCS solution from the Final Pareto front, the SOC information is provided to the short-term stage.

In this case, the SOC information of the ESS and the EV system is used to define the operational schedule of all distributed generation systems and the MV grid power for the next operational hour. To do this, 24 ELD problems are solved independently.

In Figure 42 it is shown the operational schedule for the Min OC, Min PL and BCS Solution for the Perfect Forecast case once the short-term stage has solved the 24 ELD problems.



a) Min OC Solution



b) Min PL Solution

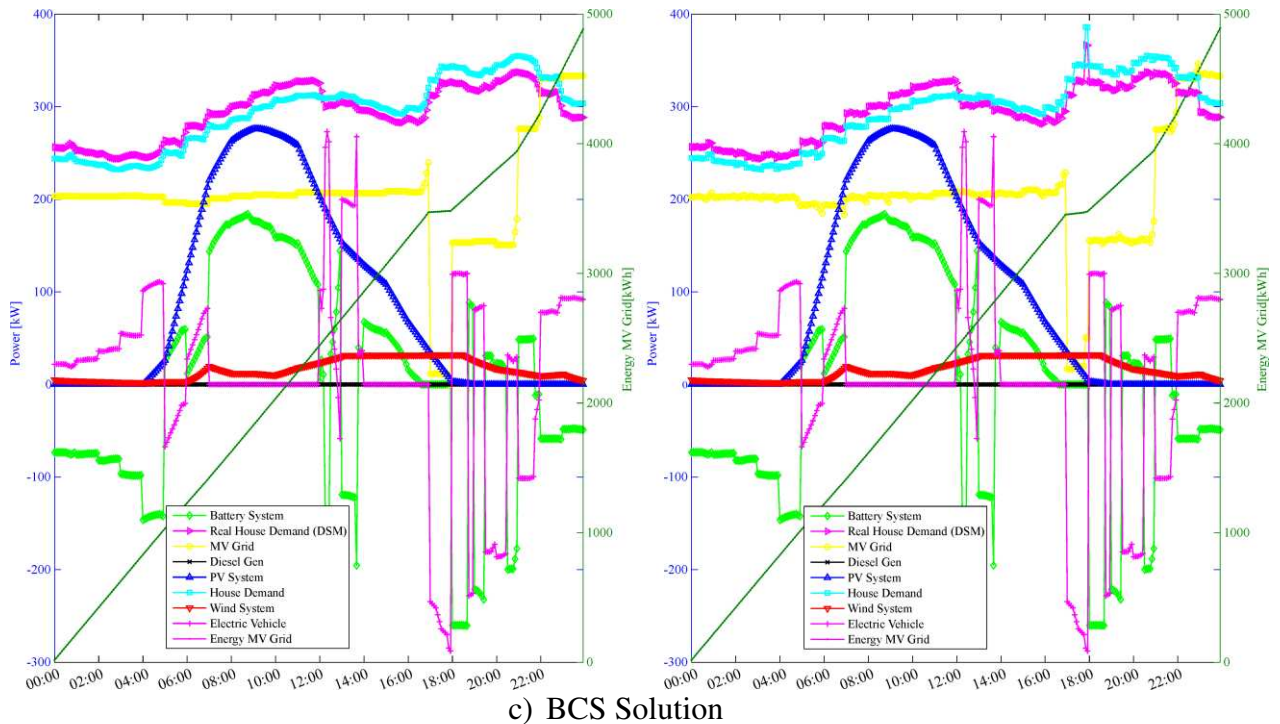


Figure 42. Scenario II: Output power for the battery system, PV and wind system, diesel generator and main grid for the Perfect Forecast case given by the short-term stage.

It is important to notice that the similarity of solutions obtained in Figure 32 (solution by the long-term stage) and Figure 42 (solution by the short-term stage) is also a result of the use of the same weight factor ( $\eta$ ) for both objectives considered in the optimization problem, described in Figure 17. In this manner, it is possible to conclude that the long-term stage and the short-term stage can provide the same operational schedule under some special conditions, even considering that the short-term stage solve 24 ELD problems independently. However, this strategy is developed to adapt the operational schedule of the LV Microgrid to consider sudden load changes and reduce the error in the management due to the forecast error.

Finally, in Figure 42 the main difference between the solution obtained using the short-term stage of the EMS (left) and the solution implemented in GridLab-D (right) is related to imperfect knowledge of the load consumption and the PL models used, which increase the final OC and PL of the solution. Considering this, in Table 19 it is shown comparative results

for the solutions obtained using the EMS and GridLab-D. According to these results, the major error can be seen in the PL objective, with a RE near to 18%, while lower errors were obtained to model the OC objective and the Energy provided by the MV grid.

Table 19. Scenario II: Comparative results for the solution obtained using the EMS and the simulated solution in GridLab-D for the Perfect Forecast case.

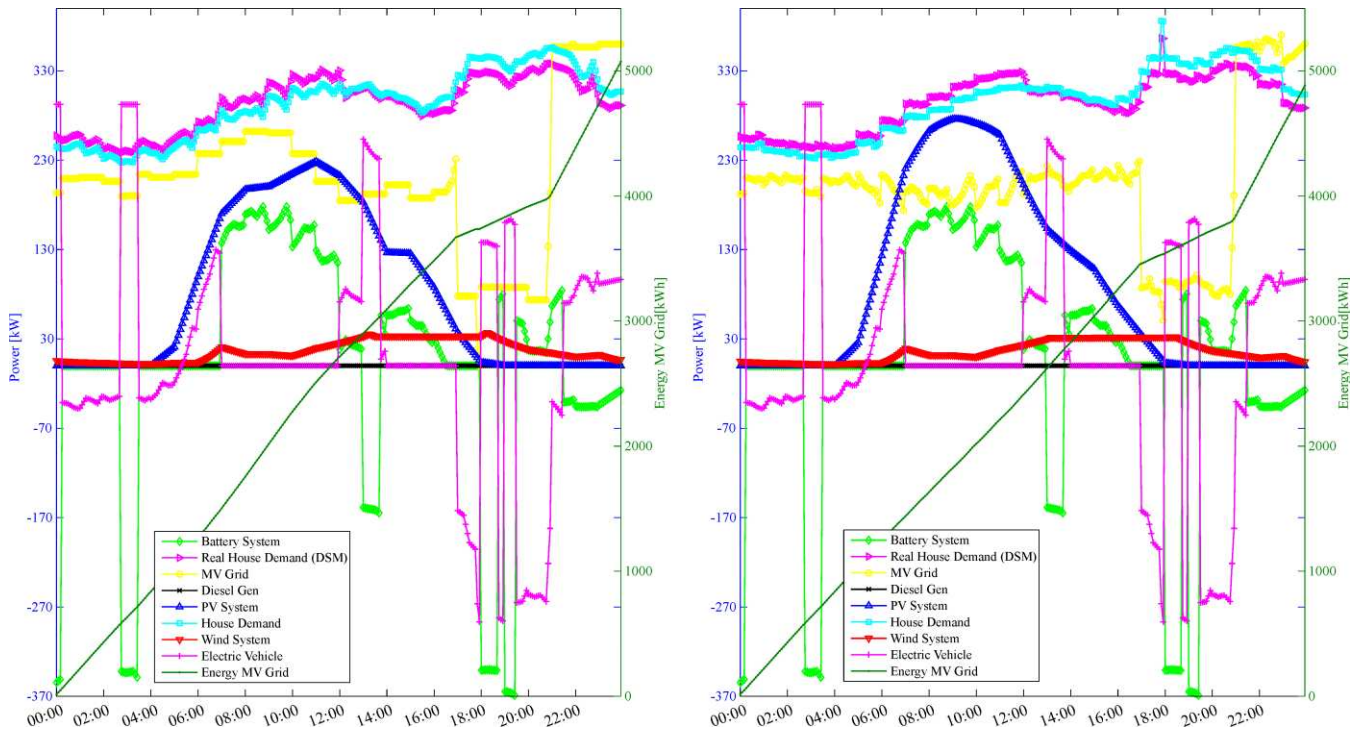
		Min OC	Min PL	BCS
OC [USD\$]	Short-term EMS	493.54	566.93	509.96
	GridLab-D	495.70	571.94	512.20
	RE[%]	<b>-0.43</b>	<b>-0.87</b>	<b>-0.43</b>
PL [kW]	Short-term EMS	860.81	847.65	832.05
	GridLab-D	1042.57	949.11	998.64
	RE[%]	<b>-17.43</b>	<b>-10.69</b>	<b>-16.68</b>
Energy [kWh]	Short-term EMS	4883.51	5133.32	4884.30
	GridLab-D	4888.28	5170.43	4892.02
	RE[%]	<b>-0.09</b>	<b>-0.71</b>	<b>-0.15</b>

For the Real Operational case, the load consumption and the RES generation considered is provided by a forecast module, obtaining the output power schedule of the distribution generation systems and the MV grid shown in Figure 43. As for the Perfect Forecast case, the solution obtained using the short-term stage varies from the solution simulated in GridLab-D as a results of the forecast error and the PL models used. However, the dispatch profile for the ESS and the EV system remains similar to the Perfect Forecast case and the long-term stage. The main variations of the solutions for both operational cases considered is due to the load consumption and the RES system generation.

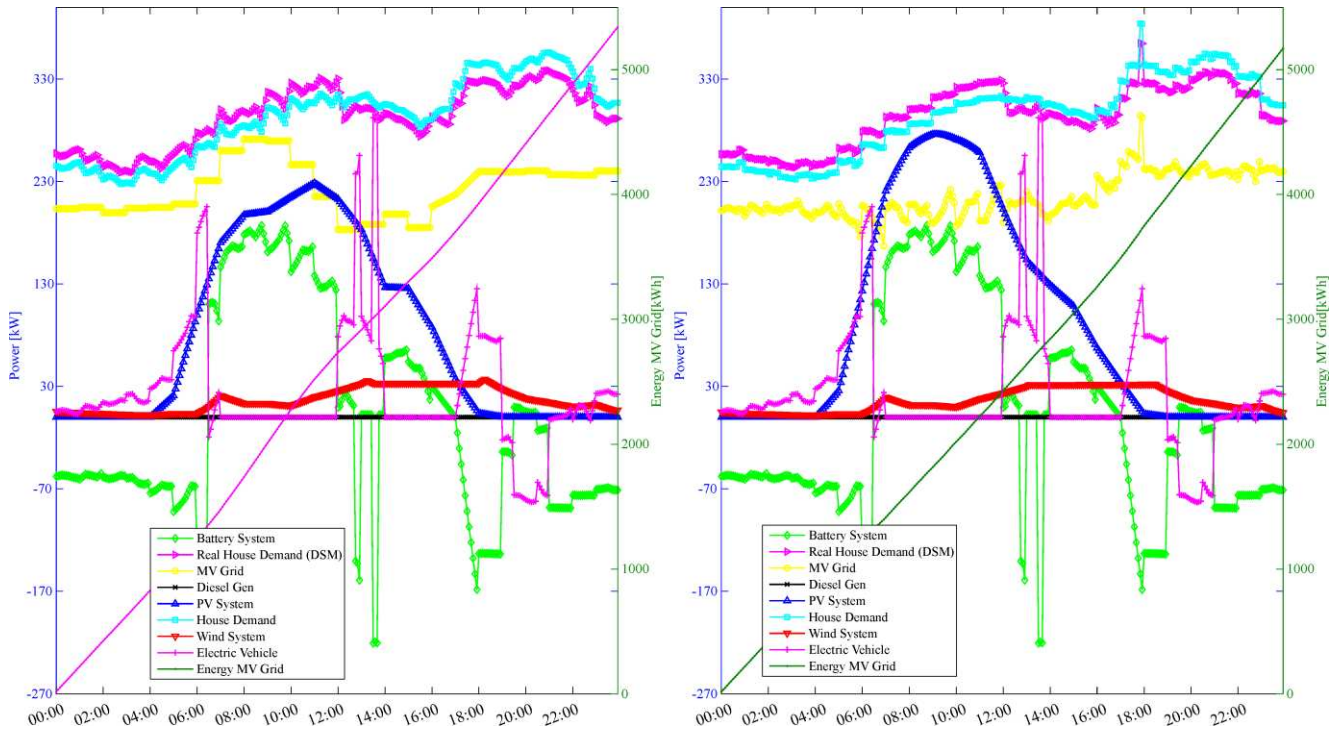
As already discussed, the short-term stage re-defines the power input/output of the ESS and the EV system to follow the variation of the load consumption. These variations are followed by the ESS and the EV system, while the power purchased from the MV grid is maintain constant. It is important to notice in Figure 43 that, as the long-term stage expects

high PV generation, it increases the amount of power that the ESS and the EV purchased from the MV grid to reach a SOC of 100% near noon. However, the real PV generation considered for the short-term stage is lower than the value expected, and as a consequence the EMS increase the amount of power purchased from the MV grid to fulfill the SOC constraint defined by the long-term stage for both storage system. As a results, the OC of the final solutions for the Real Operational cases have higher values.

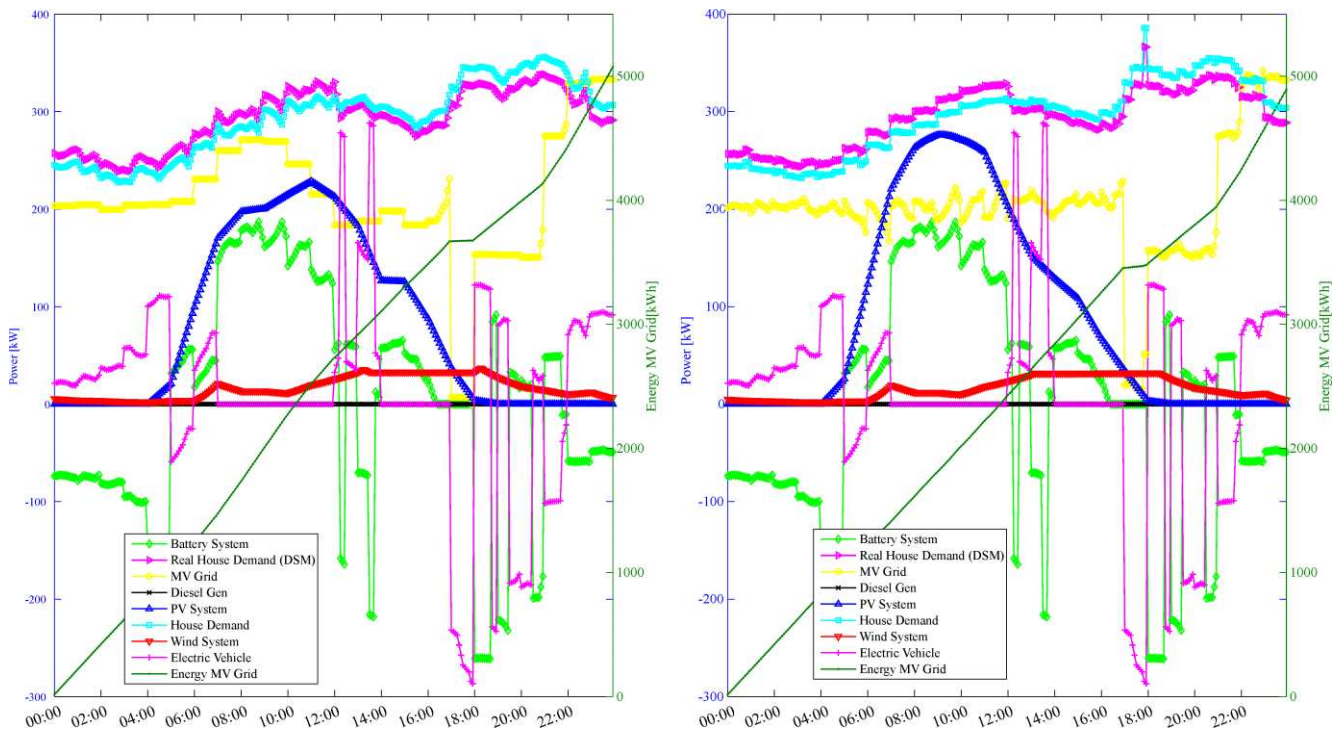
Finally, if the Min OC, the Min PL and BCS Sol for both operational cases considered are compared, as in Table 20, it is possible to observe that due to the forecast error in the load consumption and the RES generation, there is an RE near to 3.5% for the OC and 7% for the PL for the three solutions analyzed.



a) Min OC Solution



a) Min PL Solution



b) BCS Solution

Figure 43. Scenario II: Output power for the battery system, PV and wind system, diesel generator and main grid for the Real Operational case given by the short-term stage.

Table 20. Scenario II: Comparative results for the Min OC, the Min PL and the BCS Sol for both operational cases considered.

Total	Case	Min OC	Min PL	BCS
OC [USD\$]	PF	493.54	566.93	509.96
	RO	510.89	586.17	527.32
	RE[%]	<b>3.51</b>	<b>3.39</b>	<b>3.40</b>
PL [kW]	PF	860.81	847.65	832.05
	RO	914.01	907.34	888.08
	RE[%]	<b>6.18</b>	<b>7.04</b>	<b>6.73</b>
Energy [kWh]	PF	4883.51	5133.32	4884.30
	RO	5073.98	5342.39	5074.79
	RE[%]	<b>3.09</b>	<b>3.91</b>	<b>3.90</b>

---

## 7 TECHNICAL ASSESSMENT OF THE EMS IN THE DISTRIBUTION SYSTEM

---

Once the EMS has obtained the Final Pareto Front and the NSGA-II+QP algorithm has selected the Best Compromise Solution, a dynamic simulation can be carried on in GridLabD to assess technically the impact of this solution in the distribution system. Considering this, the Best Compromise Solution has to guarantee safety operational conditions in the distribution system, operating according to the Power Quality regulations given by PRODIST in its Module 8.

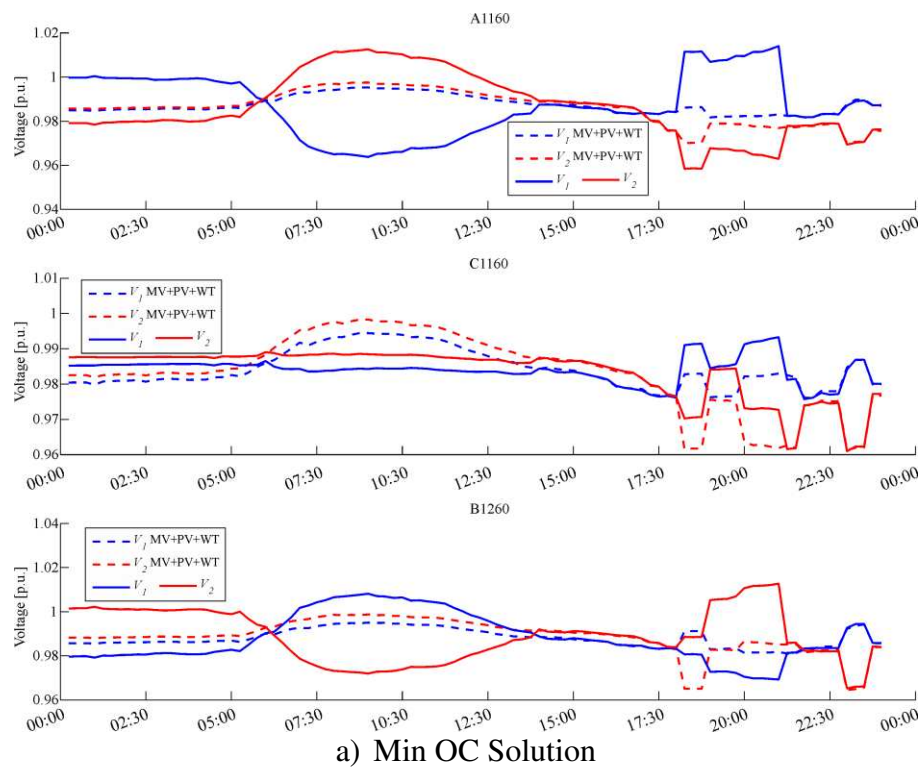
Based on this, in this chapter it is presented a technical assessment of the optimal solutions previously studied for both scenarios considered and presented in Chapter 5 and 6. This technical assessment includes an analysis of the voltage variations at the most remote nodes of the distribution system. In addition, simulation of the voltage unbalance (VU) factor described in Section 3.8.1 is also presented.

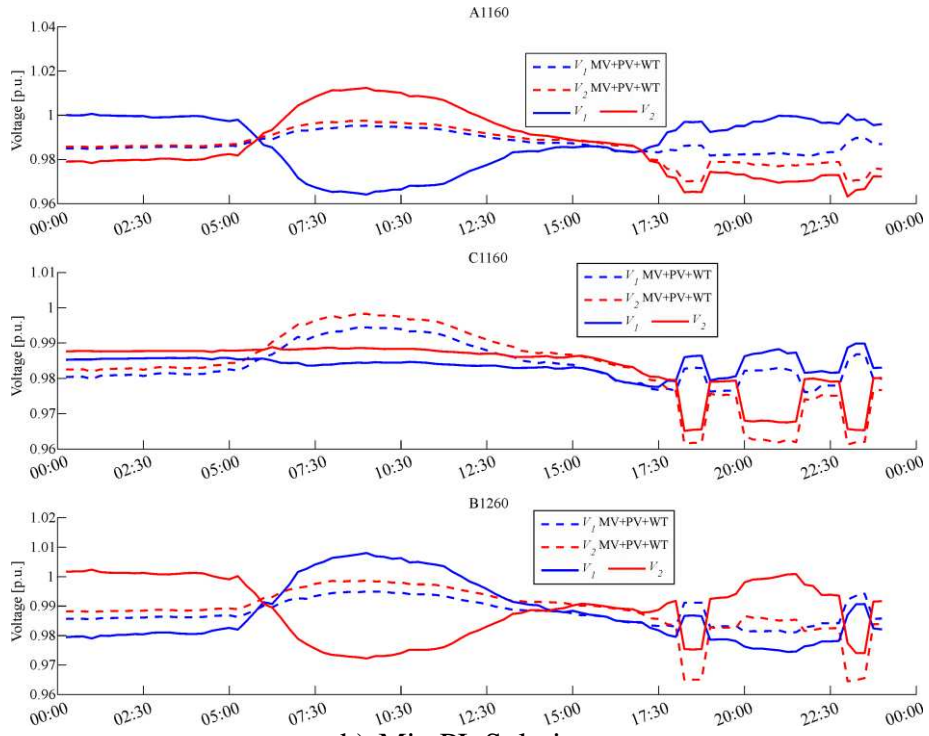
### 7.1 SCENARIO I: BASIC MICROGRID

According to [76], in LV distribution systems the low relation ratio of the reactance/resistance ( $X/R$ ) creates a coupling behavior between the active power and the voltage, as well as between the reactive power and the voltage angle. Thus, to ensure power flow between two bars it is necessary to have different voltage values between these two bars. Therefore, if a distributed generator is connected in certain bar inside a distribution system, its voltage has to increase to ensure that the generator is supplying active power to the system.

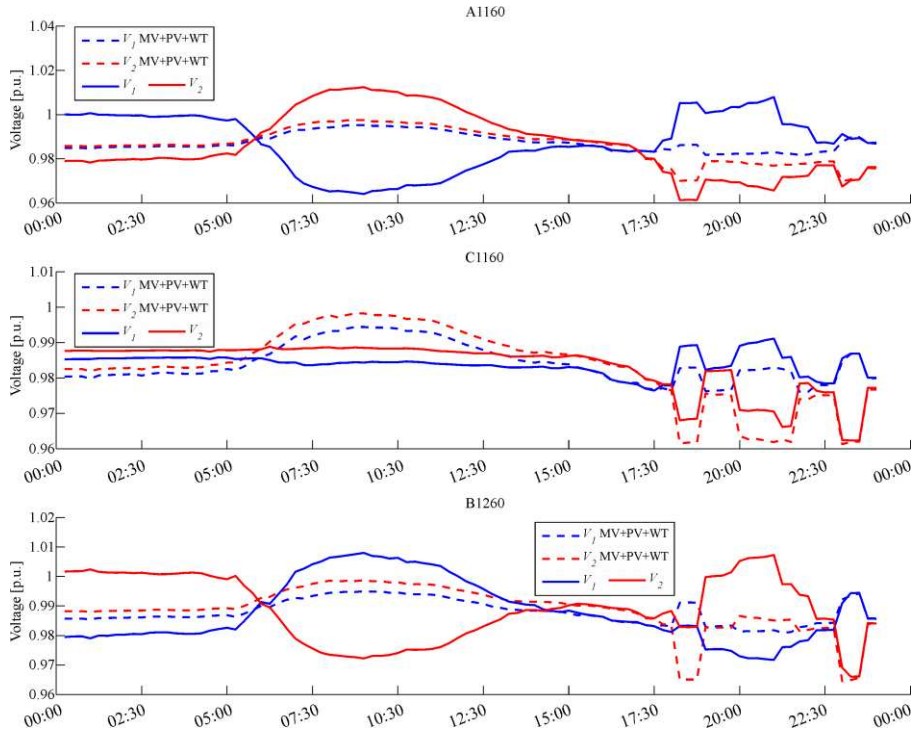
Considering this, it is expected high voltage variations at the most remote nodes of the distribution system due to the high penetration level of Distributed Energy Resources (generation and storage) in the LV microgrid considered. As discussed before, the voltage variations at the most remotes nodes should be between 108 V (0.90 *p.u.*) and 127 V (1.05 *p.u.*). These voltage values are defined by the Power Quality Module of the PRODIST for 127 V distribution systems [73]. The nodes considered for the technical assessment corresponds to the nodes A1160, C1160 and B1260 in the distribution system shown in Figure 8.

In Figure 44 it is shown the triplex line voltage variations for nodes A1160, C1160 and B1260 for the three solutions analyzed in Chapter 5 for the Perfect Forecast case. The voltage variation of all nodes is compared to the voltage variation for the case where it is only considered the MV grid and the PV and wind system (MV+PV+WT).





b) Min PL Solution



c) BCS Solution

Figure 44. Scenario I: Triplex line voltage variations: Line 1 (red) and Line 2(blue).

According to Figure 44, in general all the voltage profiles are inside the voltage range defined by the Power Quality Module of the PRODIST. In particular, for the Min OC Sol, there is a voltage increment at noon for the nodes A1160 and B1260, when the long-term stage dispatch the battery in charging mode. Similarly, at the peak periods, when the long-term stage dispatch the system in discharging mode to reduce the power purchased from the MV grid. This increment is near to 0.02. On the other hand, for the node C1160, when the MV+PV+WT case is compared to the Min OC Sol, it is possible to observe a reduction in the voltage variation at noon, as a consequence of the increment of the power purchased by the battery system.

Similar voltage variations can be seen for the Min PL Sol and the BCS Sol, shown in Figure 44b) and Figure 44c), respectively. In particular, in Figure 44b) it is possible to observe how the voltage variations for all the nodes are smoother when compared to the voltage variation for the Min OC Sol. This behavior is a consequence of the final operational schedule of the Min PL Sol, in which the long-term stage reduce the MV power variations. Finally, in terms of voltage variation, it is possible to observe how the BCS solution represent a compromise between the two extreme solutions of the Final Pareto front.

Considering these results and based on this analysis, the battery system can be used to regulate the voltage variation at the residential node connections, increasing or decreasing the voltage variations according to the battery's system power input/output. Thus, the ESS can not only be used to store energy, but also to provide ancillary services to improve the quality of the final voltage profile.

Now, related to the voltage at the PCC of the distribution system (node N4), in Figure 45 it is shown the VU factor for the 24-hours horizon of scheduled. As it can be seen, the VU factor does not exceed 1% for all the solutions analyzed, which means that all of them satisfy

the voltage unbalance operational constraint. In addition, in Figure 45 it is possible to observe how the long-term stage reduce the VU variations near to the noon. This reduction is a consequence of the operational strategy developed by the long-term stage, which maintain constant the amount of power purchased from the MV grid, while the PV system is generating its maximum output power and the ESS store the remaining of this energy. In terms of the final compromise and quality, the best VU profile is shown by the BCS Sol when compared to the MV+PV+WT case, reducing the VU factor to a 0.04% maximum value. It is important to highlight that these low values for the VU factor, even for the MV+PV+WT case, is directly related to the low level of load unbalance for the phases A, B and C of the distribution system.

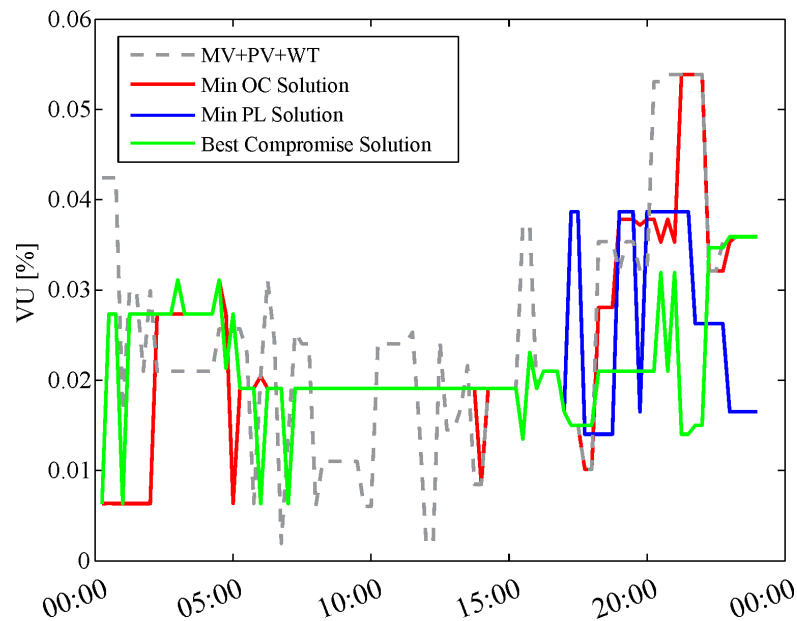
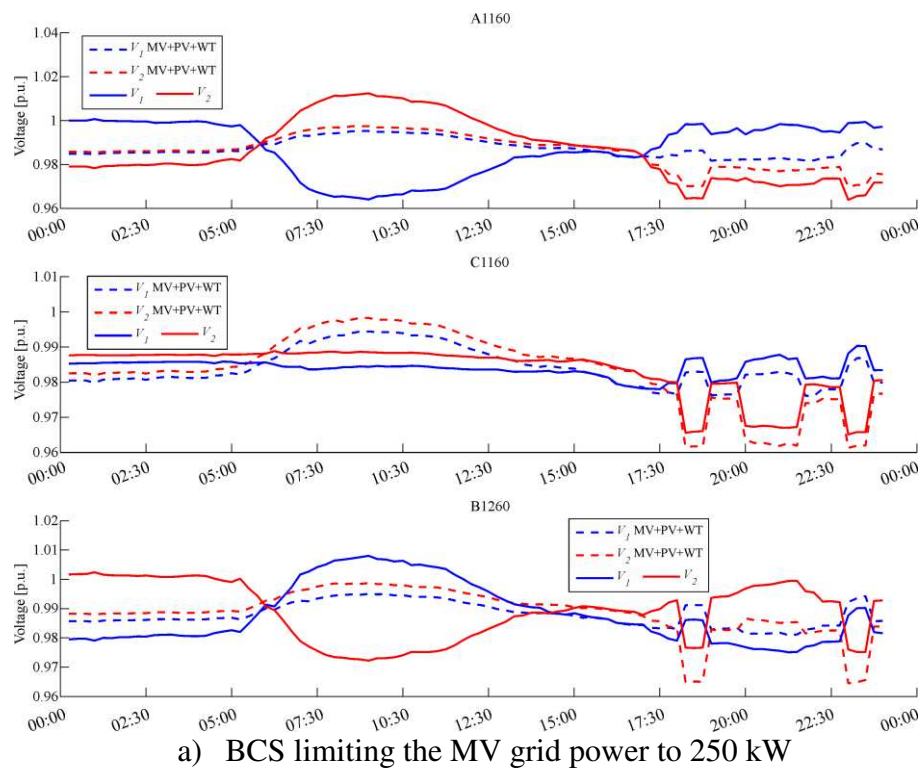


Figure 45. Scenario I: Voltage Unbalance (VU) at the PCC, node N4. Scenario I.

To show the impact of the long-term stage when the diesel generator is dispatched, in Figure 46 it is shown the voltage variations at nodes A1160, C1160 and B1260 for the cases when the MV grid power is limited and the LLC of the ESS is considered. According to Figure 46, the increase in the voltage at noon and at peak periods is result of the PV generation and battery system which is operating in charging and discharging mode,

respectively. Moreover, when the diesel generator is dispatched from 19:00 pm to 22:00 pm in Figure 27, a higher voltage variation is not seen in Figure 46a). This is mainly due to the location of the diesel generator, out-side of the distribution system. Similarly, for the BCS when the LLC is considered, when the diesel generator is dispatched at intermediary and peak periods in Figure 28, a major variation in the voltage of the nodes at the distribution system is not seen in Figure 46b).



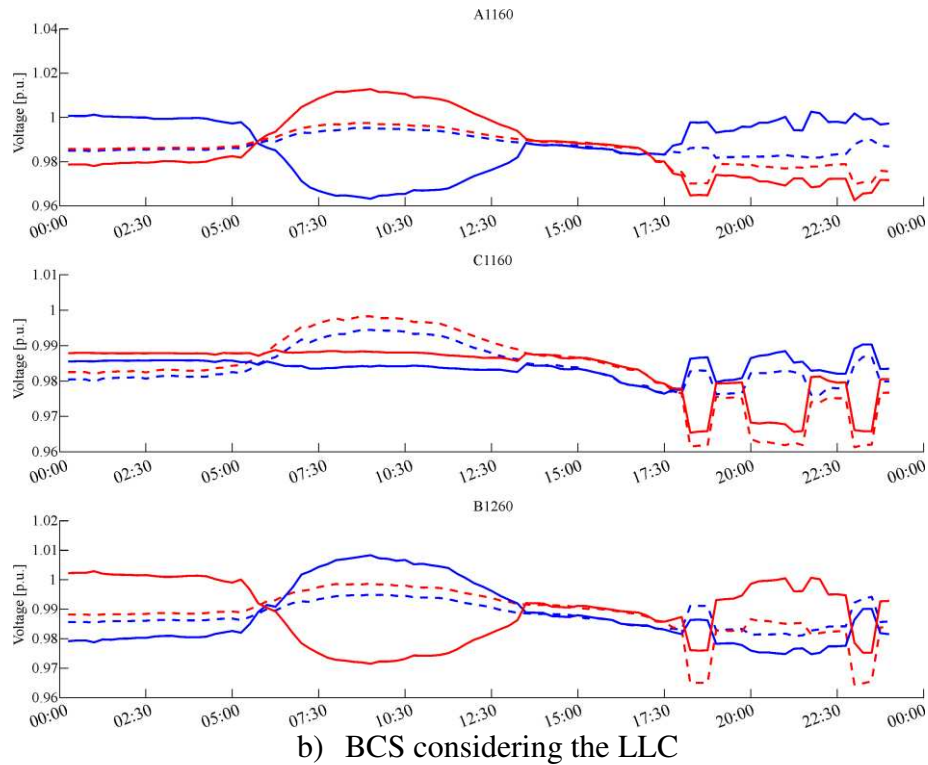


Figure 46. Scenario I: Triplex line voltage variations: Line 1 (red) and Line 2 (blue) for the cases where the diesel generator is dispatched.

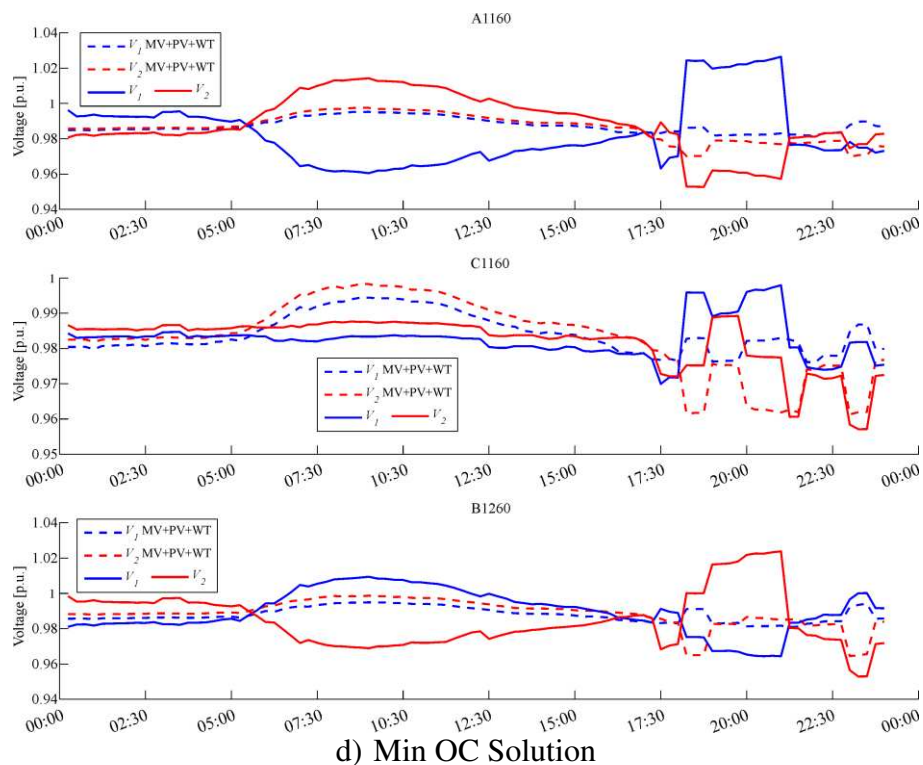
## 7.2 SCENARIO II: A MORE INTELLIGENT MICROGRID

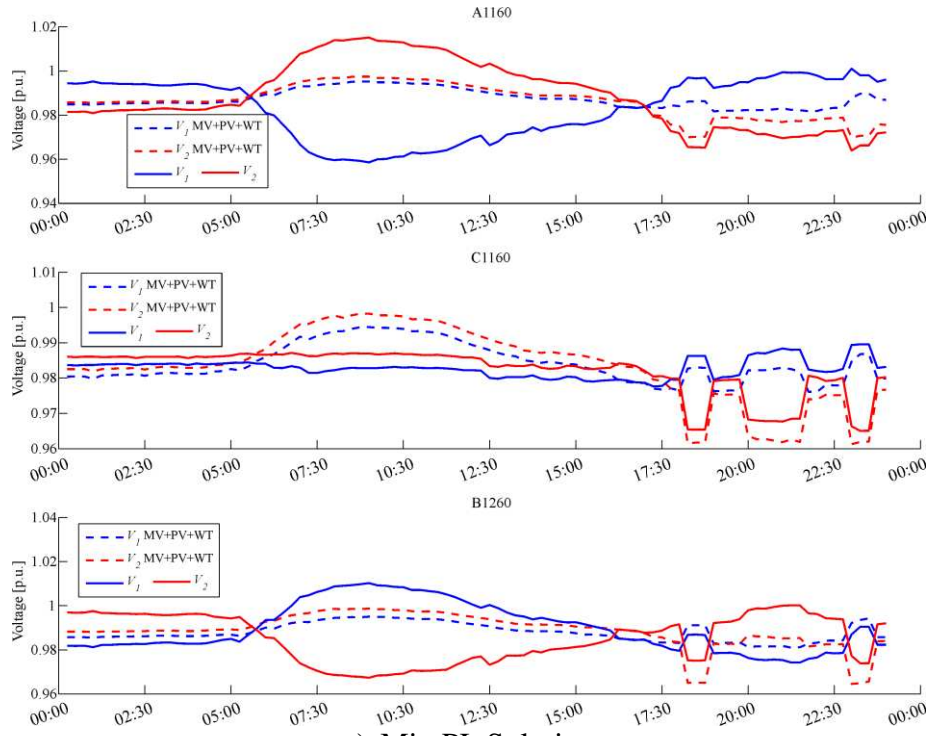
As described in Chapter 6, in this scenario the EMS considers a DSM strategy and an EV system. The inclusion of the EVs increases the storage capacity of the LV Microgrid. To evaluate the impact of the EMS when a DSM strategy and the EV system is considered, in Figure 47 it is shown the voltage variation of the nodes A1160, C1160 and B1260 for the Min OC Sol, Min PL Sol and the BCS Solution described in Figure 32.

According to Figure 47, the voltage increment at the nodes A1160 and B1260 is related to the PV generation and the charging mode of operation of the battery system. On the other hand, the node C1160 shows a voltage decrease at the same operational periods. These results are similar to those obtained and discussed previously in Section 7.1. However, as in this case the LV Microgrid has a major storage capacity (due to the EV system), the voltage increment at peak period is greater when compared to the results obtained in Section 7.1. The maximum

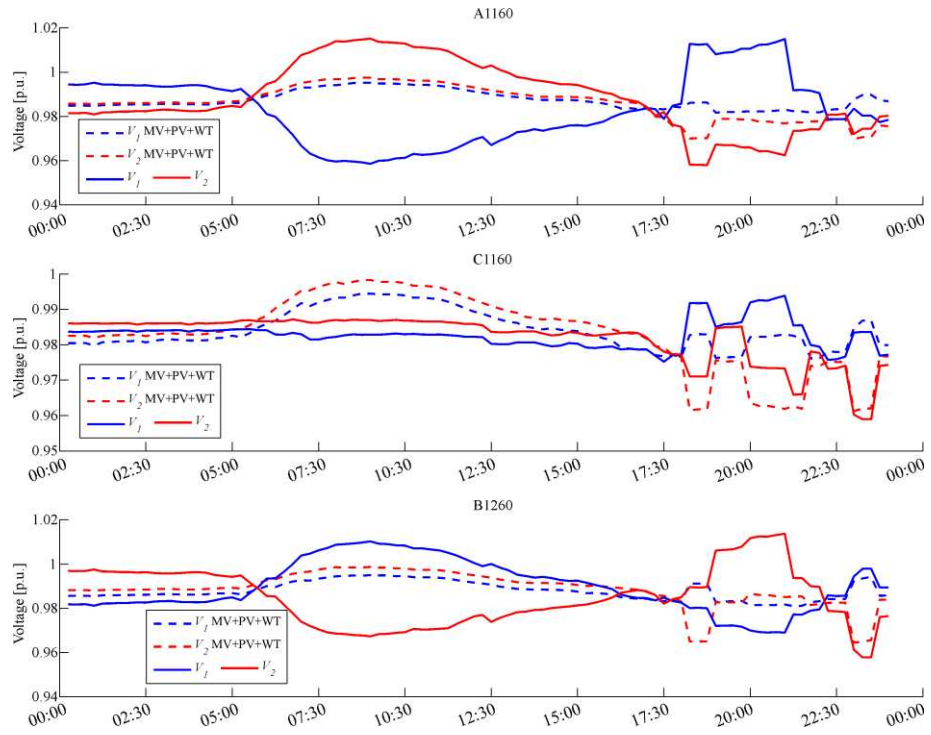
voltage for node A1160 is near to 1.04 p.u., 0.02 greater than the same value for the case analyzed in Section 7.1 for the Min OC Sol. This is a result of the discharging mode of operation of the ESS and the EV to reduce the amount of power purchased from the MV grid at intermediary and peak periods.

Considering these results, it is important to highlight that if the capacity of the ESS and the EV is incremented to reduce even more the energy purchased from the MV grid (as in the Min OC Sol), the probability that the voltage at node A1160 and B1260 exceeds its maximum value will increase. However, as the BCS solution give the same priority for both objectives considered, the voltage is inside its normal operational range.





e) Min PL Solution



f) BCS Solution

Figure 47. Scenario II: Triplex line voltage variations: Line 1 (red) and Line 2 (blue).

Related to the VU factor, in Figure 48 it is shown its variation profile for the 24-hours horizon. According to Figure 48, the VU factor is inside its normal operational range, with a maximum value of 0.06% for the Min OC Sol. In addition, it is observed how the profile of the BCS solutions shows low variations during the operational day when compared to the Min PL and Min OC solution. Furthermore, the profile of the BCS solution shows a maximum VU value of 0.04%, lower than the value obtained when is not performed energy management (MV+PV+WT case), showing the capabilities of the EMS to improve the final VU profile of the LV Microgrid.

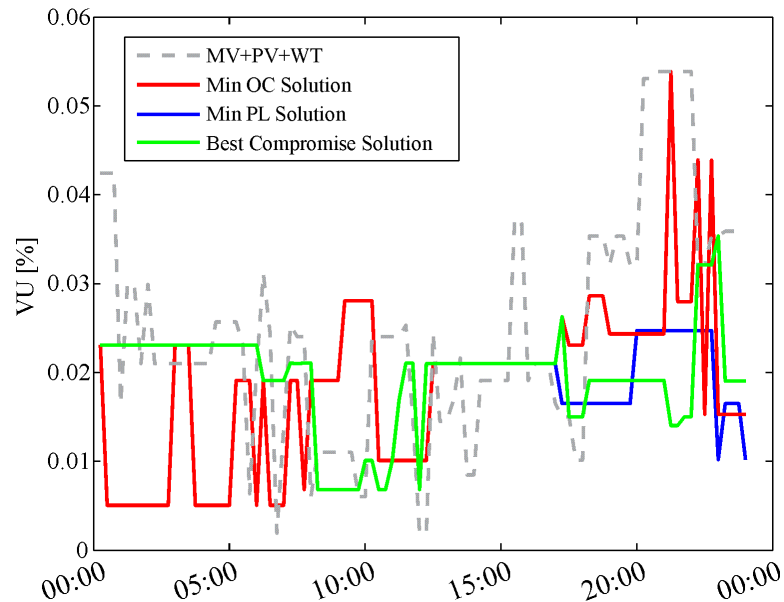


Figure 48. Scenario II: Voltage Unbalance (VU) at the PCC, node N4.

---

## 8 CONCLUSIONS

---

An Energy Management System to control and dispatch all the generation and storage units of a MG has been developed in this master dissertation. In addition, a Demand Side Management strategy has been considered to assess the impact of the load consumption management in the economic operation of the LV distribution system. The EMS developed is composed of two optimization stages: a long-term and a short-term stage. The main function of the long-term stage is to reduce the operational cost and the power losses simultaneously, considering an operational horizon of 24-hours ahead. To do this, the algorithm NSGA-II complemented with a QP technique has been used.

Once the long-term stage has defined the operational schedule of all the generation and storage units, as well as the shifting coefficients of the DSM, the hourly SOC information of the ESS is supplied to the short-term stage. The main function of the short-term is to re-define the power output of all the generation and storage units considering the unit commitment and SOC of the ESS information provided by the long-term stage for an operational horizon of 1-hour. This is done to manage power unbalance and reduce the impact of the forecast error in the operation of the distribution system. Considering this, the main findings of this thesis are summarized as follows:

- The proposed algorithm proposed for the long-term stage, the NSGA-II+QP algorithm, and the strategy developed (including the heuristic procedure to handle the diesel generation constraints and, the crossover and mutation operators) has

been proved to solve the energy management problem efficiently, providing a good quality final Pareto front. Moreover, as at the final generation all the individuals belongs to the final Pareto front, the algorithm has shown good convergence capabilities, identifying a set of trade-off solutions according to the objectives considered.

- From an economic point of view, fuel-based generation systems are not attractive to be dispatched when the MV grid is operating at normal conditions. This is mainly due to the higher cost of the diesel fuel when compared with the cost of the energy that can be provided by the main grid. To conclude this, different cases were studied considering even the higher energy cost defined by all the utilities in Brazil, obtaining for all the cases that the diesel generator is never dispatched.
- For the cases studied in Chapter 5, when the distribution system include the renewable-based generation systems (PV and wind systems), the final OC can be reduced in 30.7%, while the final PL can be reduced in 31.9%. This is due to the reduction of power that is purchased from the MV grid. Moreover, when the EMS is included, the final OC can be reduced in 5.3 % more (for the BCS Sol). This reduction is a result of the management performed by the long-term stage. It is important to notice that without an ESS it would be possible to perform management in the distribution system.
- Also for Chapter 5, when the RES generation and the load consumption are forecasted with a maximum RE of 5%, the impact of this forecast error is an increase in the final OC near to 5% and in the final PL near to 7.5%. This increment in the final OC is a result of the 9% decrease in the final energy supplied

by the ESS and the increment in 4.3% in the energy supplied by the MV grid. This increment in the energy supplied by the MV grid can be considered small enough to be neglected for one day of operation. However, this error may have a major impact in the economic operation of the microgrid in an annual operation basis.

- If the SOC of the ESS for both operational cases described in Chapter 5 are compared, it is possible to notice that the shape of the SOC, i.e., the charging/discharging pattern, was not affected significantly due to forecast error. This means that, if the forecast module can predict the trend in the load consumption (low and high demand periods) and the RES generation accurately, the short-term stage will be less affected by the forecast error.
- For the cases studied in Chapter 6, when it is considered a DSM strategy in conjunction with the EV technologies, a reduction of 2.55% in the final OC can be achieved (for the Min OC Sol). On the other hand, the final PL and energy provided by the MV are increased. This increment is a result of the inclusion of the EVs, which act as load when dispatched in charging mode. In addition, it was possible to observe that the forecast error has an impact near to 3.3% for the OC objective and 5.6% for the PL objective. This increment in the final OC and PL, is a consequence of the increment in 3.7% of the energy purchased from the MV grid and the reduction of the amount of energy supplied by the ESS.
- For the cases studied, when the EV is considered, an interesting and complementary behavior between the PV system, the ESS and the EV was observed. In this complementary behavior, part of the energy generated by the PV system is used to charge the EV system and the ESS, reducing the power purchased

from the MV grid. Furthermore, at night periods, part of the energy is exchanged between the two storage systems to fulfill all the operational constraints and reduce the final OC.

- According to the dynamic simulation performed, it was possible to conclude that the ESS and the EV system can be used to regulate the voltage variation at the residential node connections. This can be done increasing or decreasing the battery power input/output. Thus, the ESS and the EV can be used not only as storage system, but also to provide ancillary services to improve the quality of the final voltage profile. In terms of the VU factor, it was observed that the final VU profile shows low variations during the operational day when compared to the case when it is not performed energy management. According to this, the EMS has shown good capabilities to improve power quality.

## **8.1 FUTURE WORKS**

The following outlines suggestions for future research works:

- Include an investment analysis, including an economical and financial evaluation of the implementation of renewable based generation system under the current incentive and tax regulated by the resolution 482/2012.
- Improve power losses models to reduce the RE when comparing to GridLabD. This can be done considering others variables such as the ambient temperature. However, these improvements can results in more mathematical complex models, which would require a more advanced optimization software.

- Include a contingency policy to operate the LV Microgrid under an unexpected disconnection of the MV grid. This contingency policy will allow the EMS to operate the LV Microgrid in grid-connected and stand-alone mode of operation.
- Develop an uncertainty assessment study of the load consumption and the RES generation in the long-term stage. This can be done using a Monte-Carlo Simulation framework.

## 8.2 PUBLICATIONS

The publications resulting directly from this research are shown below:

*Conference publications:*

1. **P. Vergara**, R. Torquato, L.C.P. da Silva, “Towards a real-time Energy Management System for a Microgrid using a Multi-Objective Genetic Algorithm”, in *2015 IEEE Power and Energy Society General Meeting*, Denver, Estados Unidos, 2015.

## 9 REFERENCES

- [1] J. del R. L. Proaño, D. S. Hueichpan, and R. P. Behnke, “Método para gerar perfis de demanda em comunidades isoladas e previsão de demanda de curto prazo para as micro-redes baseadas em energias renováveis,” Universidade de Chile, 2012.
- [2] E. R. Sanseverino, M. L. Di Silvestre, M. G. Ippolito, A. De Paola, and G. Lo Re, “An execution, monitoring and replanning approach for optimal energy management in microgrids,” *Energy*, vol. 36, no. 5, pp. 3429–3436, May 2011.
- [3] D. E. Olivares, C. A. Canizares, and M. Kazerani, “A centralized optimal energy management system for microgrids,” in *2011 IEEE Power and Energy Society General Meeting*, 2011, pp. 1–6.
- [4] F. Katiraei, R. Iravani, N. Hatziargyriou, and A. Dimeas, “Microgrids management,” *IEEE Power Energy Mag.*, vol. 6, no. 3, pp. 54–65, May 2008.
- [5] C. M. Colson, M. H. Nehrir, and S. A. Pourmousavi, “Towards real-time microgrid power management using computational intelligence methods,” in *IEEE PES General Meeting*, 2010, pp. 1–8.
- [6] V. Hamidi, K. S. Smith, and R. C. Wilson, “Smart Grid technology review within the Transmission and Distribution sector,” in *2010 IEEE PES Innovative Smart Grid Technologies Conference Europe (ISGT Europe)*, 2010, pp. 1–8.
- [7] G. Kyriakarakos, A. I. Dounis, K. G. Arvanitis, and G. Papadakis, “A fuzzy logic energy management system for polygeneration microgrids,” *Renew. Energy*, vol. 41, pp. 315–327, May 2012.
- [8] M. Marzband, A. Sumper, A. Ruiz-Álvarez, J. L. Domínguez-García, and B. Tomoiagă, “Experimental evaluation of a real time energy management system for stand-alone microgrids in day-ahead markets,” *Appl. Energy*, vol. 106, pp. 365–376, Jun. 2013.
- [9] R. H. Lasseter, “MicroGrids,” *2002 IEEE Power Eng. Soc. Winter Meet. Conf. Proc. (Cat. No.02CH37309)*, vol. 1, pp. 305–308, 2002.
- [10] T. L. Vandoorn, J. C. Vasquez, J. De Kooning, J. M. Guerrero, and L. Vandeveld, “Microgrids: Hierarchical Control and an Overview of the Control and Reserve Management Strategies,” *IEEE Ind. Electron. Mag.*, vol. 7, no. 4, pp. 42–55, Dec. 2013.
- [11] N. Hatziargyriou, H. Asano, R. Iravani, and C. Marnay, “Microgrids: An Overview of Ongoing Research, Development, and Demonstration Projects,” *IEEE Power Energy Mag. IEEE*, vol. 5, no. 4, pp. 78–94, 2007.
- [12] R. H. Lasseter, “Microgrids and Distributed Generation,” *J. Energy Eng.*, vol. 133, no. 3, pp. 144–149, Sep. 2007.
- [13] R. H. Lasseter, “Smart Distribution: Coupled Microgrids,” *Proc. IEEE*, vol. 99, no. 6, pp. 1074–1082, Jun. 2011.

- [14] “Brazilian Elect. Reg. Agency (ANEEL): General Information,” 2012. [Online]. Available: [http://www.aneel.gov.br/arquivos/PDF/informacoes\\_](http://www.aneel.gov.br/arquivos/PDF/informacoes_). [Accessed: 09-Feb-2015].
- [15] R. Torquato, F. C. L. Trindade, and W. Freitas, “Analysis of the harmonic distortion impact of photovoltaic generation in Brazilian residential networks,” in *2014 16th International Conference on Harmonics and Quality of Power (ICHQP)*, 2014, pp. 239–243.
- [16] Y. LI and F. NEJABATKHAH, “Overview of control, integration and energy management of microgrids,” *J. Mod. Power Syst. Clean Energy*, vol. 2, no. 3, pp. 212–222, Aug. 2014.
- [17] A. Bidram and A. Davoudi, “Hierarchical Structure of Microgrids Control System,” *IEEE Trans. Smart Grid*, vol. 3, no. 4, pp. 1963–1976, Dec. 2012.
- [18] D. E. Olivares, A. Mehrizi-Sani, A. H. Etemadi, C. A. Canizares, R. Iravani, M. Kazerani, A. H. Hajimiragha, O. Gomis-Bellmunt, M. Saadifard, R. Palma-Behnke, G. A. Jimenez-Estevez, and N. D. Hatziargyriou, “Trends in Microgrid Control,” *IEEE Trans. Smart Grid*, vol. 5, no. 4, pp. 1905–1919, Jul. 2014.
- [19] E. Vaahedi, “Energy Management Systems,” in *Practical Power System Operation*, 1st ed., Wiley-IEEE Press, 2014, pp. 161–175.
- [20] A. K. Basu, S. P. Chowdhury, S. Chowdhury, and S. Paul, “Microgrids: Energy management by strategic deployment of DERs—A comprehensive survey,” *Renew. Sustain. Energy Rev.*, vol. 15, no. 9, pp. 4348–4356, Dec. 2011.
- [21] M. S. Narkhede, S. Chatterji, and S. Ghosh, “Trends and challenges in optimization techniques for operation and control of Microgrid - A review,” *2012 1st Int. Conf. Power Energy NERIST*, pp. 1–7, Dec. 2012.
- [22] A. Solanki, A. Nasiri, V. Bhavaraju, T. Abdullah, and D. Yu, “A new control method for microgrid power management,” in *2013 International Conference on Renewable Energy Research and Applications (ICRERA)*, 2013, no. October, pp. 1212–1216.
- [23] H. S. V. S. Kumar Nunna and S. Doolla, “Multiagent-Based Distributed-Energy-Resource Management for Intelligent Microgrids,” *IEEE Trans. Ind. Electron.*, vol. 60, no. 4, pp. 1678–1687, Apr. 2013.
- [24] A. L. Dimeas and N. D. Hatziargyriou, “Operation of a Multiagent System for Microgrid Control,” *IEEE Trans. Power Syst.*, vol. 20, no. 3, pp. 1447–1455, Aug. 2005.
- [25] C. M. Colson and M. H. Nehrir, “Algorithms for distributed decision-making for multi-agent microgrid power management,” in *2011 IEEE Power and Energy Society General Meeting*, 2011, pp. 1–8.
- [26] D. E. Olivares, C. A. Canizares, and M. Kazerani, “A Centralized Energy Management System for Isolated Microgrids,” *IEEE Trans. Smart Grid*, vol. 5, no. 4, pp. 1864–1875, Jul. 2014.
- [27] Y. Sahraei Manjili, A. Rajaei, M. Jamshidi, and B. T. Kelley, “Intelligent decision making for energy management in microgrids with air pollution reduction policy,” in

- 2012 7th International Conference on System of Systems Engineering (SoSE), 2012, pp. 13–18.
- [28] D. Paire and A. Miraoui, “Power management strategies for microgrid—A short review,” in *2013 IEEE Industry Applications Society Annual Meeting*, 2013, pp. 1–9.
- [29] J. M. Guerrero, J. C. Vasquez, J. Matas, L. G. de Vicuna, and M. Castilla, “Hierarchical Control of Droop-Controlled AC and DC Microgrids—A General Approach Toward Standardization,” *IEEE Trans. Ind. Electron.*, vol. 58, no. 1, pp. 158–172, Jan. 2011.
- [30] J. M. Guerrero, J. C. Vasquez, and R. Teodorescu, “Hierarchical control of droop-controlled DC and AC microgrids — a general approach towards standardization,” in *2009 35th Annual Conference of IEEE Industrial Electronics*, 2009, pp. 4305–4310.
- [31] J. A. P. Lopes, C. L. Moreira, and A. G. Madureira, “Defining Control Strategies for MicroGrids Islanded Operation,” *IEEE Trans. Power Syst.*, vol. 21, no. 2, pp. 916–924, May 2006.
- [32] J. a. Peças Lopes, S. a. Polenz, C. L. Moreira, and R. Cherkaoui, “Identification of control and management strategies for LV unbalanced microgrids with plugged-in electric vehicles,” *Electr. Power Syst. Res.*, vol. 80, no. 8, pp. 898–906, Aug. 2010.
- [33] A. Bertani, A. Borghetti, C. Bossi, L. De Biase, O. Lamquet, S. Massucco, A. Morini, C. A. Nucci, M. Paolone, E. Quaia, and F. Silvestro, “Management of Low Voltage Grids with High Penetration of Distributed Generation: concepts, implementations and experiments,” Milan, Italy, 2006.
- [34] T. L. Vandoorn, B. Zwaenepoel, J. D. M. De Kooning, B. Meersman, and L. Vandeveldel, “Smart microgrids and virtual power plants in a hierarchical control structure,” *2011 2nd IEEE PES Int. Conf. Exhib. Innov. Smart Grid Technol.*, pp. 1–7, Dec. 2011.
- [35] Q. Qin, Z. Chen, and X. Wang, “Overview of micro-grid energy management system research status,” *2012 Power Eng. Autom. Conf.*, pp. 1–4, Sep. 2012.
- [36] M. a. Abido, “Environmental/economic power dispatch using multiobjective evolutionary algorithms,” *IEEE Trans. Power Syst.*, vol. 18, no. 4, pp. 1529–1537, Nov. 2003.
- [37] J. M. Lujano-Rojas, C. Monteiro, R. Dufo-López, and J. L. Bernal-Agustín, “Optimum load management strategy for wind/diesel/battery hybrid power systems,” *Renew. Energy*, vol. 44, pp. 288–295, Aug. 2012.
- [38] Y.-F. Li, N. Pedroni, and E. Zio, “A Memetic Evolutionary Multi-Objective Optimization Method for Environmental Power Unit Commitment,” *IEEE Trans. Power Syst.*, vol. 28, no. 3, pp. 2660–2669, Aug. 2013.
- [39] M. Strelec and J. Berka, “Microgrid energy management based on approximate dynamic programming,” in *IEEE PES ISGT Europe 2013*, 2013, pp. 1–5.
- [40] P. Stluka, D. Godbole, and T. Samad, “Energy management for buildings and microgrids,” in *IEEE Conference on Decision and Control and European Control Conference*, 2011, pp. 5150–5157.

- [41] X. Wu, X. Wang, and Z. Bie, "Optimal generation scheduling of a microgrid," in *2012 3rd IEEE PES Innovative Smart Grid Technologies Europe (ISGT Europe)*, 2012, pp. 1–7.
- [42] S. Chakraborty and M. G. Simoes, "PV-Microgrid Operational Cost Minimization by Neural Forecasting and Heuristic Optimization," *2008 IEEE Ind. Appl. Soc. Annu. Meet.*, pp. 1–8, Oct. 2008.
- [43] R. Palma-Behnke, C. Benavides, F. Lanas, B. Severino, L. Reyes, J. Llanos, and D. Saez, "A Microgrid Energy Management System Based on the Rolling Horizon Strategy," *IEEE Trans. Smart Grid*, vol. 4, no. 2, pp. 996–1006, Jun. 2013.
- [44] X. Wu, X. Wang, and C. Qu, "A Hierarchical Framework for Generation Scheduling of Microgrids," *IEEE Trans. Power Deliv.*, vol. 29, no. 6, pp. 2448–2457, Dec. 2014.
- [45] A. Takeuchi, T. Hayashi, Y. Nozaki, and T. Shimakage, "Optimal Scheduling Using Metaheuristics for Energy Networks," *IEEE Trans. Smart Grid*, vol. 3, no. 2, pp. 968–974, Jun. 2012.
- [46] A. R. Abul'Wafa, "Optimization of economic/emission load dispatch for hybrid generating systems using controlled Elitist NSGA-II," *Electr. Power Syst. Res.*, vol. 105, pp. 142–151, Dec. 2013.
- [47] B. Zhao, X. Zhang, P. Li, K. Wang, M. Xue, and C. Wang, "Optimal sizing, operating strategy and operational experience of a stand-alone microgrid on Dongfushan Island," *Appl. Energy*, vol. 113, pp. 1656–1666, Jan. 2014.
- [48] B. Zhao, X. Zhang, J. Chen, C. Wang, and L. Guo, "Operation Optimization of Standalone Microgrids Considering Lifetime Characteristics of Battery Energy Storage System," *IEEE Trans. Sustain. Energy*, pp. 1–10, 2013.
- [49] D. Feroldi, P. Rullo, and D. Zumoffen, "Energy management strategy based on receding horizon for a power hybrid system," *Renew. Energy*, vol. 75, pp. 550–559, Mar. 2015.
- [50] M. Marzband, M. Ghadimi, A. Sumper, and J. L. Domínguez-García, "Experimental validation of a real-time energy management system using multi-period gravitational search algorithm for microgrids in islanded mode," *Appl. Energy*, vol. 128, pp. 164–174, Sep. 2014.
- [51] L. Guo, W. Liu, X. Li, Y. Liu, B. Jiao, W. Wang, C. Wang, and F. Li, "Energy Management System for Stand-Alone Wind-Powered-Desalination Microgrid," *IEEE Trans. Smart Grid*, pp. 1–1, 2014.
- [52] S. Upadhyay and M. P. Sharma, "Development of hybrid energy system with cycle charging strategy using particle swarm optimization for a remote area in India," *Renew. Energy*, vol. 77, pp. 586–598, May 2015.
- [53] M. Hemmati, N. Amjady, and M. Ehsan, "System modeling and optimization for islanded micro-grid using multi-cross learning-based chaotic differential evolution algorithm," *Int. J. Electr. Power Energy Syst.*, vol. 56, pp. 349–360, Mar. 2014.

- [54] I. Prodan and E. Zio, "A model predictive control framework for reliable microgrid energy management," *Int. J. Electr. Power Energy Syst.*, vol. 61, pp. 399–409, Oct. 2014.
- [55] E. Kuznetsova, C. Ruiz, Y. Li, and E. Zio, "Analysis of robust optimization for decentralized microgrid energy management under uncertainty," *Int. J. Electr. Power Energy Syst.*, vol. 64, pp. 815–832, Jan. 2015.
- [56] Y. Jaganmohan Reddy, Y. V Pavan Kumar, V. Sunil Kumar, and K. Padma Raju, "Distributed ANNs in a layered architecture for energy management and maintenance scheduling of renewable energy HPS microgrids," *2012 Int. Conf. Adv. Power Convers. Energy Technol.*, no. 1, pp. 1–6, Aug. 2012.
- [57] "GRIDLAB-D," 2015. [Online]. Available: <https://www.girdlabd.org>.
- [58] K. P. Schneider, J. C. Fuller, and D. P. Chassin, "Multi-State Load Models for Distribution System Analysis," *IEEE Trans. Power Syst.*, vol. 26, no. 4, pp. 2425–2433, Nov. 2011.
- [59] G. Cau, D. Cocco, M. Petrollese, S. Knudsen Kær, and C. Milan, "Energy management strategy based on short-term generation scheduling for a renewable microgrid using a hydrogen storage system," *Energy Convers. Manag.*, vol. 87, pp. 820–831, Nov. 2014.
- [60] M. M. Jalali and A. Kazemi, "Demand side management in a smart grid with multiple electricity suppliers," *Energy*, vol. 81, pp. 766–776, Feb. 2015.
- [61] T. Logenthiran, D. Srinivasan, and T. Z. Shun, "Demand Side Management in Smart Grid Using Heuristic Optimization," *IEEE Trans. Smart Grid*, vol. 3, no. 3, pp. 1244–1252, Sep. 2012.
- [62] D. Müller, A. Monti, S. Stinner, T. Schlösser, T. Schütz, P. Matthes, H. Wolisz, C. Molitor, H. Harb, and R. Streblow, "Demand side management for city districts," *Build. Environ.*, pp. 1–11, Apr. 2015.
- [63] Z. Wu and X. Xia, "Optimal switching renewable energy system for demand side management," *Sol. Energy*, vol. 114, pp. 278–288, Apr. 2015.
- [64] E. H. Et-Tolba, M. Maaroufi, and M. Ouassaid, "Demand side management algorithms and modeling in smart grids A customer's behavior based study," in *2013 International Renewable and Sustainable Energy Conference (IRSEC)*, 2013, pp. 531–536.
- [65] R. Palma-Behnke, C. Benavides, E. Aranda, J. Llanos, and D. Saez, "Energy management system for a renewable based microgrid with a demand side management mechanism," in *2011 IEEE Symposium on Computational Intelligence Applications In Smart Grid (CIASG)*, 2011, pp. 1–8.
- [66] W. Su, H. Eichi, W. Zeng, and M. Chow, "A Survey on the Electrification of Transportation in a Smart Grid Environment," *IEEE Trans. Ind. Informatics*, vol. 8, no. 1, pp. 1–10, Feb. 2012.
- [67] C. Zhou, K. Qian, M. Allan, and W. Zhou, "Modeling of the Cost of EV Battery Wear Due to V2G Application in Power Systems," *IEEE Trans. Energy Convers.*, vol. 26, no. 4, pp. 1041–1050, Dec. 2011.

- [68] N. Leemput, J. Van Roy, F. Geth, P. Tant, B. Claessens, and J. Driesen, "Comparative Analysis of Coordination Strategies for Electric Vehicles," in *2011 2nd IEEE PES International Conference and Exhibition on Innovative Smart Grid Technologies*, 2011, pp. 1–8.
- [69] P. Grahn, J. Munkhammar, J. Widen, K. Alvehag, and L. Soder, "PHEV Home-Charging Model Based on Residential Activity Patterns," *IEEE Trans. Power Syst.*, vol. 28, no. 3, pp. 2507–2515, Aug. 2013.
- [70] K. Qian, C. Zhou, M. Allan, and Y. Yuan, "Modeling of Load Demand Due to EV Battery Charging in Distribution Systems," *IEEE Trans. Power Syst.*, vol. 26, no. 2, pp. 802–810, May 2011.
- [71] K. Qian, C. Zhou, M. Allan, and Y. Yuan, "Modeling of Load Demand Due to EV Battery Charging in Distribution Systems," *IEEE Trans. Power Syst.*, vol. 26, no. 2, pp. 802–810, May 2011.
- [72] A. Damnjanovic and G. Feruson, "The measurement and evaluation of distribution transformer losses under nonlinear loading," in *IEEE Power Engineering Society General Meeting, 2004.*, vol. 2, no. 3, pp. 1416–1419.
- [73] "Brazilian Elect. Reg. Agency (ANEEL):Module 8 -Power Quality," 2010. [Online]. Available:  
[http://www.aneel.gov.br/arquivos/pdf/modulo8\\_revisao\\_1\\_retificacao\\_1.pdf](http://www.aneel.gov.br/arquivos/pdf/modulo8_revisao_1_retificacao_1.pdf).  
[Accessed: 19-Feb-2015].
- [74] C. A. C. Coello, G. B. Lamont, and D. A. Van Veldhuizen, *Evolutionary Algorithms for Solving Multi-Objective Problems*, Second Edi. New York, Untied States of America: Springer, 2007, p. 810.
- [75] K. Deb, A. Pratap, S. Agarwal, and T. Meyarivan, "A fast and elitist multiobjective genetic algorithm: NSGA-II," *IEEE Trans. Evol. Comput.*, vol. 6, no. 2, pp. 182–197, Apr. 2002.
- [76] N. Jenkins, J. B. Ekanayake, and G. Strbac, *Distributed Generation*, First. London, England: Institution of Engineering and Technology, 2010.

## 10 APPENDIX

### 10.1 APPENDIX A

Table A1. LV single-phase transformers specifications.

Low Voltage Transformer	Connection Type	SINGLE PHASE CENTER TAPPED
	Install Type	PADMOUNT
	Power rating [kVA]	200
	Primary voltage [kV]	13.2
	Secondary voltage [kV]	0.120
	Impedance [ $\Omega$ ]	$0.00033 + 0.0022j$
	Shunt impedance [k $\Omega$ ]	$10 + 10j$

Table A2. MV transformers specifications.

MV Transformer	Connection Type	DELTA-DELTA
	Power rating [kVA] (Wind System)	40
	Power rating [kVA] (Diesel Generator System)	60
	Primary voltage [V]	207.846
	Secondary voltage [kV]	13.2
	Resistance [ $\Omega$ ]	0.01
	Reactance [H]	0.06

Table A3. House specifications.

House	Heating and cooling system type	Electric
	Light power factor [-]	0.95
Inverter	Power factor [-]	1.0
	Efficiency [-]	0.95
	Panel type	SINGLE CRISTAL SILICON
	Nominal voltage [V]	220
Solar System	Installation type	FIXED AXIS, ROOF MOUNTED
	Efficiency [-]	0.18

Table A4. Length of lines.

From	To	Length [m]	Type
N1	N2	100	Underground Line
N3	N2	100	Underground Line
N2	N4	100	Underground Line
A-1000	A-1100	60	Triplex Line
A-1100	A-1110	50	Triplex Line
A-1100	A-1120	50	Triplex Line
A-1110	A-1150	100	Triplex Line
A-1120	A-1160	100	Triplex Line
B-1000	B-1100	60	Triplex Line
B-1100	B-1110	50	Triplex Line
B-1100	B-1120	50	Triplex Line
B-1110	B-1150	100	Triplex Line
B-1120	B-1160	100	Triplex Line
C-1000	C-1100	60	Triplex Line
C-1100	C-1110	50	Triplex Line
C-1100	C-1120	50	Triplex Line
C-1110	C-1150	100	Triplex Line
C-1120	C-1160	100	Triplex Line

Table A5. Conductor specifications.

Underground Line	Conductor diameter [in]	0.567
	Outer diameter [in]	1.29
	GMR [in]	0.0171
	Resistance [ $\Omega$ /ml]	0.410
Triplex Line	GMR [in]	0.0111
	Resistance [ $\Omega$ /ml]	0.97
	Insulation thickness [in]	0.08
	Diameter [in]	0.368

## 10.2 APPENDIX B

Meteorological data for the Congonhas Airport (São Paulo). SWERA Project.

Table B.1. Hourly weather data for the State of São Paulo.

	Temp [°C]	Wind Speed [m/s]	Solar Direct [W/m <sup>2</sup> ]	Solar Difuse [W/m <sup>2</sup> ]	Solar Normal [W/m <sup>2</sup> ]	Humidity [%]	Pressure [mbar]
00:00:00	18,1	2,5	0	0	0	86	920,43
01:00:00	17,9	2,3	0	0	0	85	920,43
02:00:00	17,7	2,2	0	0	0	87	920,43
03:00:00	17,6	2	0	0	0	88	920,43
04:00:00	17,4	1,9	0	0	0	89	920,43
05:00:00	17,5	2,2	39	20	23	86	920,43
06:00:00	18,3	2,2	185	80	131	82	920,43
07:00:00	19,3	4	316	156	310	78	920,43
08:00:00	20,5	3,4	366	217	466	73	920,43
09:00:00	21,7	3,4	372	284	595	69	920,43
10:00:00	22,6	3,2	399	316	692	65	920,43
11:00:00	23,4	3,9	424	360	781	64	920,43
12:00:00	24,1	4,3	395	346	735	61	920,43
13:00:00	24,2	4,7	340	339	651	62	920,43
14:00:00	23,6	5,3	235	290	477	65	920,43
15:00:00	22,4	6	233	244	392	71	920,43
16:00:00	21,5	5,8	163	153	223	73	920,43
17:00:00	20,3	5,5	69	79	94	78	920,43
18:00:00	19,3	5,1	7	7	8	81	920,43
19:00:00	18,8	4,4	0	0	0	82	920,43
20:00:00	18,5	3,8	0	0	0	83	920,43
21:00:00	18,4	3,5	0	0	0	84	920,43
22:00:00	18,2	3,1	0	0	0	86	920,43
23:00:00	18,1	3,3	0	0	0	85	920,43